

# On the spherical cardioid distribution and its goodness-of-fit

Eduardo García-Portugués<sup>1,2</sup>

## Abstract

In this paper, we study the spherical cardioid distribution, a higher-dimensional and higher-order generalization of the circular cardioid distribution. This distribution is rotationally symmetric and generates unimodal, multimodal, axial, and girdle-like densities. We show several characteristics of the spherical cardioid that make it highly tractable: simple density evaluation, closedness under convolution, explicit expressions for vectorized moments, and efficient simulation. The moments of the spherical cardioid up to a given order coincide with those of the uniform distribution on the sphere, highlighting its closeness to the latter. We derive estimators by the method of moments and maximum likelihood, their asymptotic distributions, and their asymptotic relative efficiencies. We give the machinery for a bootstrap goodness-of-fit test based on the projected-ecdf approach, including the projected distribution and closed-form expressions for test statistics. An application to modeling the orbits of long-period comets shows the usefulness of the spherical cardioid distribution in real data analyses.

**Keywords:** Directional Statistics; Gegenbauer Polynomials; Chebyshev Polynomials; Projections.

## 1 Introduction

The (*circular*) *cardioid distribution* was introduced by Harold Jeffreys in 1948 (Eq. (1) in p. 328 of Jeffreys, 2003, reprint) as that with density

$$f_{C_k}(\theta; \mu, \rho) := \frac{1}{2\pi} \{1 + \rho \cos(\theta - \mu)\}, \quad \theta \in [0, 2\pi), \quad (1)$$

for a concentration  $\rho \in [-1, 1]$  and a location  $\mu \in [0, 2\pi)$ . The name “cardioid” stems from the fact that the polar curve  $r(\theta) = f_{C_k}(\theta; \mu, \rho)$  traces a cardioid when  $|\rho| = 1$  and a limaçon when  $|\rho| < 1$ . Originally proposed as a “continuous departure from a uniform distribution of chance”, the cardioid distribution is arguably the simplest non-uniform distribution on the circle  $\mathbb{S}^1 \equiv [0, 2\pi)$ , with  $0 \equiv 2\pi$  identified. It reduces to the uniform density on the circle for  $\rho = 0$  and gives a unimodal density for  $\rho > 0$  with mode at  $\mu$ . In the literature, the cardioid density is often parametrized as  $\theta \mapsto (2\pi)^{-1}(1 + 2\rho \cos(\theta - \mu))$  and  $|\rho| \in [0, 1/2)$  (Mardia and Jupp, 1999, Section 3.5.5; Jammalamadaka and SenGupta, 2001, Section 2.2.2) or  $\rho \in [0, 1/2]$  (Pewsey et al., 2013, Section 4.3.4), but we adopt the original parametrization in (1) for later convenience.

The cardioid distribution has received considerable attention in the literature. The main reasons are threefold. First, the model is highly tractable, which makes it particularly easy to understand and rich in terms of available results that are scarcer for other circular distributions: closedness under convolution, closed-form cumulative distribution function, straightforward trigonometric moments, and direct estimation and inference. Pewsey (2026) gave a recent and critical revision of these basic properties. Second, the density (1) arises as a submodel of general circular models that have been proposed in the literature, like the  $M$ -truncated nonnegative Fourier series models of Fernández-Durán (2004) ((1) arises with the choice  $M = 1$ ), the symmetric and unimodal family of circular distributions of Jones and Pewsey (2005) (choice  $\psi = 1$ ), and the unimodal family of Kato and Jones (2015) (choice  $\rho = 0$ ). Third, due to its simplicity, the cardioid density has been used as the building

---

<sup>1</sup>Department of Statistics, Carlos III University of Madrid (Spain).

<sup>2</sup>Corresponding author. e-mail: edgarcia@est-econ.uc3m.es.

block for more flexible models, through generators and transformations. We refer to Pewsey (2026) for references on the latter use.

Generalizations of (1) to higher-dimensional supports have been mainly concentrated on the two-dimensional torus ( $\mathbb{S}^1$ )<sup>2</sup>. Wehrly and Johnson (1980)'s approach can be used to construct bivariate distributions with cardioid marginals and/or cardioid link density, an approach which Fernández-Durán (2007) exploited with  $M$ -truncated nonnegative Fourier series. Wang and Shimizu (2012) proposed two toroidal models with cardioid marginals using Möbius transformations. More recently, Banerjee and Biswas (2024) proposed a toroidal model with cardioid marginals and a cardioid conditional distribution. As pointed out by Shogo Kato in Pewsey and García-Portugués (2021, Eq. (1)), it is possible to construct cardioid-like densities on the two-dimensional torus that have both marginal and conditional cardioid distributions, such as

$$(\theta_1, \theta_2) \mapsto \frac{1}{4\pi^2} \{1 + \rho_1 \cos(\theta_1 - \mu_1) + \rho_2 \cos(\theta_2 - \mu_2) + \rho_{12} \cos(\theta_1 - \mu_1) \cos(\theta_2 - \mu_2)\}.$$

Extensions of (1) to the sphere  $\mathbb{S}^d := \{\mathbf{x} \in \mathbb{R}^{d+1} : \|\mathbf{x}\| = 1\}$  have been scarcer, more recent, and also closely related. As a mixing base to represent rotationally symmetric distributions on  $\mathbb{S}^d$ , Baringhaus and Grübel (2024) considered a distribution generalizing (1) to  $\mathbb{S}^d$ , using zonal spherical harmonics. We refer to this distribution as the *spherical cardioid distribution*. This spherical cardioid distribution exactly coincides with the “Legendre polynomial distributions” used in Borodavka and Ebner (2026) as a device to study the power of maximal projection-based uniformity tests on  $\mathbb{S}^d$ . To the best of the author's knowledge, no substantial investigation of the spherical cardioid distribution as a statistical model has been conducted so far.

This paper studies in depth the spherical cardioid distribution on  $\mathbb{S}^d$ ,  $d \geq 1$ . Its density is a  $k$ -order generalization of the circular cardioid density (1) based on Chebyshev and Gegenbauer polynomials. Our main methodological contributions are threefold. First, we show several characteristics and properties of the spherical cardioid that make it an appealing model: ability to produce unimodal/multimodal patterns, connections with the von Mises–Fisher and Watson distributions, explicit vectorized moments of arbitrary order, closedness under convolution, a simple characteristic function, and efficient simulation. The  $m$ -moments of the cardioid of order  $k$ , with  $k > m$ , are shown to coincide with those of the uniform distribution. This makes a large- $k$  spherical cardioid distribution a formidably challenging alternative for uniform tests. Second, we derive estimation and inference by the method of moments, for  $k = 1, 2$ , and a moment estimator for the concentration parameter when the location is known. We also study maximum likelihood estimation and inference for  $k \geq 1$ . We obtain the asymptotic distributions of these estimators and their asymptotic relative efficiencies, showing that moment estimators lose more efficiency for large absolute values of the concentration. Third, we give the machinery for a bootstrap goodness-of-fit test based on a statistic that integrates, across projecting directions, discrepancies between the projected empirical cumulative distribution function and the null projected cumulative distribution function. To that aim, we provide closed forms for the projected distribution and several test statistics. Numerical experiments corroborate the adequate empirical behavior of the estimators and the goodness-of-fit test. In an application to modeling the orbits of long-period comets, we show that the spherical cardioid distribution of order two on  $\mathbb{S}^2$  is a practically relevant model.

The rest of this paper is organized as follows. Section 2 provides general notation and background on orthogonal polynomials used throughout the paper. Section 3 introduces the spherical cardioid distribution (Section 3.1) and its basic properties: closedness under convolution (Section 3.2), moments (Section 3.3), characteristic function (Section 3.4), and simulation (Section 3.5). Section 4 deals with estimation and inference by the method of moments (Section 4.1) and maximum likelihood (Section 4.2), and inspects asymptotic relative efficiencies (Section 4.3). A goodness-of-fit test for spherical cardioidness is provided in Section 5, which is based on the projected cumulative distribution function (Section 5.1), a closed form of the test statistic (Section 5.2), and a parametric bootstrap procedure (Section 5.3). Section 6 reports numerical experiments on the finite-sample

performance of the estimators and bootstrap test. An application to modeling the orbits of comets is presented in Section 7. Some concluding remarks are given in Section 8. Proofs are deferred to Appendices A–C.

## 2 Background on orthogonal polynomials

We denote the surface area of  $\mathbb{S}^d = \{\mathbf{x} \in \mathbb{R}^{d+1} : \|\mathbf{x}\| = 1\}$ ,  $d \geq 1$ , as  $\omega_d := 2\pi^{(d+1)/2}/\Gamma((d+1)/2)$ . The surface area measure on  $\mathbb{S}^d$  is denoted by  $\sigma_d$ . We set  $\mathbb{S}^0 := \{-1, 1\}$ ,  $\sigma_0$  as the counting measure on  $\mathbb{S}^0$ , and  $\omega_0 := 2$ . The uniform distribution on  $\mathbb{S}^d$ , denoted  $\text{Unif}(\mathbb{S}^d)$ , has constant density  $1/\omega_d$  with respect to  $\sigma_d$ . In the paper, densities on  $\mathbb{S}^d$  are always with respect to  $\sigma_d$ .

Gegenbauer and Chebyshev polynomials are central to the spherical cardioid construction. Both are orthogonal polynomial families on the space of square-integrable functions on  $[-1, 1]$  with respect to the weight functions  $x \mapsto (1-x^2)^{d/2-1}$ ,  $d \geq 2$ , and  $x \mapsto (1-x^2)^{-1/2}$ , respectively. We denote by  $L_d^2([-1, 1])$  this weighted  $L^2$  space.

The Gegenbauer polynomials  $\{C_k^{(d-1)/2}\}_{k=0}^\infty$  of index  $\lambda = (d-1)/2$ ,  $d \geq 2$ , form an orthogonal basis on  $L_d^2([-1, 1])$ . They satisfy the orthogonality relation

$$\int_{-1}^1 C_k^{(d-1)/2}(x) C_\ell^{(d-1)/2}(x) (1-x^2)^{d/2-1} dx = \delta_{k,\ell} c_{k,d},$$

where  $\delta_{k,\ell}$  denotes the Kronecker delta and

$$c_{k,d} := \frac{2^{3-d} \pi \Gamma(d+k-1)}{(d+2k-1)k! \Gamma((d-1)/2)^2} = \frac{\omega_d}{\omega_{d-1}} \left(1 + \frac{2k}{d-1}\right)^{-2} d_{k,d}, \quad (2)$$

$$d_{k,d} := \left(1 + \frac{2k}{d-1}\right) \frac{\Gamma(d-1+k)}{\Gamma(d-1)k!} = \left(1 + \frac{2k}{d-1}\right) C_k^{(d-1)/2}(1). \quad (3)$$

Above,  $d_{k,d}$  is the dimension of the vector space of spherical harmonics of degree  $k$ , i.e., the harmonic homogeneous polynomials of degree  $k$  defined on  $\mathbb{S}^d$ . The first Gegenbauer polynomials are  $C_0^{(d-1)/2}(x) = 1$ ,  $C_1^{(d-1)/2}(x) = (d-1)x$ , and  $C_2^{(d-1)/2}(x) = [(d-1)/2][(d+1)x^2 - 1]$ , while the next follow from the recurrence relation

$$C_{k+1}^{(d-1)/2}(x) = \frac{2k+d-1}{k+1} x C_k^{(d-1)/2}(x) - \frac{k+d}{k+1} C_{k-1}^{(d-1)/2}(x), \quad k \geq 1.$$

The Chebyshev polynomials (of the first kind)  $\{T_k\}_{k=0}^\infty$  are expressible as  $T_k(x) = \cos(k \cos^{-1}(x))$  for  $x \in [-1, 1]$ . They form an orthogonal basis on  $L_1^2([-1, 1])$ , satisfying

$$\int_{-1}^1 T_k(x) T_\ell(x) (1-x^2)^{-1/2} dx = \delta_{k,\ell} c_{k,1},$$

where

$$c_{k,1} := \frac{1 + \delta_{k,0}}{2} \pi = \frac{\omega_1}{\omega_0} (2 - \delta_{k,0})^{-2} d_{k,1}, \quad d_{k,1} := 2 - \delta_{k,0} = (2 - \delta_{k,0}) T_k(1). \quad (4)$$

The first Chebyshev polynomials are  $T_0(x) = 1$ ,  $T_1(x) = x$ , and  $T_2(x) = 2x^2 - 1$ , with the next following from

$$T_{k+1}(x) = 2x T_k(x) - T_{k-1}(x), \quad k \geq 1.$$

Chebyshev polynomials can be seen as the scaled limit of Gegenbauer polynomials when their index shrinks to zero:  $\lim_{\lambda \rightarrow 0^+} \lambda^{-1} C_k^\lambda(x) = (2/k) T_k(x)$  for  $k \geq 1$ . To unify notation, we adopt the convention  $C_k^0(x) := T_k(x)$  for  $k \geq 0$ . By defining

$$\tau_{k,d} := \begin{cases} 2 - \delta_{k,0}, & d = 1, \\ 1 + 2k/(d-1), & d \geq 2, \end{cases}$$

for  $k \geq 0$ , it follows that (2)–(4) are expressible, for  $d \geq 1$ , as

$$c_{k,d} = \frac{\omega_d}{\omega_{d-1}} \tau_{k,d}^{-2} d_{k,d}, \quad C_k^{(d-1)/2}(1) = \tau_{k,d}^{-1} d_{k,d}. \quad (5)$$

Using this notation, we define the normalized polynomials

$$\tilde{C}_k^{(d-1)/2}(x) := \frac{C_k^{(d-1)/2}(x)}{C_k^{(d-1)/2}(1)} = \frac{C_k^{(d-1)/2}(x)}{\tau_{k,d}^{-1} d_{k,d}} = \frac{\omega_d}{\omega_{d-1}} \frac{C_k^{(d-1)/2}(x)}{c_{k,d} \tau_{k,d}}$$

for  $k \geq 0$  and  $d \geq 1$ . In particular,  $\tilde{C}_0^{(d-1)/2}(x) = 1$ ,  $\tilde{C}_1^{(d-1)/2}(x) = x$ , and  $\tilde{C}_2^{(d-1)/2}(x) = d^{-1}[(d+1)x^2 - 1]$  for  $d \geq 1$ . The normalized polynomials satisfy  $|\tilde{C}_k^{(d-1)/2}(x)| \leq 1$  for  $x \in [-1, 1]$ ,  $k \geq 0$ , and  $d \geq 1$ . The parity of  $C_k^{(d-1)/2}$  and  $\tilde{C}_k^{(d-1)/2}$  is that of  $k$ , i.e., they are even (odd) functions when  $k$  is even (odd).

Since  $\{C_k^{(d-1)/2}\}_{k=0}^{\infty}$  form an orthogonal basis of  $L_d^2([-1, 1])$ , any function  $g \in L_d^2([-1, 1])$ ,  $d \geq 1$ , admits the expansion

$$g(x) = \sum_{k=0}^{\infty} b_{k,d}(g) C_k^{(d-1)/2}(x), \quad (6)$$

$$b_{k,d}(g) := \frac{1}{c_{k,d}} \int_{-1}^1 g(x) C_k^{(d-1)/2}(x) (1-x^2)^{d/2-1} dx,$$

with the series (6) converging in  $L_d^2([-1, 1])$ . As a consequence of (6), a function  $f \in L^2(\mathbb{S}^d)$  rotationally symmetric about  $\mu \in \mathbb{S}^d$ , defined as  $f(\mathbf{x}) := g(\mathbf{x}^\top \mu)$ , admits the zonal spherical harmonics expansion

$$f(\mathbf{x}) = \sum_{k=0}^{\infty} b_{k,d}(g) C_k^{(d-1)/2}(\mathbf{x}^\top \mu), \quad (7)$$

with the series converging in  $L^2(\mathbb{S}^d)$ . Kalf (1995, Theorem 2) can be applied to guarantee uniform convergence of (7) if  $f$  is sufficiently smooth. Indeed, if  $f \in C^\infty(\mathbb{S}^d)$ , then (7) is uniformly absolutely convergent.

A useful result involving Gegenbauer and Chebyshev polynomials is the formula

$$\frac{1}{\omega_d} \int_{\mathbb{S}^d} C_k^{(d-1)/2}(\gamma^\top \mathbf{u}) C_m^{(d-1)/2}(\gamma^\top \mathbf{v}) \sigma_d(d\gamma) = \tau_{k,d}^{-1} C_k^{(d-1)/2}(\mathbf{u}^\top \mathbf{v}) \delta_{k,m} \quad (8)$$

for  $k, m \geq 0$  and  $d \geq 1$ . A proof of (8) can be found in García-Portugués et al. (2023, Lemma B.7).

### 3 Spherical cardioid distribution

#### 3.1 Genesis

The generalization of (1) to the sphere is motivated by the fact that  $\cos(\theta - \mu)$  can be expressed as the Chebyshev polynomial  $\tilde{C}_1^0(\cos(\theta - \mu)) = \cos(\theta - \mu)$ . Switching to Cartesian coordinates on  $\mathbb{S}^1$ ,  $\mathbf{x} = (\cos \theta, \sin \theta)^\top$  and  $\mu = (\cos \mu, \sin \mu)^\top$ , it follows that  $\cos(\theta - \mu) = \cos \theta \cos \mu + \sin \theta \sin \mu = \mathbf{x}^\top \mu$ , and hence  $\cos(\theta - \mu) = \tilde{C}_1^0(\mathbf{x}^\top \mu)$ . The generalization to the sphere  $\mathbb{S}^d$ ,  $d \geq 1$ , and higher orders  $k \geq 1$  is then evident.

**Definition 3.1** (Spherical cardioid distribution). *The spherical cardioid distribution on  $\mathbb{S}^d$ ,  $d \geq 1$ , with location  $\mu \in \mathbb{S}^d$ , concentration  $\rho \in [-1, 1]$ , and (integer) order  $k \geq 1$ , has density*

$$f_{C_k}(\mathbf{x}; \mu, \rho) := \frac{1}{\omega_d} \left\{ 1 + \rho \tilde{C}_k^{(d-1)/2}(\mathbf{x}^\top \mu) \right\} \quad (9)$$

with respect to the surface area measure  $\sigma_d$  on  $\mathbb{S}^d$ . The distribution is denoted  $C_k(\mu, \rho)$ .

Just like the circular cardioid is the simplest Fourier-based density, the spherical cardioid is the simplest spherical harmonic-based density (see (7)). Baringhaus and Grübel (2024, Eq. (27)) and Borodavka and Ebner (2026, Eq. (5.3)) had considered (9) before as auxiliary means for infinite mixture representation and power investigation in uniformity tests on  $\mathbb{S}^d$ , respectively. As a particular spherical harmonics-based density, more general instances of (9) can be traced back to Giné (1975, Theorem 5.3, Proposition 6.5) in the context of Sobolev tests of uniformity on  $\mathbb{S}^d$ .

The density (9) is well-defined since  $|\tilde{C}_k^{(d-1)/2}(\mathbf{x}^\top \boldsymbol{\mu})| \leq 1$  and  $\int_{\mathbb{S}^d} C_k^{(d-1)/2}(\mathbf{x}^\top \boldsymbol{\mu}) \sigma_d(d\mathbf{x}) = 0$  for  $k \geq 1$  (e.g., by (8)). For  $d = 1$ , using polar coordinates, (9) reduces to

$$f_{C_k}(\theta; \mu, \rho) = \frac{1}{2\pi} \{1 + \rho \cos(k(\theta - \mu))\},$$

which yields the circular cardioid density (1) when  $k = 1$ . When  $d = 2$  and  $k = 1, 2$ , (9) becomes

$$f_{C_k}(\mathbf{x}; \boldsymbol{\mu}, \rho) = \begin{cases} \frac{1}{4\pi} \left\{ 1 + \rho \mathbf{x}^\top \boldsymbol{\mu} \right\}, & k = 1, \\ \frac{1}{4\pi} \left\{ 1 + \rho \frac{3(\mathbf{x}^\top \boldsymbol{\mu})^2 - 1}{2} \right\}, & k = 2. \end{cases}$$

For large  $d$ , the density (9) converges to  $(1/\omega_d) \{1 + \rho (\mathbf{x}^\top \boldsymbol{\mu})^k\}$  since  $\lim_{d \rightarrow \infty} \tilde{C}_k^{(d-1)/2}(x) = x^k$  for  $x \in [-1, 1]$  and  $k \geq 1$  (DLMF, 2025, Eq. 18.6.4).

If  $\mathbf{X} \sim C_k(\boldsymbol{\mu}, \rho)$ , then for any  $(d+1) \times (d+1)$  orthogonal matrix  $\mathbf{O}$ ,  $\mathbf{O}\mathbf{X} \sim C_k(\mathbf{O}\boldsymbol{\mu}, \rho)$ . Therefore,  $C_k(\boldsymbol{\mu}, \rho)$  is rotationally symmetric about  $\boldsymbol{\mu} \in \mathbb{S}^d$ , since  $\mathbf{O}\mathbf{X}$  and  $\mathbf{X}$  are equal in distribution for any orthogonal transformation  $\mathbf{O}$  such that  $\mathbf{O}\boldsymbol{\mu} = \boldsymbol{\mu}$ . Thus, in particular,  $f_{C_k}(\mathbf{x}; \boldsymbol{\mu}, \rho) = f_{C_k}(\boldsymbol{\mu}; \mathbf{x}, \rho) = f_{C_k}(-\mathbf{x}; -\boldsymbol{\mu}, \rho)$ . When  $\rho = 0$ ,  $C_k(\boldsymbol{\mu}, 0) = \text{Unif}(\mathbb{S}^d)$  for any  $k \geq 1$ .

Because the parity of  $\tilde{C}_k^{(d-1)/2}$  is that of  $k$ , the density (9) is non-identifiable on  $(\boldsymbol{\mu}, \rho) \in \mathbb{S}^d \times [-1, 1]$  for odd  $k$ , as  $f_{C_k}(\mathbf{x}; \boldsymbol{\mu}, \rho) = f_{C_k}(\mathbf{x}; -\boldsymbol{\mu}, -\rho)$ . Therefore, we can restrict the parameter space to  $\rho \in [0, 1]$  for odd  $k$  without loss of generality. In contrast, for even  $k$ , both signs of  $\rho$  yield different densities for  $d \geq 2$  (see Figure 2), but  $\pm \boldsymbol{\mu}$  give the same density. In particular, the density is axially symmetric, i.e.,  $f_{C_k}(\mathbf{x}; \boldsymbol{\mu}, \rho) = f_{C_k}(-\mathbf{x}; \boldsymbol{\mu}, \rho) = f_{C_k}(\mathbf{x}; -\boldsymbol{\mu}, \rho)$ . The parameter space of  $\boldsymbol{\mu}$  can be thus restricted to  $\mathbb{S}_+^d := \{\boldsymbol{\mu} \in \mathbb{S}^d : \mu_1 > 0\}$  for  $k$  even without loss of generality. This symmetry also makes the density non-identifiable in  $\rho$  for  $d = 1$ , as  $f_{C_k}(\theta; \mu, \rho) = f_{C_k}(\theta; \mu + \pi/k, -\rho)$  since  $\cos(k(\theta - (\mu + \pi/k))) = -\cos(k(\theta - \mu))$  (see Figure 1); a restriction to  $\rho \in [0, 1]$  prevents it. Actually, for  $d = 1$  and any  $k \geq 1$ , the density is  $k$ -fold symmetric, so only values of  $\boldsymbol{\mu}$  in  $\mathbb{S}_k^1 := \{(\cos(\theta), \sin(\theta))^\top : \theta \in [0, 2\pi/k]\}$  give different densities.

To remove all these non-identifiabilities from the full parameter space  $\mathbb{S}^d \times [-1, 1]$ , we reduce the parameter space of  $(\boldsymbol{\mu}, \rho)$  in (9) to

$$\Theta_{k,d} := \begin{cases} \mathbb{S}_k^1 \times [0, 1], & d = 1, k \geq 1, \\ \mathbb{S}^d \times [0, 1], & d \geq 2, k \text{ odd}, \\ \mathbb{S}_+^d \times [-1, 1], & d \geq 2, k \text{ even}. \end{cases}$$

We may further restrict to  $\rho \neq 0$  (excludes uniform density;  $\boldsymbol{\mu}$  is not identifiable) and  $|\rho| < 1$  (ensures the density is always strictly positive). We denote this reduced parameter space as  $\Theta_{k,d}^\circ$ .

Figure 1 shows the shapes of the density (9) on  $\mathbb{S}^1$  when  $\boldsymbol{\mu} = \mathbf{e}_2$ ,  $k = 1, 2, 3, 4$  and  $\rho \in \{-1, 1\}$ . For  $k \geq 1$  and  $\rho > 0$ , there are  $k$  modes located at  $\mu + 2\pi j/k$  and  $k$  antimodes (local minima) located at  $\mu + 2\pi(j + 1/2)/k$ ,  $j = 0, 1, \dots, k-1$ . The density vanishes at the antimodes only if  $\rho = 1$ . The figure illustrates how negative values of  $\rho$ , also for even  $k$ , result in non-identifiability.

The shapes of the spherical cardioid density are more intricate, with multiple girdle-like patterns appearing for  $k > 1$ . Figure 2 shows them on  $\mathbb{S}^2$  for  $\boldsymbol{\mu} = \mathbf{e}_3$ ,  $k = 1, 2, 3, 4$  and  $\rho \in \{-1, 1\}$ . Because  $f_{C_k}(\mathbf{x}; \boldsymbol{\mu}, \rho)$  depends on  $\mathbf{x}$  only through  $t = \mathbf{x}^\top \boldsymbol{\mu}$ , its critical sets are either the poles  $\pm \boldsymbol{\mu}$  (corresponding to  $t = \pm 1$ ) or latitude subspheres  $\{\mathbf{x} \in \mathbb{S}^d : \mathbf{x}^\top \boldsymbol{\mu} = t\}$ , creating density

ridges or valleys. The  $t$ -latitudes,  $t \in (-1, 1)$ , of the density ridges/valleys correspond to the zeros of  $[C_k^{(d-1)/2}(t)]' = (d-1)C_{k-1}^{(d+1)/2}(t)$ , which can be obtained numerically or localized through inequalities (DLMF, 2025, Section 18.16(ii)). In general, the location and type of the extrema depend on the parity of  $k$  and the sign of  $\rho$ : (i) for  $k = 1$  and  $\rho > 0$ , there is a single mode at  $\mu$  and a single antinode at  $-\mu$ ; (ii) for  $k = 2$  and  $\rho > 0$ , there are two antipodal modes at  $\pm\mu$  and one density valley at the equator; (iii) for  $k \geq 3$  and  $\rho > 0$ , there is a mode at  $\mu$ ,  $\lfloor (k-1)/2 \rfloor$  density ridges, and a mode (antinode) at  $-\mu$  if  $k$  is even (odd); (iv) for even  $k$  and  $\rho < 0$ , the poles  $\pm\mu$  are antinodes and there are  $k/2$  density ridges, distributed on latitude subspheres symmetric with respect to the equator (with the central ridge at the equator when  $k/2$  is odd). These statements hold for all  $d \geq 2$ .

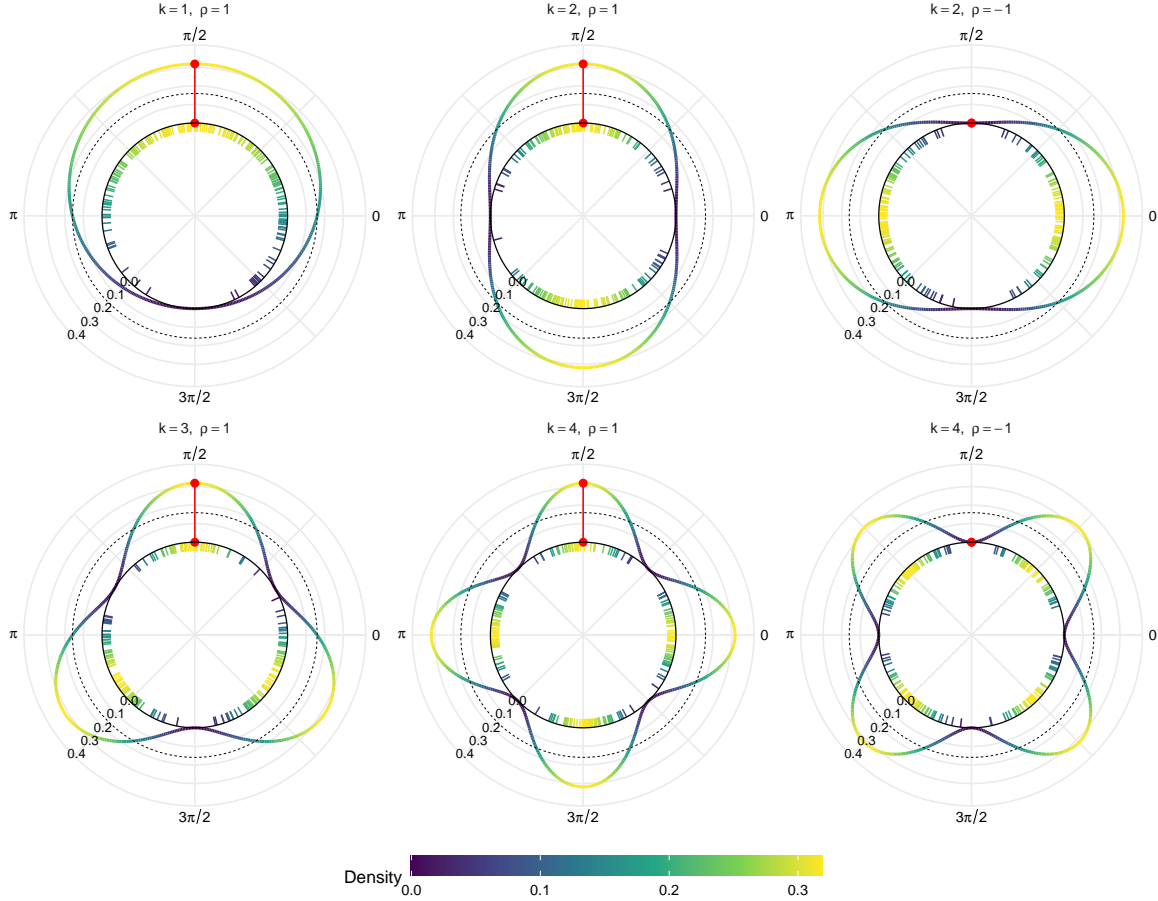


Figure 1: Samples and density of the spherical cardioid on  $\mathbb{S}^1$  with  $\mu = e_2$  (red point, north) and  $(k, \rho) \in \{(1, 1), (2, 1), (2, -1), (3, 1), (4, 1), (4, -1)\}$ . For each panel, a random sample of  $n = 200$  observations is shown. The dashed curve gives the uniform density  $1/(2\pi)$  as reference. Negative- $\rho$  panels illustrate overparametrization.

Just like the von Mises distribution with low concentration is approximately a circular cardioid (see, e.g., Mardia and Jupp, 1999, Eq. (3.5.20)), the von Mises–Fisher distribution  $\text{vMF}(\mu, \kappa)$  on  $\mathbb{S}^d$ ,  $d \geq 1$ , with location  $\mu \in \mathbb{S}^d$  and concentration  $\kappa \geq 0$ , is connected with the spherical cardioid. Precisely,

$$\text{vMF}(\mu, \kappa) \approx C_1(\mu, \kappa) \quad \text{when } \kappa \approx 0, \quad (10)$$

as  $\exp\{\kappa \mathbf{x}^\top \mu\} \approx 1 + \kappa \mathbf{x}^\top \mu = 1 + \kappa \tilde{C}_1^{(d-1)/2}(\mathbf{x}^\top \mu)$ . Similarly, the Watson distribution  $\text{W}(\mu, \kappa)$ ,

with density proportional to  $\mathbf{x} \mapsto \exp\{\kappa(\mathbf{x}^\top \boldsymbol{\mu})^2\}$  for  $\kappa \in \mathbb{R}$ , satisfies

$$W(\boldsymbol{\mu}, \kappa) \approx C_2 \left( \boldsymbol{\mu}, \frac{d\kappa}{d+1+\kappa} \right) \quad \text{when } \kappa \approx 0, \quad (11)$$

as  $\exp\{\kappa(\mathbf{x}^\top \boldsymbol{\mu})^2\} \approx 1 + \kappa(\mathbf{x}^\top \boldsymbol{\mu})^2 = [1 + \kappa/(d+1)]\{1 + [(d\kappa)/(d+1+\kappa)]\tilde{C}_2^{(d-1)/2}(\mathbf{x}^\top \boldsymbol{\mu})\}$ . Approximations (10)–(11) are useful because it is easier to evaluate the density of  $C_k(\boldsymbol{\mu}, \kappa)$  and to simulate from it (Section 3.5) than from the von Mises–Fisher or Watson distributions. The distribution  $C_1(\boldsymbol{\mu}, \rho)$  is a special case (choice  $\psi = 1$ ) of the extension to  $\mathbb{S}^d$  of the unimodal family of circular distributions of Jones and Pewsey (2005). Baringhaus and Grübel (2024, Section 3) show how rotationally symmetric distributions on  $\mathbb{S}^d$  about  $\boldsymbol{\mu}$ , particularly the von Mises–Fisher and Cauchy-like distributions, can be expressed in terms of infinite mixtures of  $\{C_k(\boldsymbol{\mu}, \rho)\}_{k=1}^\infty$ , a result related to (9).

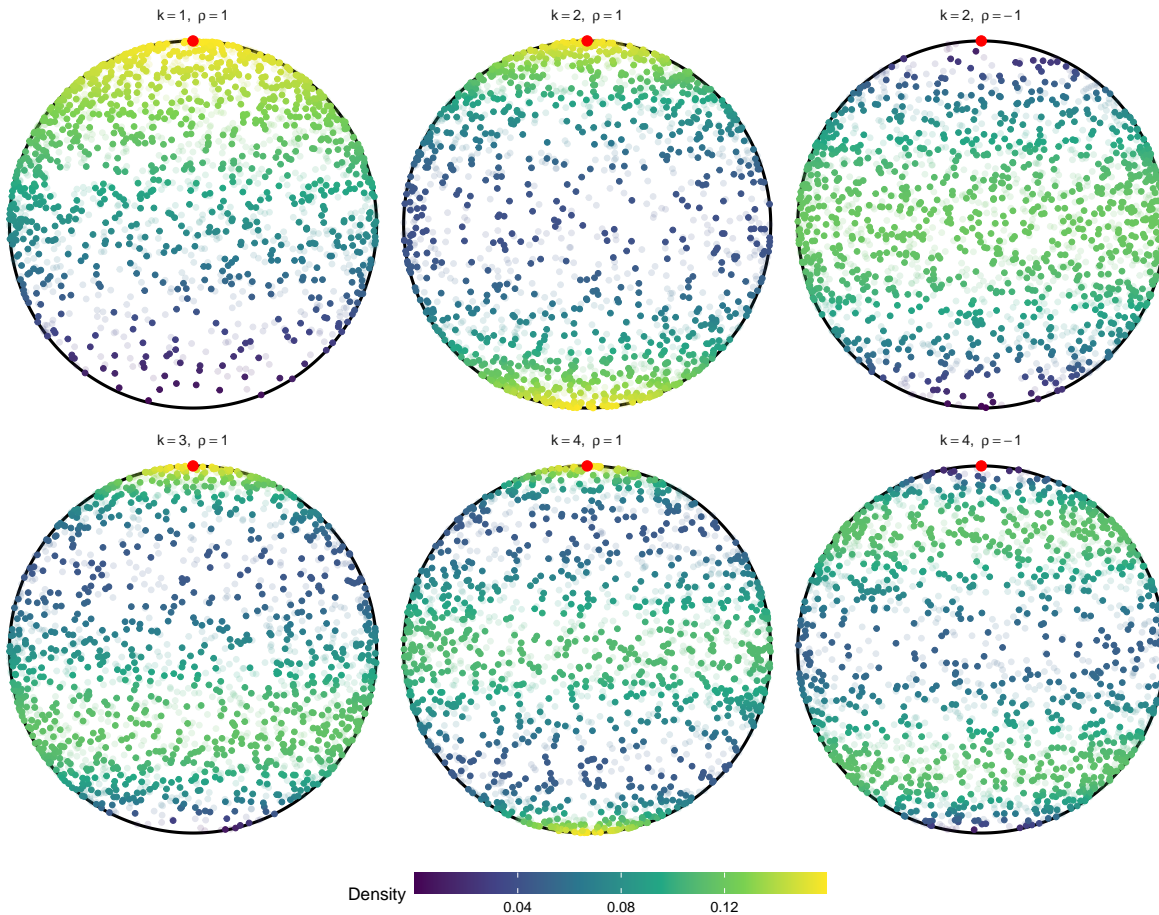


Figure 2: Samples and density of the spherical cardioid on  $\mathbb{S}^2$  with  $\boldsymbol{\mu} = \mathbf{e}_3$  (red point, north) and  $(k, \rho) \in \{(1, 1), (2, 1), (2, -1), (3, 1), (4, 1), (4, -1)\}$ . The plots show the front hemisphere of  $\mathbb{S}^2$ , with shading applied to the points in the back hemisphere. The sample, with  $n = 2000$  observations, is colored according to the value of the density at the observations.

### 3.2 Closedness under convolution

The circular cardioid family is closed under convolution, in the sense that if  $\Theta_1 \sim C_1(\mu_1, \rho_1)$  and  $\Theta_2 \sim C_1(\mu_2, \rho_2)$  independently, then  $(\Theta_1 + \Theta_2) \bmod 2\pi \sim C_1(\mu_1 + \mu_2, \rho_1 \rho_2 / 2)$  (see, e.g., Pewsey, 2026, p. 2, under a slightly different parametrization). For brevity, we write this result as  $C_1(\mu_1, \rho_1) + C_1(\mu_2, \rho_2) \stackrel{d}{=} C_1(\mu_1 + \mu_2, \rho_1 \rho_2 / 2)$ .

The spherical cardioid family defined by (9) is also closed under convolution in the following general sense.

**Proposition 3.1** (Closedness under convolution). *Let  $\boldsymbol{\mu}_1, \boldsymbol{\mu}_2 \in \mathbb{S}^d$ ,  $\rho_1, \rho_2 \in [-1, 1]$ , and  $k_1, k_2 \geq 1$ . Then,*

$$\int_{\mathbb{S}^d} f_{C_{k_1}}(\mathbf{x}; \boldsymbol{\mu}_1, \rho_1) f_{C_{k_2}}(\mathbf{x}; \boldsymbol{\mu}_2, \rho_2) \sigma_d(d\mathbf{x}) = f_{C_{k_1}}\left(\boldsymbol{\mu}_1; \boldsymbol{\mu}_2, \delta_{k_1, k_2} \frac{\rho_1 \rho_2}{d_{k_1, d}}\right)$$

and, if  $\mathbf{X} \mid \boldsymbol{\Xi} \sim C_{k_1}(\boldsymbol{\Xi}, \rho_1)$  and  $\boldsymbol{\Xi} \sim C_{k_2}(\boldsymbol{\mu}_2, \rho_2)$ , then  $\mathbf{X} \sim C_{k_1}(\boldsymbol{\mu}_2, \delta_{k_1, k_2} \rho_1 \rho_2 / d_{k_1, d})$ .

For  $d = 1$ , using polar coordinates, the previous result readily implies that

$$\begin{aligned} (f_{C_{k_1}}(\cdot; \boldsymbol{\mu}_1, \rho_1) * f_{C_{k_2}}(\cdot; \boldsymbol{\mu}_2, \rho_2))(\theta) &= \int_0^{2\pi} f_{C_{k_1}}(\theta - \varphi; \boldsymbol{\mu}_1, \rho_1) f_{C_{k_2}}(\varphi; \boldsymbol{\mu}_2, \rho_2) d\varphi \\ &= f_{C_{k_1}}\left(\theta; \boldsymbol{\mu}_1 + \boldsymbol{\mu}_2, \delta_{k_1, k_2} \frac{\rho_1 \rho_2}{2}\right). \end{aligned}$$

Hence,  $C_{k_1}(\boldsymbol{\mu}_1, \rho_1) + C_{k_2}(\boldsymbol{\mu}_2, \rho_2) \stackrel{d}{=} C_{k_1}(\boldsymbol{\mu}_1 + \boldsymbol{\mu}_2, \delta_{k_1, k_2} \rho_1 \rho_2 / 2)$ , which in particular shows that  $\text{Unif}(\mathbb{S}^1)$  can arise as the convolution of two non-uniform cardioid distributions of different orders.

Alternatively, for  $d \geq 1$ , Proposition 3.1 gives the closedness under the Cartesian-coordinates “convolution” on  $\mathbb{S}^d$

$$\begin{aligned} (f_{C_{k_1}}(\cdot; \cdot, \rho_1) * f_{C_{k_2}}(\cdot; \boldsymbol{\mu}, \rho_2))(\mathbf{x}) &:= \int_{\mathbb{S}^d} f_{C_{k_1}}(\mathbf{x}; \mathbf{y}, \rho_1) f_{C_{k_2}}(\mathbf{y}; \boldsymbol{\mu}, \rho_2) \sigma_d(d\mathbf{y}) \\ &= f_{C_{k_1}}\left(\mathbf{x}; \boldsymbol{\mu}, \delta_{k_1, k_2} \frac{\rho_1 \rho_2}{d_{k_1, d}}\right) \end{aligned}$$

considered in, e.g., Klemelä (2000) in the context of kernel smoothing on the sphere.

### 3.3 Moments

We compute in this section the vectorized moments of the  $C_k(\boldsymbol{\mu}, \rho)$  distribution. These moments allow quantifying the degree of similarity of  $C_k(\boldsymbol{\mu}, \rho)$  to  $\text{Unif}(\mathbb{S}^d)$ , and are key to derive the inference in Section 4.1.

We require some matrix notation. We use  $\text{vec} : \mathcal{M}_{p,q} \rightarrow \mathbb{R}^{pq}$  to denote the vectorization map that stacks the columns of a  $p \times q$  matrix into a  $pq$ -dimensional vector, and  $\text{vec}_{p,q}^{-1}$  to denote the inverse map. We denote  $\mathbf{S}_{d+1,r}$  as the *symmetrizer*  $(d+1)^r \times (d+1)^r$  matrix such that

$$\mathbf{S}_{d+1,r}(\mathbf{v}_1 \otimes \cdots \otimes \mathbf{v}_r) = \frac{1}{r!} \sum_{\sigma \in S_r} \mathbf{v}_{\sigma(1)} \otimes \cdots \otimes \mathbf{v}_{\sigma(r)}$$

for any collection  $\{\mathbf{v}_1, \dots, \mathbf{v}_r\} \subset \mathbb{R}^{d+1}$  and  $S_r$  being the set of permutations of  $\{1, \dots, r\}$  (see, e.g., Chacón and Duong, 2018, p. 95). The symmetrizer matrix satisfies  $\mathbf{S}_{d+1,r}^2 = \mathbf{S}_{d+1,r}$  and  $\mathbf{S}_{d+1,r}^\top = \mathbf{S}_{d+1,r}$ . The standard Kronecker product of matrices is denoted with  $\otimes$ , and  $\mathbf{x}^{\otimes r} = \otimes_{j=1}^r \mathbf{x}$  represents the  $r$ -fold Kronecker product of the column vector  $\mathbf{x}$ .

Our first result shows, in particular, that all the moments of order  $m < k$  of  $C_k(\boldsymbol{\mu}, \rho)$  coincide with those of  $\text{Unif}(\mathbb{S}^d)$ , and so do the moments of order  $m > k$  with  $m - k$  odd.

**Theorem 3.1** (Vectorized moments). *Let  $\mathbf{X} \sim C_k(\boldsymbol{\mu}, \rho)$  for  $(\boldsymbol{\mu}, \rho) \in \mathbb{S}^d \times [-1, 1]$ ,  $k \geq 1$ , and  $d \geq 1$ . Let  $m \geq 1$ . The  $m$ th vectorized moment of  $\mathbf{X}$ ,  $\mathbb{E}[\mathbf{X}^{\otimes m}]$ , is given by:*

(i). For  $m < k$ ,  $\mathbb{E}[\mathbf{X}^{\otimes m}] = \boldsymbol{\mu}_{d+1,m}$ , where

$$\boldsymbol{\mu}_{d+1,m} := \mathbb{E}[\mathbf{U}^{\otimes m}] = \frac{(m-1)!!}{\prod_{r=0}^{m/2-1} (d+1+2r)} \mathbf{S}_{d+1,m} (\text{vec } \mathbf{I}_{d+1})^{\otimes m/2} \mathbf{1}_{\{m \text{ even}\}} \quad (12)$$

for  $\mathbf{U} \sim \text{Unif}(\mathbb{S}^d)$ .

(ii). For  $m = k$ ,

$$\mathbb{E}[\mathbf{X}^{\otimes k}] = \boldsymbol{\mu}_{d+1,k} + \frac{\rho}{d_{k,d}} \mathbf{S}_{d+1,k} \sum_{j=0}^{\lfloor k/2 \rfloor} a_{k,j} (\text{vec } \mathbf{I}_{d+1})^{\otimes j} \otimes \boldsymbol{\mu}^{\otimes k-2j},$$

where

$$a_{k,j} = (-1)^j \frac{k!}{2^j (k-2j)! j!} \frac{1}{\prod_{r=1}^j (2(k-r)+d-1)}, \quad a_{k,0} = 1.$$

(iii). For  $m > k$  and  $m - k$  odd,  $\mathbb{E}[\mathbf{X}^{\otimes m}] = \boldsymbol{\mu}_{d+1,m}$ .

(iv). For general  $m \geq 1$ ,

$$\begin{aligned} \mathbb{E}[\mathbf{X}^{\otimes m}] &= \boldsymbol{\mu}_{d+1,m} \\ &+ \frac{\rho}{C_k^{(d-1)/2}(1)} \frac{\omega_{d-1}}{\omega_d} \mathbf{S}_{d+1,m} \sum_{j=0}^{\lfloor m/2 \rfloor} e_{j,k,m} \boldsymbol{\mu}^{\otimes(m-2j)} \otimes \left\{ (\text{vec } \mathbf{I}_{d+1} - \boldsymbol{\mu}^{\otimes 2})^{\otimes j} \right\}, \end{aligned}$$

where

$$\begin{aligned} e_{j,k,m} &:= \binom{m}{2j} \frac{(2j-1)!!}{\prod_{r=0}^{j-1} (d+2r)} f_{j,m,k} \mathbf{1}_{\{m+k \text{ even}\}}, \\ f_{j,m,k} &:= \int_{-1}^1 t^{m-2j} (1-t^2)^{d/2-1+j} C_k^{(d-1)/2}(t) dt \\ &= \frac{\Gamma(d/2+j)}{g_{k,d}} \\ &\times \sum_{s=0}^{\lfloor k/2 \rfloor} (-1)^s \frac{2^{k-2s} \Gamma((d-1)/2+k-s)}{s!(k-2s)!} \frac{\Gamma((m+k+1)/2-j-s)}{\Gamma((d+k+m+1)/2-s)}, \\ g_{k,d} &:= \begin{cases} k/2, & d = 1, \\ [\Gamma((d-1)/2)]^{-1}, & d \geq 2. \end{cases} \end{aligned}$$

The next two corollaries exploit Theorem 3.1 to provide explicit expressions for particular moments and their covariance matrices, useful for Section 4.1.

**Corollary 3.1** (Specific moments). *Let  $\mathbf{X}_k \sim \text{C}_k(\boldsymbol{\mu}, \rho)$  for  $(\boldsymbol{\mu}, \rho) \in \mathbb{S}^d \times [-1, 1]$ ,  $k \geq 1$ , and  $d \geq 1$ . Then, the  $k$ th moments for  $k = 1, \dots, 4$  are:*

$$\begin{aligned} \mathbb{E}[\mathbf{X}_1] &= \frac{\rho}{d+1} \boldsymbol{\mu}, \\ \mathbb{E}[\mathbf{X}_2^{\otimes 2}] &= \frac{1}{d+1} \text{vec } \mathbf{I}_{d+1} + \frac{2\rho}{d(d+3)} \left\{ \boldsymbol{\mu}^{\otimes 2} - \frac{1}{d+1} \text{vec } \mathbf{I}_{d+1} \right\}, \\ \mathbb{E}[\mathbf{X}_3^{\otimes 3}] &= \frac{6\rho}{d(d+1)(d+5)} \mathbf{S}_{d+1,3} \left\{ \boldsymbol{\mu}^{\otimes 3} - \frac{3}{d+3} \text{vec } \mathbf{I}_{d+1} \otimes \boldsymbol{\mu} \right\}, \\ \mathbb{E}[\mathbf{X}_4^{\otimes 4}] &= \frac{3}{(d+1)(d+3)} \mathbf{S}_{d+1,4} (\text{vec } \mathbf{I}_{d+1})^{\otimes 2} \\ &+ \frac{24\rho}{d(d+1)(d+2)(d+7)} \mathbf{S}_{d+1,4} \left\{ \boldsymbol{\mu}^{\otimes 4} - \frac{6}{d+5} \text{vec } \mathbf{I}_{d+1} \otimes \boldsymbol{\mu}^{\otimes 2} \right. \\ &\left. + \frac{3}{(d+3)(d+5)} (\text{vec } \mathbf{I}_{d+1})^{\otimes 2} \right\}. \end{aligned}$$

**Corollary 3.2** (Covariance matrices of vectorized moments). *Let  $\mathbf{X} \sim \mathbf{C}_k(\boldsymbol{\mu}, \rho)$  for  $(\boldsymbol{\mu}, \rho) \in \mathbb{S}^d \times [-1, 1]$ ,  $k \geq 1$ , and  $d \geq 1$ . Let  $m \geq 1$ . The covariance matrix of  $\mathbf{X}^{\otimes m}$  is*

$$\text{Var}[\mathbf{X}^{\otimes m}] = \text{vec}_{(d+1)^m, (d+1)^m}^{-1} \left( \mathbb{E}[\mathbf{X}^{\otimes 2m}] - \mathbb{E}[\mathbf{X}^{\otimes m}]^{\otimes 2} \right).$$

If  $k$  is odd, then  $\mathbb{E}[\mathbf{X}^{\otimes 2m}] = \boldsymbol{\mu}_{d+1, 2m}$ . In particular, for  $k = 1$ ,

$$\text{Var}[\mathbf{X}] = \frac{1}{d+1} \mathbf{I}_{d+1} - \frac{\rho^2}{(d+1)^2} \boldsymbol{\mu} \boldsymbol{\mu}^\top.$$

As a consequence of the previous result, we have the following Central Limit Theorem (CLT) for the sample  $m$ th vectorized moment:

$$\sqrt{n}(\overline{\mathbf{X}^{\otimes m}} - \mathbb{E}[\mathbf{X}^{\otimes m}]) \rightsquigarrow \mathcal{N}(\mathbf{0}, \text{Var}[\mathbf{X}^{\otimes m}]),$$

with relatively explicit forms for  $k = m = 1$  and  $k = m = 2$ .

### 3.4 Characteristic function

The characteristic and moment generating functions,  $\varphi_{\mathbf{X}}(\mathbf{t}) := \mathbb{E}[e^{i\mathbf{t}^\top \mathbf{X}}]$  and  $M_{\mathbf{X}}(\mathbf{t}) := \mathbb{E}[e^{\mathbf{t}^\top \mathbf{X}}]$ , admit explicit expressions for  $\mathbf{X} \sim \mathbf{C}_k(\boldsymbol{\mu}, \rho)$ , as shown next.

**Proposition 3.2** (Characteristic and moment generating functions). *Let  $\mathbf{X} \sim \mathbf{C}_k(\boldsymbol{\mu}, \rho)$  for  $(\boldsymbol{\mu}, \rho) \in \mathbb{S}^d \times [-1, 1]$ ,  $k \geq 1$ , and  $d \geq 1$ . Then, for  $\mathbf{t} \in \mathbb{R}^{d+1} \setminus \{\mathbf{0}\}$  ( $\mathbf{t} = \mathbf{0}$  follows by continuity),*

$$M_{\mathbf{X}}(\mathbf{t}) = \left( \frac{2}{\|\mathbf{t}\|} \right)^{(d-1)/2} \left\{ e_{0,d} \mathcal{I}_{(d-1)/2}(\|\mathbf{t}\|) + \frac{\rho}{d_{k,d}} e_{k,d} \mathcal{I}_{(2k+d-1)/2}(\|\mathbf{t}\|) C_k^{(d-1)/2} \left( \frac{\boldsymbol{\mu}^\top \mathbf{t}}{\|\mathbf{t}\|} \right) \right\},$$

where  $\mathcal{I}_\nu$  is the modified Bessel function of the first kind and order  $\nu$ , and

$$e_{\ell,d} := \begin{cases} \Gamma((d-1)/2)(\ell + (d-1)/2), & d \geq 2, \\ 2 - \delta_{\ell,0}, & d = 1. \end{cases}$$

$\varphi_{\mathbf{X}}(\mathbf{t})$  is obtained by replacing  $\mathcal{I}_{(2\ell+d-1)/2}(\|\mathbf{t}\|)$  with  $i^\ell \mathcal{J}_{(2\ell+d-1)/2}(\|\mathbf{t}\|)$ ,  $\ell = 0, k$ , in the expression of  $M_{\mathbf{X}}(\mathbf{t})$ , where  $\mathcal{J}_\nu$  is the Bessel function of the first kind and order  $\nu$ .

The explicit form of the characteristic function can be used to derive goodness-of-fit tests based on the squared distance between the population and empirical characteristic functions, as in Ebner et al. (2024). We do not pursue this direction here, and instead focus on a different goodness-of-fit test strategy in Section 5.

### 3.5 Simulation

Simulation from  $\mathbf{C}_k(\boldsymbol{\mu}, \rho)$  is immediate by rejection sampling from  $\text{Unif}(\mathbb{S}^d)$ , since

$$\frac{f_{\mathbf{C}_k}(\mathbf{x}; \boldsymbol{\mu}, \rho)}{1/\omega_d} = 1 + \rho \tilde{C}_k^{(d-1)/2}(\mathbf{x}^\top \boldsymbol{\mu}) \leq 1 + |\rho| =: M.$$

The acceptance probability is  $1/M \in [1/2, 1]$ . Algorithm 1 sets out the steps.

Rejection-free simulation can be derived using the rotational symmetry of the model and either the parity of  $k$  or the forthcoming Theorem 5.1. Because of rotational symmetry, if  $\mathbf{X} := T\boldsymbol{\mu} + \sqrt{1-T^2} \mathbf{B}_{\boldsymbol{\mu}} \boldsymbol{\Xi}$ , where  $\boldsymbol{\Xi} \sim \text{Unif}(\mathbb{S}^{d-1})$  is independent of the random variable  $T \sim F_{\boldsymbol{\mu}}$  on  $[-1, 1]$  (see Theorem 5.1) and  $\mathbf{B}_{\boldsymbol{\mu}}$  is a semi-orthogonal  $(d+1) \times d$  matrix such that  $\boldsymbol{\mu}^\top \mathbf{B}_{\boldsymbol{\mu}} = \mathbf{0}$ , then  $\mathbf{X} \sim \mathbf{C}_k(\boldsymbol{\mu}, \rho)$ . For example, for  $d = 2$  and  $k = 2$ , Theorem 5.1 gives

$$F_{\boldsymbol{\mu}}(x) = \frac{\rho x^3 + (2 - \rho)x + 2}{4},$$

which enables inverse transform sampling by solving  $T = F_{\boldsymbol{\mu}}^{-1}(U)$  for  $U \sim \text{Unif}(0, 1)$ . In particular, for  $\rho > 0$ , the cubic equation has an explicit valid root given by  $T = \sqrt[3]{-q/2 + \sqrt{\Delta}} + \sqrt[3]{-q/2 - \sqrt{\Delta}}$ , where  $q = 2(1 - 2u)/\rho$ ,  $p = (2 - \rho)/\rho$ , and  $\Delta = (q/2)^2 + (p/3)^3$ .

---

**Algorithm 1:** Rejection sampling from  $C_k(\boldsymbol{\mu}, \rho)$

---

- i. Simulate  $\mathbf{U} \sim \text{Unif}(\mathbb{S}^d)$ .
- ii. Simulate  $V \sim \text{Unif}(0, 1)$ .
- iii. If  $V \leq (1 + \rho \tilde{C}_k^{(d-1)/2}(\mathbf{U}^\top \boldsymbol{\mu}))/M$ , accept  $\mathbf{U}$ , else return to the first step.

---

The inverse transformation method is rarely preferable over rejection sampling besides  $k = 1, 2$ . However, for odd  $k \geq 1$ , we can borrow from the stochastic representation of skew symmetric distributions (e.g., Azzalini and Capitanio, 2014, Proposition 1.3) to simulate  $C_k(\boldsymbol{\mu}, \rho)$  exactly without rejections due to the parity of  $f_d$  (see (17)) and oddness of  $\tilde{C}_k^{(d-1)/2}$ . Algorithm 2 and the proof of Proposition 3.3 give the specifics.

---

**Algorithm 2:** Rejection-free sampling from  $C_k(\boldsymbol{\mu}, \rho)$  for odd  $k$

---

- i. Simulate  $\mathbf{U} \sim \text{Unif}(\mathbb{S}^d)$ .
- ii. Set  $X = \mathbf{U}^\top \mathbf{e}_1$  and  $R = |X|$ .
- iii. Simulate  $S \in \{-1, 1\}$  with  $P\{S = 1 \mid R\} = \{1 + \rho \tilde{C}_k^{(d-1)/2}(R)\}/2$  and set  $T = SR$ .
- iv. Simulate  $\boldsymbol{\Xi} \sim \text{Unif}(\mathbb{S}^{d-1})$  independent of  $(R, S)$ .
- v. Return  $\mathbf{X} = T\boldsymbol{\mu} + \sqrt{1 - T^2} \mathbf{B}_{\boldsymbol{\mu}} \boldsymbol{\Xi}$ .

---

**Proposition 3.3.** *The random vector  $\mathbf{X}$  generated in Algorithm 2 is distributed as  $C_k(\boldsymbol{\mu}, \rho)$ .*

## 4 Estimation and inference

Let  $\mathbf{X}_1, \dots, \mathbf{X}_n$  be an independent and identically distributed (iid) sample from  $C_k(\boldsymbol{\mu}, \rho)$ . We address in this section the estimation of  $(\boldsymbol{\mu}, \rho)$  and asymptotic results allowing for their inference.

### 4.1 Method of moments

The moments obtained in Theorem 3.1 can be used for estimation of  $(\boldsymbol{\mu}, \rho)$  through the method of moments. Its applicability, as anticipated by the expressions of the moments in Corollary 3.1, depends on the order  $k$ . We provide next moment estimators of  $(\boldsymbol{\mu}, \rho)$  for the specific orders  $k = 1, 2$ . We then follow a different approach to obtain an estimator of  $\rho$  for arbitrary  $k \geq 1$ , when  $\boldsymbol{\mu}$  is known, using Gegenbauer moments.

Our first result concerns the case  $k = 1$ , for which  $E[\mathbf{X}] = [\rho/(d+1)]\boldsymbol{\mu}$ , and hence  $\hat{\boldsymbol{\mu}}_{\text{MM},1} := \bar{\mathbf{X}}/\|\bar{\mathbf{X}}\|$  and  $\hat{\rho}_{\text{MM},1} := (d+1)\|\bar{\mathbf{X}}\|$  are natural moment estimators. The estimators  $(\hat{\boldsymbol{\mu}}_{\text{MM},1}, \hat{\rho}_{\text{MM},1})$ , computed from the sample  $\mathbf{X}_1, \dots, \mathbf{X}_n$ , are *rotationally equivariant*: if they are computed from the rotated sample  $\mathbf{O}\mathbf{X}_1, \dots, \mathbf{O}\mathbf{X}_n$ , their resulting values are  $(\mathbf{O}\hat{\boldsymbol{\mu}}_{\text{MM},1}, \hat{\rho}_{\text{MM},1})$ .

**Theorem 4.1** (Moment estimators when  $k = 1$ ). *Let  $\mathbf{X}_1, \dots, \mathbf{X}_n \sim C_1(\boldsymbol{\mu}, \rho)$ , for  $(\boldsymbol{\mu}, \rho) \in \Theta_{1,d}^\circ$  and  $d \geq 1$ . Let*

$$\hat{\boldsymbol{\mu}}_{\text{MM},1} = \frac{\bar{\mathbf{X}}}{\|\bar{\mathbf{X}}\|} \quad \text{and} \quad \hat{\rho}_{\text{MM},1} = (d+1)\|\bar{\mathbf{X}}\|.$$

Then:

(i). The estimators are strongly consistent:  $(\hat{\boldsymbol{\mu}}_{\text{MM},1}, \hat{\rho}_{\text{MM},1}) \rightarrow (\boldsymbol{\mu}, \rho)$  a.s. as  $n \rightarrow \infty$ .

(ii). The estimators are asymptotically normal:

$$\sqrt{n} \begin{pmatrix} \hat{\boldsymbol{\mu}}_{\text{MM},1} - \boldsymbol{\mu} \\ \hat{\rho}_{\text{MM},1} - \rho \end{pmatrix} \rightsquigarrow \mathcal{N}_{d+2} \begin{pmatrix} \mathbf{0} & \begin{pmatrix} \sigma_{\text{MM},1}^2(\boldsymbol{\mu})(\mathbf{I}_{d+1} - \boldsymbol{\mu}\boldsymbol{\mu}^\top) & \mathbf{0}^\top \\ \mathbf{0} & \sigma_{\text{MM},1}^2(\rho) \end{pmatrix} \end{pmatrix}$$

as  $n \rightarrow \infty$ , where  $\sigma_{\text{MM},1}^2(\boldsymbol{\mu}) = (d+1)\rho^{-2}$  and  $\sigma_{\text{MM},1}^2(\rho) = d+1-\rho^2$ .

The asymptotic covariance matrix is block-diagonal and singular. The former gives the asymptotic independence of  $(\hat{\boldsymbol{\mu}}_{\text{MM},1}, \hat{\rho}_{\text{MM},1})$ , as in any rotationally symmetric model, while the latter is a consequence of the constraint  $\|\boldsymbol{\mu}\| = 1$ , and is ubiquitous in models in directional statistics (see, e.g., Mardia and Jupp, 1999, p. 199).

Specializing Theorem 4.1(ii) to  $d = 1$  and taking polar coordinates, the result in Pewsey (2026, Eq. (10)) follows after adjusting for the different parameterization of  $\rho$ .

In the case  $k = 2$ , the first moment of  $\text{C}_2(\boldsymbol{\mu}, \rho)$  is null and the second is required to identify both parameters. By Corollary 3.1, we know that

$$\begin{aligned} \mathbb{E}[\mathbf{X}\mathbf{X}^\top] &= \frac{1}{d+1}\mathbf{I}_{d+1} + \frac{2\rho}{d(d+3)} \left\{ \boldsymbol{\mu}\boldsymbol{\mu}^\top - \frac{1}{d+1}\mathbf{I}_{d+1} \right\} \\ &= \frac{d+3+2\rho}{(d+1)(d+3)}\boldsymbol{\mu}\boldsymbol{\mu}^\top + \frac{(d+3)-2\rho/d}{(d+1)(d+3)}(\mathbf{I}_{d+1} - \boldsymbol{\mu}\boldsymbol{\mu}^\top) \\ &=: a(\rho)\boldsymbol{\mu}\boldsymbol{\mu}^\top + b(\rho)(\mathbf{I}_{d+1} - \boldsymbol{\mu}\boldsymbol{\mu}^\top). \end{aligned}$$

Note that  $a(\rho) > b(\rho)$  for any  $\rho > 0$ , and  $a(\rho) < b(\rho)$  for any  $\rho < 0$ . Hence,

$$(\lambda_\pm, \mathbf{u}_\pm) = (a(\rho), \boldsymbol{\mu}) \tag{13}$$

is the first (+) or last (-) eigenpair of  $\boldsymbol{\Sigma}$ , depending on the sign of  $\rho$ .

The eigenpair (13) suggests the following estimators based on the sample scatter matrix  $\mathbf{S} = (1/n) \sum_{i=1}^n \mathbf{X}_i \mathbf{X}_i^\top$ :

$$\hat{\boldsymbol{\mu}}_{\text{MM},2} := \mathbf{u}_\pm(\mathbf{S}), \quad \hat{\rho}_{\text{MM},2} := \frac{d+3}{2} ((d+1)\lambda_\pm(\mathbf{S}) - 1),$$

where  $\lambda_+(\mathbf{S})$  is the largest (resp.,  $\lambda_-(\mathbf{S})$  is the smallest) eigenvalue of  $\mathbf{S}$  for  $\text{C}_2(\boldsymbol{\mu}, \rho)$  with  $\rho > 0$  (resp.,  $\rho < 0$ ) and  $\mathbf{u}_\pm(\mathbf{S})$  is its associated unit eigenvector. Since the scatter matrix of the rotated sample  $\mathbf{O}\mathbf{X}_1, \dots, \mathbf{O}\mathbf{X}_n$  is  $\mathbf{O}\mathbf{S}\mathbf{O}^\top$ , the estimators for the rotated sample are  $(\mathbf{O}\hat{\boldsymbol{\mu}}_{\text{MM},2}, \hat{\rho}_{\text{MM},2})$ , showing their rotational equivariance. To avoid testing for the eigenpair with single multiplicity in  $\mathbf{S}$ , we assume the sign of  $\rho$  is fixed in advance.

**Theorem 4.2** (Moment estimators when  $k = 2$ ). *Let  $\mathbf{X}_1, \dots, \mathbf{X}_n \sim \text{C}_2(\boldsymbol{\mu}, \rho)$ , for  $(\boldsymbol{\mu}, \rho) \in \Theta_{2,d}^\circ$  and  $d \geq 1$ . Let*

$$\hat{\boldsymbol{\mu}}_{\text{MM},2} = \mathbf{u}_\pm(\mathbf{S}) \quad \text{and} \quad \hat{\rho}_{\text{MM},2} = \frac{d+3}{2} ((d+1)\lambda_\pm(\mathbf{S}) - 1),$$

*with  $(\hat{\boldsymbol{\mu}}_{\text{MM},2}, \hat{\rho}_{\text{MM},2}) \in \Theta_{2,d}^\circ$ , where the sign in  $\mathbf{u}_\pm(\mathbf{S})$  and  $\lambda_\pm(\mathbf{S})$  is chosen according to the sign of  $\rho$ . Then:*

(i). The estimators are strongly consistent:  $(\hat{\boldsymbol{\mu}}_{\text{MM},2}, \hat{\rho}_{\text{MM},2}) \rightarrow (\boldsymbol{\mu}, \rho)$  a.s. as  $n \rightarrow \infty$ .

(ii). The estimators are asymptotically normal:

$$\sqrt{n} \begin{pmatrix} \hat{\boldsymbol{\mu}}_{\text{MM},2} - \boldsymbol{\mu} \\ \hat{\rho}_{\text{MM},2} - \rho \end{pmatrix} \rightsquigarrow \mathcal{N}_{d+2} \left( \mathbf{0}, \begin{pmatrix} \sigma_{\text{MM},2}^2(\boldsymbol{\mu})(\mathbf{I}_{d+1} - \boldsymbol{\mu}\boldsymbol{\mu}^\top) & \mathbf{0}^\top \\ \mathbf{0} & \sigma_{\text{MM},2}^2(\rho) \end{pmatrix} \right)$$

as  $n \rightarrow \infty$ , where

$$\begin{aligned} \sigma_{\text{MM},2}^2(\boldsymbol{\mu}) &= \frac{d(d+3)[d(d+5) + 2(d-1)\rho]}{4\rho^2(d+1)(d+5)}, \\ \sigma_{\text{MM},2}^2(\rho) &= \frac{d(d+3)}{2} + \frac{2(d-1)(d+3)}{d+5}\rho - \rho^2. \end{aligned}$$

For  $d = 1$ ,  $\sigma_{\text{MM},2}^2(\boldsymbol{\mu}) = \sigma_{\text{MM},1}^2(\boldsymbol{\mu})$  and  $\sigma_{\text{MM},2}^2(\rho) = \sigma_{\text{MM},1}^2(\rho)$ .

When  $\boldsymbol{\mu}$  is known, a natural estimator for  $\rho$  is obtained by equating the theoretical and sample Gegenbauer moments. The estimator has the advantage of being straightforward for any integer  $k \geq 1$  and handling the cases of  $\rho$  positive or negative in a seamless way. Its asymptotic variance for  $k = 1, 2$  coincides with that of the method of moments estimators in Theorems 4.1–4.2, but this estimator is unbiased.

**Theorem 4.3** (Estimation of  $\rho$  via Gegenbauer moments). *Let  $\mathbf{X}_1, \dots, \mathbf{X}_n \sim \text{C}_k(\boldsymbol{\mu}, \rho)$  for  $\boldsymbol{\mu} \in \mathbb{S}^d$  (known),  $\rho \in [-1, 1]$ , and  $d \geq 1$ . Define the estimator*

$$\hat{\rho}_{\text{GM}} := \frac{\tau_{k,d}}{n} \sum_{i=1}^n C_k^{(d-1)/2}(\boldsymbol{\mu}^\top \mathbf{X}_i).$$

Then:

- (i). The estimator is unbiased.
- (ii). The estimator is strongly consistent:  $\hat{\rho}_{\text{GM}} \rightarrow \rho$  a.s. as  $n \rightarrow \infty$ .
- (iii). The estimator is asymptotically normal:

$$\sqrt{n}(\hat{\rho}_{\text{GM}} - \rho) \rightsquigarrow \mathcal{N}(0, \sigma_{\text{GM},k}^2(\rho))$$

as  $n \rightarrow \infty$ , where

$$\sigma_{\text{GM},k}^2(\rho) = d_{k,d} + \rho \eta_{k,d} \mathbf{1}_{\{k \text{ even}\}} - \rho^2,$$

with

$$\eta_{k,d} = \frac{(2k+d-1)^2}{(3k+d-1)(d-1)} \frac{k!}{((k/2)!)^3} \frac{\Gamma((d+k-1)/2)^3 \Gamma(d+3k/2-1)}{\Gamma(d+k-1) \Gamma((d-1)/2)^2 \Gamma((d+3k-1)/2)}$$

for  $d \geq 2$  and  $\eta_{k,1} = 0$  for  $d = 1$ . For  $k = 1, 2$ ,  $\sigma_{\text{GM},k}^2(\rho) = \sigma_{\text{MM},k}^2(\rho)$ .

Note that the moment estimators  $\hat{\rho}_{\text{MM},k}$ ,  $k = 1, 2$ , and  $\hat{\rho}_{\text{GM}}$  may fall outside  $[-1, 1]$  or  $[0, 1]$  for finite sample sizes. Hence, in practice they should be truncated to ensure valid parameter estimates.

## 4.2 Maximum likelihood

It is operationally convenient to reparametrize the model in terms of a less constrained parameter  $\boldsymbol{\xi} := \rho \boldsymbol{\mu} \in \{\mathbf{x} \in \mathbb{R}^{d+1} : \|\mathbf{x}\| \leq 1\}$ , for  $\rho > 0$ . With this parametrization, (9) becomes

$$f_{\text{C}_k}(\mathbf{x}; \boldsymbol{\xi}) := \frac{1}{\omega_d} \left\{ 1 + \|\boldsymbol{\xi}\| \tilde{C}_k^{(d-1)/2}(\mathbf{x}^\top \boldsymbol{\xi} / \|\boldsymbol{\xi}\|) \right\} \quad (14)$$

for  $\boldsymbol{\xi} \neq \mathbf{0}$ , with the convention that  $f_{C_k}(\mathbf{x}; \mathbf{0}) = 1/\omega_d$ . For  $\rho < 0$  and even  $k$ , an analogous reparametrization follows with  $f_{C_k}(\mathbf{x}; -\boldsymbol{\xi})$ .

The Maximum Likelihood (ML) estimator of  $\boldsymbol{\xi}$  is

$$\hat{\boldsymbol{\xi}}_{\text{ML}} := \arg \max_{\|\boldsymbol{\xi}\| \leq 1} \ell_n(\boldsymbol{\xi}), \quad \ell_n(\boldsymbol{\xi}) := \sum_{i=1}^n \log f_{C_k}(\mathbf{X}_i; \boldsymbol{\xi}),$$

with  $\ell_n(\boldsymbol{\xi})$  denoting the log-likelihood in terms of  $\boldsymbol{\xi}$ . It readily follows that  $\hat{\boldsymbol{\mu}}_{\text{ML}} = \hat{\boldsymbol{\xi}}_{\text{ML}} / \|\hat{\boldsymbol{\xi}}_{\text{ML}}\|$  and  $\hat{\rho}_{\text{ML}} = \|\hat{\boldsymbol{\xi}}_{\text{ML}}\|$ . Maximization of  $\boldsymbol{\xi} \mapsto \ell_n(\boldsymbol{\xi})$  can be done by inspecting its local maxima, related with the roots  $\hat{\boldsymbol{\xi}}_n$  of the score equations:

$$\frac{\partial}{\partial \boldsymbol{\xi}} \ell_n(\hat{\boldsymbol{\xi}}_n) = \mathbf{0}.$$

Both  $\hat{\boldsymbol{\xi}}_{\text{ML}}$  and the roots  $\hat{\boldsymbol{\xi}}_n$  are rotationally equivariant, as implied by the rotational equivariance of the density function:  $f_{C_k}(\mathbf{O}\mathbf{x}; \mathbf{O}\boldsymbol{\xi}) = f_{C_k}(\mathbf{x}; \boldsymbol{\xi})$  for any orthogonal matrix  $\mathbf{O}$ . Hence, the corresponding estimators computed from the rotated sample  $\mathbf{O}\mathbf{X}_1, \dots, \mathbf{O}\mathbf{X}_n$  are  $\mathbf{O}\hat{\boldsymbol{\xi}}_{\text{ML}}$  and  $\mathbf{O}\hat{\boldsymbol{\xi}}_n$ .

The following result establishes the existence of a consistent sequence of roots  $\hat{\boldsymbol{\xi}}_n$  that are local maxima of  $\boldsymbol{\xi} \mapsto \ell_n(\boldsymbol{\xi})$  and the asymptotic normality of that sequence. The result is stated in terms of  $(\boldsymbol{\mu}, \rho)$  rather than  $\boldsymbol{\xi}$  to ease interpretation.

**Theorem 4.4** (Maximum likelihood estimation). *Let  $\mathbf{X}_1, \dots, \mathbf{X}_n \sim C_k(\boldsymbol{\mu}, \rho)$  for*

$$(\boldsymbol{\mu}, \rho) \in \Theta_{k,d}^* := \begin{cases} \{(\cos(\theta), \sin(\theta))^\top : \theta \in (0, 2\pi/k)\} \times (0, \rho_\star), & d = 1, k \geq 1, \\ \mathbb{S}^d \times (0, \rho_\star), & d \geq 2, k \text{ odd}, \\ \mathbb{S}_+^d \times (0, \rho_\star), & d \geq 2, k \text{ even}, \end{cases} \quad (15)$$

with  $0 < \rho_\star < 1$ . Then:

(i). *The probability that  $(\boldsymbol{\mu}, \rho) \mapsto \ell_n(\boldsymbol{\mu}, \rho)$  has at least one local maximum tends to one as  $n \rightarrow \infty$ .*

(ii). *There exists a sequence of local maxima  $(\hat{\boldsymbol{\mu}}_n, \hat{\rho}_n)$  such that  $(\hat{\boldsymbol{\mu}}_n, \hat{\rho}_n) \rightarrow (\boldsymbol{\mu}, \rho)$  in probability as  $n \rightarrow \infty$ .*

(iii). *The sequence  $(\hat{\boldsymbol{\mu}}_n, \hat{\rho}_n)$  is asymptotically normal:*

$$\sqrt{n} \begin{pmatrix} \hat{\boldsymbol{\mu}}_n - \boldsymbol{\mu} \\ \hat{\rho}_n - \rho \end{pmatrix} \rightsquigarrow \mathcal{N}_{d+2} \left( \mathbf{0}, \begin{pmatrix} \sigma_{\text{ML}}^2(\boldsymbol{\mu})(\mathbf{I}_{d+1} - \boldsymbol{\mu}\boldsymbol{\mu}^\top) & \mathbf{0}^\top \\ \mathbf{0} & \sigma_{\text{ML}}^2(\rho) \end{pmatrix} \right)$$

as  $n \rightarrow \infty$ , where, for  $d = 1$ ,

$$\sigma_{\text{ML}}^2(\rho) = \frac{\rho^2 \sqrt{1 - \rho^2}}{1 - \sqrt{1 - \rho^2}}, \quad \sigma_{\text{ML}}^2(\boldsymbol{\mu}) = \frac{1}{k^2(1 - \sqrt{1 - \rho^2})}$$

and, for  $d \geq 2$ ,

$$\begin{aligned} [\sigma_{\text{ML}}^2(\rho)]^{-1} &= \frac{\omega_{d-1}}{\omega_d C_k^{(d-1)/2}(1)} \int_{-1}^1 \frac{C_k^{(d-1)/2}(t)^2 (1-t^2)^{d/2-1}}{C_k^{(d-1)/2}(1) + \rho C_k^{(d-1)/2}(t)} dt, \\ [\sigma_{\text{ML}}^2(\boldsymbol{\mu})]^{-1} &= \rho^2 \frac{\omega_{d-1}}{\omega_d C_k^{(d-1)/2}(1)} \frac{(d-1)^2}{d} \int_{-1}^1 \frac{C_{k-1}^{(d+1)/2}(t)^2 (1-t^2)^{d/2}}{C_k^{(d-1)/2}(1) + \rho C_k^{(d-1)/2}(t)} dt. \end{aligned}$$

When  $d = 2$  and  $k = 1$ ,

$$\sigma_{\text{ML}}^2(\rho) = \frac{\rho^3}{\tanh^{-1}(\rho) - \rho}, \quad \sigma_{\text{ML}}^2(\boldsymbol{\mu}) = \frac{2\rho}{\rho - (1 - \rho^2) \tanh^{-1}(\rho)}.$$

Specializing to  $d = 1$  and  $k = 1$ , Theorem 4.4(ii) gives the statements in Pewsey (2026, p. 5) after adjusting for the different parameterization of  $\rho$ .

### 4.3 Asymptotic relative efficiency

We conclude this section by inspecting the Asymptotic Relative Efficiencies (AREs) of the moment estimators with respect to the maximum likelihood estimators. These AREs are defined as

$$\text{ARE}_{\text{MM}}(\rho) := \frac{\sigma_{\text{ML}}^2(\rho)}{\sigma_{\text{MM}}^2(\rho)}, \quad \text{ARE}_{\text{MM}}(\boldsymbol{\mu}) := \frac{\sigma_{\text{ML}}^2(\boldsymbol{\mu})}{\sigma_{\text{MM}}^2(\boldsymbol{\mu})}, \quad \text{ARE}_{\text{GM}}(\rho) := \frac{\sigma_{\text{ML}}^2(\rho)}{\sigma_{\text{GM},k}^2(\rho)}.$$

Figure 3 shows the ARE curves  $\rho \mapsto \text{ARE}_{\text{MM}}(\boldsymbol{\mu})$  and  $\rho \mapsto \text{ARE}_{\text{MM}}(\rho)$  for  $\rho \in (0, 1)$ ,  $k = 1, 2$ , and  $d = 1, \dots, 10$ . As expected, the AREs are smaller than one. The efficiency of both moment estimators is maximal for  $\rho = 0$  and decreases as  $\rho$  increases, but differently for  $\hat{\boldsymbol{\mu}}_{\text{MM}}$  and  $\hat{\rho}_{\text{MM}}$ . Indeed,  $\text{ARE}_{\text{MM}}(\boldsymbol{\mu})$  is almost always above 0.8, while  $\text{ARE}_{\text{MM}}(\rho)$  can attain minima below 0.25 for  $\rho \approx 1$ . The AREs are larger for  $k = 2$  than for  $k = 1$  when  $d > 1$ , except for  $d = 1$  where  $\rho \mapsto \text{ARE}_{\text{MM}}(\boldsymbol{\mu})$  and  $\rho \mapsto \text{ARE}_{\text{MM}}(\rho)$  coincide for  $k = 1, 2$ . Recall that in the displayed case  $\rho > 0$  (assumption of Theorem 4.4),  $(\hat{\boldsymbol{\mu}}_{\text{MM},2}, \hat{\rho}_{\text{MM},2})$  are based on the largest eigenpair of  $\mathbf{S}$ , i.e., its the most stable version of the estimator. The efficiency of moment estimators increases with the dimension  $d$ .

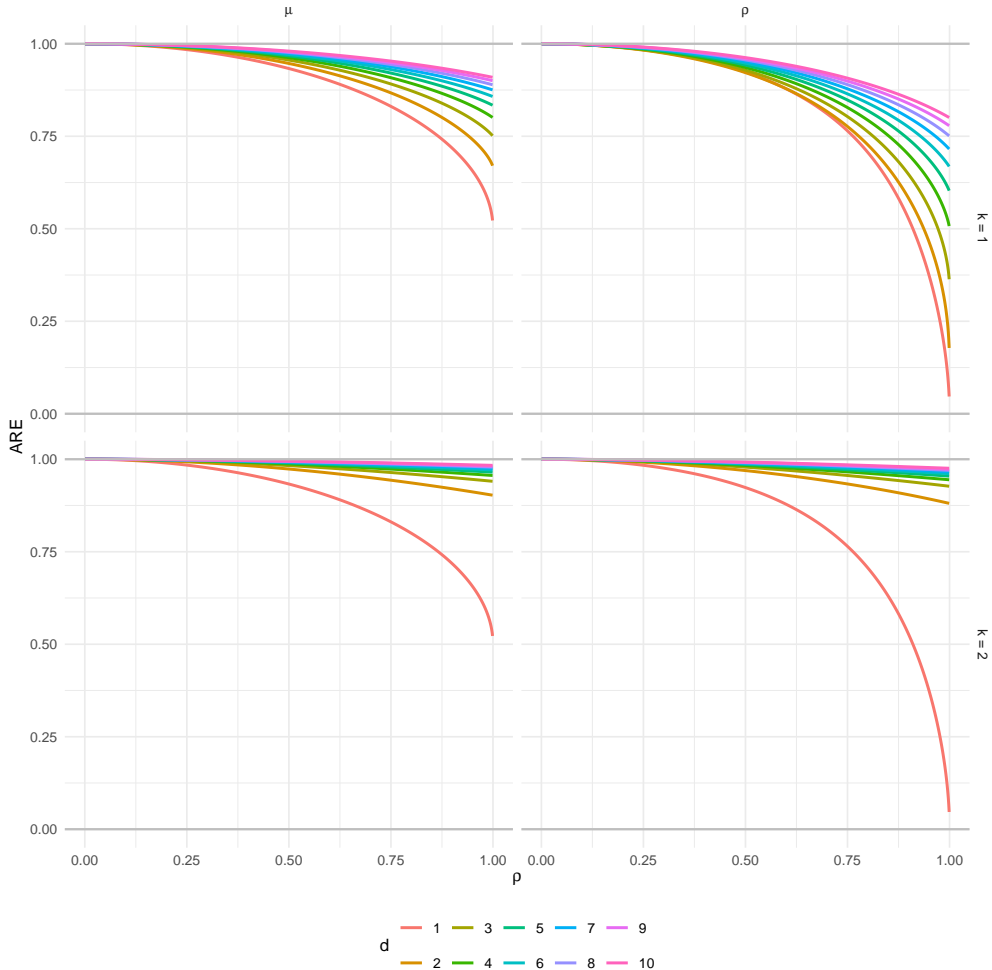


Figure 3: Asymptotic relative efficiencies  $\rho \mapsto \text{ARE}_{\text{MM}}(\boldsymbol{\mu})$  and  $\rho \mapsto \text{ARE}_{\text{MM}}(\rho)$  for  $k = 1, 2$  and  $d = 1, \dots, 10$ .

Figure 4 shows the ARE curves  $\rho \mapsto \text{ARE}_{\text{GM}}(\rho)$  for several choices of  $d$  and  $k$ . For  $k = 1, 2$ , the ARE curves coincide with those of  $\text{ARE}_{\text{MM}}(\rho)$  shown in Figure 3. For  $k = 3$  fixed, the efficiency pattern is similar to that of  $\text{ARE}_{\text{MM}}(\rho)$ : maximum ARE at  $\rho = 0$ , decay as  $\rho$  increases, and increase

as  $d$  grows. Despite knowing  $\mu$ , efficiency of  $\hat{\rho}_{GM}$  is still smaller than that of  $\hat{\rho}_{ML}$ . With  $d = 2$  fixed it is seen that the AREs increase with  $k$ , in an uneven fashion depending of the parity of  $k$ : even  $k$  yield larger AREs, presumably because the estimation of  $\mu$  becomes harder because of axial patterns, to which  $\hat{\rho}_{GM}$  is unaffected.

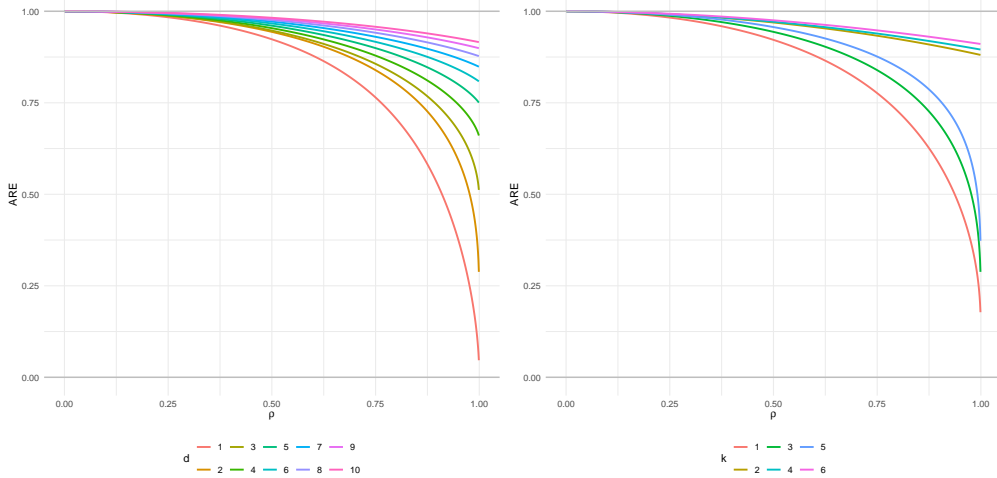


Figure 4: Asymptotic relative efficiencies  $\rho \mapsto \text{ARE}_{GM}(\rho)$  for  $k = 3$  and  $d = 1, \dots, 10$  (left panel) and  $k = 1, \dots, 6$  and  $d = 2$  (right panel).

## 5 Goodness-of-fit

We turn now our attention to the goodness-of-fit testing for the  $C_k(\mu, \rho)$  distribution. Given an iid sample  $\mathbf{X}_1, \dots, \mathbf{X}_n \sim P$ , we aim at testing the spherical cardioidness of  $P$  through the null hypothesis

$$H_0: P \in \left\{ C_k(\mu, \rho) : (\mu, \rho) \in \mathbb{S}^d \times [-1, 1] \right\},$$

for a fixed  $k \geq 1$ . We build on the integrated projected-ecdf approach employed in García-Portugués et al. (2023) by using a test statistic that integrates, across projecting directions, the quadratic discrepancies between the null cumulative distribution function (cdf) of the projected data and the empirical cdf (ecdf) of these projections.

Let  $F_\gamma$  the cdf of the spherical cardioid distribution projected along direction  $\gamma \in \mathbb{S}^d$ . That is, if  $\mathbf{X} \sim C_k(\mu, \rho)$ , then  $T = \gamma^\top \mathbf{X} \sim F_\gamma$ . Let  $F_{n, \gamma}(x) = (1/n) \sum_{i=1}^n 1_{\{\gamma^\top \mathbf{X}_i \leq x\}}$  denote the ecdf of the projected data  $\{\gamma^\top \mathbf{X}_i\}_{i=1}^n$ . We consider the test statistic

$$P_n^{W, \lambda} := n \int_{\mathbb{S}^d} \int_{-1}^1 (F_{n, \gamma}(x) - F_\gamma(x))^2 dW(F_\gamma(x)) \lambda(d\gamma), \quad (16)$$

where  $\lambda$  is a distribution on  $\mathbb{S}^d$  and  $W$  a measure on  $[0, 1]$ . Large values of  $P_n^{W, \lambda}$  provide evidence against  $H_0$ . To obtain a simpler form of (16) we need explicit expressions for  $F_\gamma$ , which we investigate next.

### 5.1 Projected distributions

We focus first on the uniform case  $\mathbf{X} \sim \text{Unif}(\mathbb{S}^d)$ . The distribution of  $\gamma^\top \mathbf{X}$  is independent of  $\gamma$ . Its density and cdf are, respectively,

$$f_d(x) := \frac{\omega_{d-1}}{\omega_d} (1 - x^2)^{d/2-1} \quad (17)$$

and

$$F_d(x) := \frac{\omega_{d-1}}{\omega_d} \int_{-1}^x (1-t^2)^{d/2-1} dt = \frac{1}{2} \{1 + \text{sign}(x) \text{I}_{x^2}(1/2, d/2)\}, \quad (18)$$

where  $x \in [-1, 1]$  and  $\text{I}_x(a, b) := \text{B}(a, b)^{-1} \int_0^x t^{a-1} (1-t)^{b-1} dt$ ,  $a, b > 0$ , is the regularized incomplete beta function. For  $x \in [-1, 1]$ ,  $F_1(x) = 1 - \cos^{-1}(x)/\pi$  and  $F_2(x) = (x+1)/2$ . For  $d \geq 3$  we have that

$$F_d(x) = F_{d-2}(x) + \frac{x(1-x^2)^{d/2-1}}{(d-2)\text{B}(1/2, (d-2)/2)},$$

reducing the evaluation of  $F_d(x)$  to polynomials on  $x$  and  $\{\text{B}(1/2, (d-2k)/2)\}_{k=0}^{\lfloor d/2 \rfloor}$ .

The following result gives a closed-form expression of the density and cdf of  $\boldsymbol{\gamma}^\top \mathbf{X}$  when  $\mathbf{X} \sim \text{C}_k(\boldsymbol{\mu}, \rho)$ , evidencing their perturbation from the projected uniform cdf.

**Theorem 5.1** (Projected distribution of  $\text{C}_k(\boldsymbol{\mu}, \rho)$ ). *Let  $\mathbf{X} \sim \text{C}_k(\boldsymbol{\mu}, \rho)$  for  $(\boldsymbol{\mu}, \rho) \in \mathbb{S}^d \times [-1, 1]$ ,  $k \geq 1$ , and  $d \geq 1$ . Let  $\boldsymbol{\gamma} \in \mathbb{S}^d$ . Then, the density and cdf of  $\boldsymbol{\gamma}^\top \mathbf{X}$  are, respectively,*

$$f_{\boldsymbol{\gamma}}(x) = f_d(x) \left\{ 1 + \rho \tilde{C}_k^{(d-1)/2}(\boldsymbol{\gamma}^\top \boldsymbol{\mu}) \tilde{C}_k^{(d-1)/2}(x) \right\}, \quad (19)$$

and

$$F_{\boldsymbol{\gamma}}(x) = F_d(x) - \rho \eta_k(\boldsymbol{\gamma}^\top \boldsymbol{\mu}) G_k(x), \quad (20)$$

where  $x \in [-1, 1]$ ,

$$\eta_k(\boldsymbol{\gamma}^\top \boldsymbol{\mu}) := \frac{\omega_{d-1}}{\omega_d} \frac{C_k^{(d-1)/2}(\boldsymbol{\gamma}^\top \boldsymbol{\mu})}{[C_k^{(d-1)/2}(1)]^2},$$

and

$$G_k(x) := \begin{cases} \frac{1}{k} \sin(k \cos^{-1}(x)), & d = 1, \\ \frac{d-1}{k(k+d-1)} C_{k-1}^{(d+1)/2}(x) (1-x^2)^{d/2}, & d \geq 2. \end{cases}$$

When  $\boldsymbol{\gamma} = \boldsymbol{\mu}$ , the density simplifies to  $f_{\boldsymbol{\mu}}(x) = f_d(x) \{1 + \rho \tilde{C}_k^{(d-1)/2}(x)\}$  and (20) can be used for simulation in Section 3.5.

## 5.2 Test statistic

We discuss two main choices for the distribution  $\lambda$  in (16). First, let us consider  $\boldsymbol{\gamma} \sim \text{Unif}(\mathbb{S}^d)$ , that is,  $\lambda = \sigma_d/\omega_d$ . This is the choice in García-Portugués et al. (2023) for testing  $H_0: \mathbf{P} = \text{Unif}(\mathbb{S}^d)$  and naturally aggregates deviations from the null hypothesis for all possible directions. It is also a conservative choice, as it does not favor any particular direction to detect departures from the null hypothesis. The test statistic becomes

$$P_n^{W, \text{Unif}} := \frac{n}{\omega_d} \int_{\mathbb{S}^d} \int_{-1}^1 (F_{n, \boldsymbol{\gamma}}(x) - F_{\boldsymbol{\gamma}}(x))^2 dW(F_{\boldsymbol{\gamma}}(x)) \sigma_d(d\boldsymbol{\gamma}). \quad (21)$$

Alternatively, let us consider  $\boldsymbol{\gamma}$  distributed as the empirical distribution  $\mathbf{P}_n$  of the sample  $\mathbf{X}_1, \dots, \mathbf{X}_n$ :

$$P_n^{W, \mathbf{P}_n} := n \int_{\mathbb{S}^d} \int_{-1}^1 (F_{n, \boldsymbol{\gamma}}(x) - F_{\boldsymbol{\gamma}}(x))^2 dW(F_{\boldsymbol{\gamma}}(x)) \mathbf{P}_n(d\boldsymbol{\gamma})$$

$$= \frac{1}{n} \sum_{i=1}^n n \int_{-1}^1 (F_{n,\mathbf{X}_i}(x) - F_{\mathbf{X}_i}(x))^2 dW(F_{\mathbf{X}_i}(x)). \quad (22)$$

This choice weights the directions to detect departures from the null hypothesis according to  $P$ . Its main advantage is the simpler expression of the test statistic. The version of (22) with  $P_n^{W,P}$  is equivalent to (21) for testing uniformity, but not for necessarily testing spherical cardioidness.

A third alternative is to consider  $\lambda$  as  $C_k(\boldsymbol{\mu}, \rho)$ , i.e., weighting projecting directions according to the null distribution. This statistic,  $P_n^{W,C_k}$ , is aligned with the  $dW(F_{\boldsymbol{\gamma}}(x))$  weight but gives a test statistic at least as complex as (21).

Since the parameters  $(\boldsymbol{\mu}, \rho)$  are unknown, in practice  $F_{\boldsymbol{\gamma}}$  must be replaced with  $\hat{F}_{\boldsymbol{\gamma}}$  in (16), the projected cdf featuring the estimates  $(\hat{\boldsymbol{\mu}}, \hat{\rho})$  obtained under  $H_0$ . If  $(\hat{\boldsymbol{\mu}}, \hat{\rho})$  are rotation-equivariant estimators, as those in Section 4, then both statistics (21) and (22) are *rotationally invariant*. To see this, consider an orthogonal matrix  $\mathbf{O}$  and the rotated sample  $\tilde{\mathbf{X}}_i = \mathbf{O}\mathbf{X}_i$ ,  $i = 1, \dots, n$ . We denote with tilde the objects computed from the rotated sample, and set  $\tilde{\boldsymbol{\gamma}} := \mathbf{O}^\top \boldsymbol{\gamma}$ . Then

$$\tilde{F}_{n,\boldsymbol{\gamma}}(x) = \frac{1}{n} \sum_{i=1}^n 1_{\{\boldsymbol{\gamma}^\top \tilde{\mathbf{X}}_i \leq x\}} = \frac{1}{n} \sum_{i=1}^n 1_{\{(\mathbf{O}^\top \boldsymbol{\gamma})^\top \mathbf{X}_i \leq x\}} = F_{n,\tilde{\boldsymbol{\gamma}}}(x)$$

and, because of Theorem 5.1,

$$\tilde{F}_{\boldsymbol{\gamma}}(x) = F_d(x) - \hat{\rho} \eta_k(\boldsymbol{\gamma}^\top \tilde{\boldsymbol{\mu}}) G_k(x) = F_d(x) - \hat{\rho} \eta_k((\mathbf{O}^\top \boldsymbol{\gamma})^\top \hat{\boldsymbol{\mu}}) G_k(x) = \hat{F}_{\boldsymbol{\gamma}}(x). \quad (23)$$

Therefore,

$$\begin{aligned} \tilde{P}_n^{W,\lambda} &= n \int_{\mathbb{S}^d} \int_{-1}^1 (\tilde{F}_{n,\boldsymbol{\gamma}}(x) - \hat{F}_{\boldsymbol{\gamma}}(x))^2 dW(\hat{F}_{\boldsymbol{\gamma}}(x)) \lambda(d\boldsymbol{\gamma}) \\ &= n \int_{\mathbb{S}^d} \int_{-1}^1 (F_{n,\mathbf{O}^\top \boldsymbol{\gamma}}(x) - \hat{F}_{\mathbf{O}^\top \boldsymbol{\gamma}}(x))^2 dW(\hat{F}_{\mathbf{O}^\top \boldsymbol{\gamma}}(x)) \lambda(d\boldsymbol{\gamma}), \end{aligned}$$

implying that  $\tilde{P}_n^{W,\text{Unif}} = P_n^{W,\text{Unif}}$ . This argument actually shows that the uniform distribution is the only distribution  $\lambda$  independent from the sample that makes  $P_n^{W,\lambda}$  rotation-invariant. Similarly to (23),  $\tilde{F}_{n,\tilde{\mathbf{X}}_i}(x) = F_{n,\mathbf{X}_i}(x)$  and  $\hat{F}_{\tilde{\mathbf{X}}_i}(x) = \hat{F}_{\mathbf{X}_i}(x)$ , so

$$\tilde{P}_n^{W,P_n} = \frac{1}{n} \sum_{i=1}^n n \int_{-1}^1 (\tilde{F}_{n,\tilde{\mathbf{X}}_i}(x) - \hat{F}_{\tilde{\mathbf{X}}_i}(x))^2 dW(\hat{F}_{\tilde{\mathbf{X}}_i}(x)) = P_n^{W,P_n}.$$

The test statistic with  $\lambda$  as  $C_k(\hat{\boldsymbol{\mu}}, \hat{\rho})$  is also rotationally-invariant.

The evaluation of  $P_n^{W,\lambda}$  can leverage the well-known closed-form expressions for the Cramér–von Mises (CvM) and Anderson–Darling (AD) statistics. Specifically, the weights  $dW^{\text{CvM}}(u) = du$  and  $dW^{\text{AD}}(u) = [u(1-u)]^{-1} du$ ,  $u \in [0, 1]$ , yield the CvM and AD statistics, respectively:

$$\begin{aligned} W_{n,\boldsymbol{\gamma}}^2 &= n \int_{-1}^1 (F_{n,\boldsymbol{\gamma}}(x) - \hat{F}_{\boldsymbol{\gamma}}(x))^2 d\hat{F}_{\boldsymbol{\gamma}}(x) = \sum_{i=1}^n \left\{ U_{(i)}^{(\boldsymbol{\gamma})} - \frac{2i-1}{2n} \right\}^2 + \frac{1}{12n}, \\ A_{n,\boldsymbol{\gamma}}^2 &= n \int_{-1}^1 \frac{(F_{n,\boldsymbol{\gamma}}(x) - \hat{F}_{\boldsymbol{\gamma}}(x))^2}{\hat{F}_{\boldsymbol{\gamma}}(x)(1 - \hat{F}_{\boldsymbol{\gamma}}(x))} d\hat{F}_{\boldsymbol{\gamma}}(x) \\ &= -n - \frac{1}{n} \sum_{i=1}^n \left\{ (2i-1) \log(U_{(i)}^{(\boldsymbol{\gamma})}) + (2(n-i)+1) \log(1 - U_{(i)}^{(\boldsymbol{\gamma})}) \right\}, \end{aligned} \quad (24)$$

where  $\{U_{(i)}^{(\boldsymbol{\gamma})}\}_{i=1}^n$  are the ( $\boldsymbol{\gamma}$ -dependent) ordered values of  $U_i^{(\boldsymbol{\gamma})} = \hat{F}_{\boldsymbol{\gamma}}(\boldsymbol{\gamma}^\top \mathbf{X}_i)$ ,  $i = 1, \dots, n$ . These expressions can be combined with a Monte Carlo approximation of the integral over  $\mathbb{S}^d$  in (21): given

a Monte Carlo sample  $\gamma_1, \dots, \gamma_K \sim \lambda$ , then

$$\hat{P}_n^{\text{CvM}, \lambda} = \frac{1}{K} \sum_{j=1}^K W_{n, \gamma_j}^2 \quad \text{and} \quad \hat{P}_n^{\text{AD}, \lambda} = \frac{1}{K} \sum_{j=1}^K A_{n, \gamma_j}^2 \quad (25)$$

efficiently approximate  $P_n^{\text{CvM}, \lambda}$  and  $P_n^{\text{AD}, \lambda}$ . If using  $P_n$  as  $\lambda$ , then (22) are exactly computable as

$$P_n^{\text{CvM}, P_n} = \frac{1}{n} \sum_{i=1}^n W_{n, \mathbf{X}_i}^2 \quad \text{and} \quad P_n^{\text{AD}, P_n} = \frac{1}{n} \sum_{i=1}^n A_{n, \mathbf{X}_i}^2. \quad (26)$$

For the  $P_n^{\text{AD}, P_n}$  statistic, care must be taken because  $U_i^{(\mathbf{X}_i)} = U_{(n)}^{(\mathbf{X}_i)} = 1$ , which causes  $A_{n, \mathbf{X}_i}^2 = \infty$ ,  $i = 1, \dots, n$ . A simple solution is omitting the addend  $i = n$  in (24).

The exact computational form for  $P_n^{W, \lambda}$  for a general weight  $W$  and distribution  $\lambda$  is more involved. The next result provides a  $V$ -statistic expression for  $P_n^{W, \lambda}$  for a finite measure  $W$  and distribution  $\lambda$ . The follow-up corollary covers the Anderson–Darling weight, which is not integrable. For simplicity, we use the notation  $F_\gamma$  instead of  $\hat{F}_\gamma$  henceforth.

**Theorem 5.2** ( $V$ -statistic form for  $P_n^{W, \lambda}$ ). *Let  $\lambda$  be a distribution on  $\mathbb{S}^d$  and  $W$  a finite measure on  $[0, 1]$ . Denote  $W(u) \equiv W([0, u])$ ,  $u \in [0, 1]$ ,  $W_1(u) := \int_0^u v \, dW(v)$ , and  $W_2(u) := \int_0^u v^2 \, dW(v)$ . Then,*

$$\begin{aligned} P_n^{W, \lambda} = & n(W(1) + W_2(1) - W_2(0) - 2W_1(1)) \\ & + 2 \sum_{i=1}^n \mathbb{E}_\gamma \left[ W_1(F_\gamma(\gamma^\top \mathbf{X}_i)) \right] - \frac{1}{n} \sum_{i,j=1}^n \mathbb{E}_\gamma \left[ W(F_\gamma(\max(\gamma^\top \mathbf{X}_i, \gamma^\top \mathbf{X}_j))) \right]. \end{aligned} \quad (27)$$

**Corollary 5.1** ( $V$ -statistic form for  $P_n^{\text{AD}, \lambda}$ ). *Let  $|\rho| < 1$ . Let  $\lambda$  be an absolutely continuous distribution on  $\mathbb{S}^d$  with bounded density. Then,*

$$\begin{aligned} P_n^{\text{AD}, \lambda} = & -n - 2 \sum_{i=1}^n \mathbb{E}_\gamma \left[ \log(1 - F_\gamma(\gamma^\top \mathbf{X}_i)) \right] \\ & - \frac{1}{n} \sum_{i,j=1}^n \mathbb{E}_\gamma \left[ \log \left( \frac{F_\gamma(\max(\gamma^\top \mathbf{X}_i, \gamma^\top \mathbf{X}_j))}{1 - F_\gamma(\max(\gamma^\top \mathbf{X}_i, \gamma^\top \mathbf{X}_j))} \right) \right]. \end{aligned}$$

The previous results are not computationally advantageous with respect to (16), as they require evaluating the expectations with respect to  $\gamma \sim \lambda$ , which are complicated because of their dependence on the distribution of  $(\gamma^\top \boldsymbol{\mu}, \gamma^\top \mathbf{X}_i, \gamma^\top \mathbf{X}_j)$ . We therefore focus on obtaining closed forms for specific cases of the statistic  $P_n^{\text{CvM}, \text{Unif}}$ .

**Theorem 5.3** (Computational form for  $P_n^{\text{CvM}, \text{Unif}}$ ). *For the CvM weight and  $\gamma \sim \text{Unif}(\mathbb{S}^d)$ , the test statistic in (27) is*

$$P_n^{\text{CvM}, \text{Unif}} = \frac{3 - 2n}{6} - \sum_{i=1}^n \varphi(\mathbf{X}_i) + \frac{2}{n} \sum_{i < j} \psi(\mathbf{X}_i, \mathbf{X}_j). \quad (28)$$

Denote  $\mu_i := \mathbf{X}_i^\top \boldsymbol{\mu}$  and  $t_{ij} := \mathbf{X}_i^\top \mathbf{X}_j$ . The kernels  $\varphi$  and  $\psi$  are as follows:

(i). If  $d = 1$  and  $k \geq 1$ ,

$$\begin{aligned} \varphi(\mathbf{X}_i) &= \frac{\rho}{2\pi^2 k^2} \left\{ T_k(\mu_i) - \frac{\rho}{4} (2 - T_{2k}(\mu_i)) \right\}, \\ \psi(\mathbf{X}_i, \mathbf{X}_j) &= \psi_1^{\text{CvM}}(\cos^{-1}(t_{ij})) \\ &\quad - \rho \left\{ \frac{\pi - \cos^{-1}(t_{ij})}{2\pi^2 k} T_k \left( \frac{\mu_i + \mu_j}{\sqrt{2(1 + t_{ij})}} \right) \sin \left( \frac{k \cos^{-1}(t_{ij})}{2} \right) \right\}. \end{aligned}$$

(ii). If  $d = 2$  and  $k = 1$ ,

$$\varphi(\mathbf{X}_i) = \frac{\rho}{30}\mu_i - \frac{\rho^2}{4}\left\{\frac{2}{35} - \frac{4\mu_i^2}{105}\right\},$$

$$\psi(\mathbf{X}_i, \mathbf{X}_j) = \psi_2^{\text{CvM}}(\cos^{-1}(t_{ij})) - \frac{\rho}{32}\sqrt{\frac{1-t_{ij}}{2}}(\mu_i + \mu_j).$$

(iii). If  $d = 2$  and  $k = 2$ ,

$$\varphi(\mathbf{X}_i) = \frac{\rho}{420}(3\mu_i^2 - 1) - \frac{\rho^2}{4}\left\{\frac{1}{330} + \frac{3\mu_i^2}{385} - \frac{\mu_i^4}{110}\right\},$$

$$\begin{aligned}\psi(\mathbf{X}_i, \mathbf{X}_j) = & \psi_2^{\text{CvM}}(\cos^{-1}(t_{ij})) \\ & - \frac{\rho}{128}\sqrt{\frac{1-t_{ij}}{2}}\left\{\frac{1+t_{ij}}{2} + \frac{3(3t_{ij}-1)}{4(1-t_{ij})}[\mu_i^2 + \mu_j^2] + \frac{3(t_{ij}-3)}{2(1-t_{ij})}\mu_i\mu_j\right\}.\end{aligned}$$

Above,

$$\psi_d^{\text{CvM}}(\theta) = \begin{cases} \frac{1}{2} + \frac{\theta}{2\pi}\left(\frac{\theta}{2\pi} - 1\right), & d = 1, \\ \frac{1}{2} - \frac{1}{4}\sin\left(\frac{\theta}{2}\right), & d = 2. \end{cases}$$

Evaluating exactly (28) has computational complexity order  $O(n^2)$ . The Monte Carlo approximations in (25) have order  $O(Kn \log n)$ , and (26) have order  $O(n^2 \log n)$ .

### 5.3 Bootstrapping

The projection-based test statistics  $P_n^{W,\lambda}$  can be readily used to assess the goodness-of-fit of  $\text{C}_k(\boldsymbol{\mu}, \rho)$  through parametric bootstrapping. The procedure is standard and builds on the contents of Secs. 3.5, 4, and 5.2. It is detailed in Algorithm 3.

---

**Algorithm 3:** Parametric bootstrap for testing the goodness-of-fit of  $\text{C}_k(\boldsymbol{\mu}, \rho)$

---

- i. Compute  $(\hat{\boldsymbol{\mu}}, \hat{\rho})$  from  $\mathbf{X}_1, \dots, \mathbf{X}_n$  using any of the estimators in Section 4.
- ii. Compute  $P_n^{W,\lambda}$  from  $\mathbf{X}_1, \dots, \mathbf{X}_n$  and  $(\hat{\boldsymbol{\mu}}, \hat{\rho})$ , either from the exact forms (28) and (26), or the Monte Carlo approximation in (25).
- iii. For  $b = 1, \dots, B$ :
  - (a) Simulate  $\mathbf{X}_1^{*b}, \dots, \mathbf{X}_n^{*b}$  from  $\text{C}_k(\hat{\boldsymbol{\mu}}, \hat{\rho})$  using Algorithm 1 or 2.
  - (b) Compute  $(\hat{\boldsymbol{\mu}}^{*b}, \hat{\rho}^{*b})$  from  $\mathbf{X}_1^{*b}, \dots, \mathbf{X}_n^{*b}$ .
  - (c) Compute  $P_n^{W,\lambda,*b}$  from  $\mathbf{X}_1^{*b}, \dots, \mathbf{X}_n^{*b}$  and  $(\hat{\boldsymbol{\mu}}^{*b}, \hat{\rho}^{*b})$  as in step ii.
- iv. Obtain the bootstrap  $p$ -value approximation

$$p\text{-value} \approx \frac{1 + \sum_{b=1}^B \mathbb{1}_{\{P_n^{W,\lambda,*b} > P_n^{W,\lambda}\}}}{B + 1}.$$


---

The algorithm can be easily adapted to test the simple null hypothesis  $H_0: \mathbf{P} = \text{C}_k(\boldsymbol{\mu}_0, \rho_0)$  for fixed  $(\boldsymbol{\mu}_0, \rho_0)$ . In this case, simply replace  $(\hat{\boldsymbol{\mu}}, \hat{\rho})$  and  $(\hat{\boldsymbol{\mu}}^{*b}, \hat{\rho}^{*b})$  with  $(\boldsymbol{\mu}_0, \rho_0)$ , and skip the estimation

steps. If  $\rho_0 = 0$ , then the simple null hypothesis corresponds to uniformity and  $P_n^{\text{CvM, Unif}} = P_n^{\text{CvM, } C_k}$  and  $P_n^{\text{AD, Unif}} = P_n^{\text{AD, } C_k}$  coincide with the projected CvM and AD statistics in García-Portugués et al. (2023).

Percentile bootstrap  $100(1 - \alpha)\%$ -confidence intervals for  $(\boldsymbol{\mu}, \rho)$  can be obtained as a direct by-product of running Algorithm 3. The percentile bootstrap confidence interval for  $\rho$  is  $(\hat{\rho}^{*(\lceil (B+1)\alpha/2 \rceil)}, \hat{\rho}^{*(\lfloor (B+1)(1-\alpha/2) \rfloor)})$ , while, for odd  $k$ , a percentile bootstrap confidence spherical cap for  $\boldsymbol{\mu}$  is  $\{\boldsymbol{\mu} \in \mathbb{S}^d : \boldsymbol{\mu}^\top \hat{\boldsymbol{\mu}} \geq t^{*(\lceil \alpha(B+1) \rceil)}\}$ , with  $t^{*b} := \hat{\boldsymbol{\mu}}^{*b\top} \hat{\boldsymbol{\mu}}$ ,  $b = 1, \dots, B$ . For even  $k$ , the confidence region is the union of two spherical caps:  $\{\boldsymbol{\mu} \in \mathbb{S}^d : |\boldsymbol{\mu}^\top \hat{\boldsymbol{\mu}}| \geq |t|^{*(\lceil \alpha(B+1) \rceil)}\}$ , with  $|t|^{*b} := |\hat{\boldsymbol{\mu}}^{*b\top} \hat{\boldsymbol{\mu}}|$ .

## 6 Numerical experiments

### 6.1 Asymptotic distributions of estimators

We validate empirically the asymptotic distributions of  $(\hat{\mu}_{\text{MM},k}, \hat{\rho}_{\text{MM},k})$ ,  $k = 1, 2$ ,  $\hat{\rho}_{\text{GM}}$ , and  $(\hat{\mu}_{\text{ML}}, \hat{\rho}_{\text{ML}})$  obtained in Section 4. We consider  $d = 2$  and the models  $C_1(\boldsymbol{\mu}, \rho)$  and  $C_2(\boldsymbol{\mu}, \rho)$  with  $\boldsymbol{\mu} = (0, 0, 1)^\top$  and  $\rho = 0.5$ . For each model, we simulate  $M = 10^4$  samples of size  $n = 1000$ , compute the estimators  $\{(\hat{\boldsymbol{\mu}}^{(j)}, \hat{\rho}^{(j)})\}_{j=1}^M$ , and construct their standardized versions  $\{\sqrt{n}(\hat{\mu}_1^{(j)} - \mu_1)\}_{j=1}^M$  (first entries of the estimators) and  $\{\sqrt{n}(\hat{\rho}^{(j)} - \rho)\}_{j=1}^M$ .

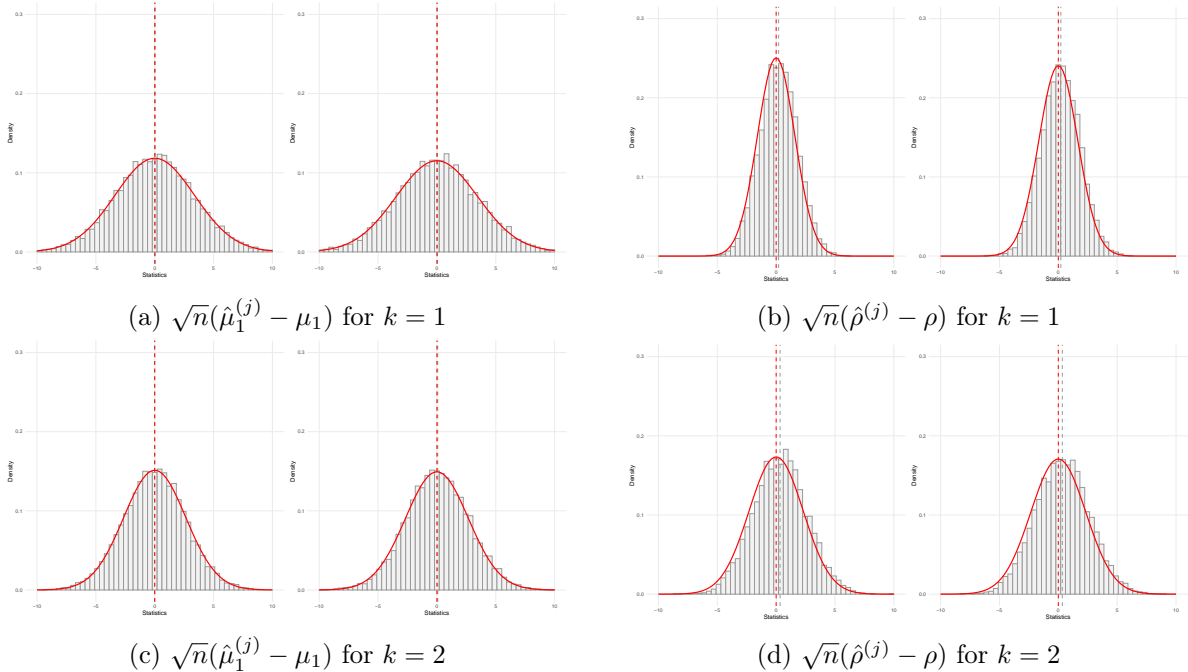


Figure 5: Histograms of  $\{\sqrt{n}(\hat{\mu}_1^{(j)} - \mu_1)\}_{j=1}^M$  and  $\{\sqrt{n}(\hat{\rho}^{(j)} - \rho)\}_{j=1}^M$  against their asymptotic normal density, for  $k = 1, 2$  and  $d = 2$ . Inside each panel, the left plot corresponds to the maximum likelihood estimator and the right plot corresponds to the method of moments estimator. The gray/red dashed lines indicate the empirical/asymptotic means.

Figure 5 shows the resulting histograms overlaid with a centered normal density with standard deviation equal to  $\sigma_{\text{MM},k}(\boldsymbol{\mu})$ ,  $\sigma_{\text{MM},k}(\rho)$ ,  $\sigma_{\text{ML}}(\boldsymbol{\mu})$ , or  $\sigma_{\text{ML}}(\rho)$ , depending on the considered estimator. The match between the empirical and asymptotic standard deviations of the estimators is tight, with relative errors smaller than 2% for  $\mu_1$  and  $\rho$ , for  $k = 1, 2$ . The bias for  $\mu_1$  has order  $10^{-2}$ , but for  $\rho$  the estimated bias  $\bar{\rho} - \rho$  is still significant: approximately 0.20 for  $k = 1$  and 0.33 for  $k = 2$  (see gray dashed lines).

## 6.2 Finite-sample behavior of goodness-of-fit test

Two numerical experiments are carried out to assess the finite-sample behavior of the goodness-of-fit test for  $H_0: P \in \{C_k(\boldsymbol{\mu}, \rho) : (\boldsymbol{\mu}, \rho) \in \mathbb{S}^d \times [-1, 1]\}$  using Algorithm 3. We consider the tests based on the test statistics  $P_n^{W, \lambda}$ , for  $W \in \{\text{CvM, AD}\}$  and  $\lambda \in \{\text{Unif, } P_n, C_k\}$ , computed using closed-form expressions or the Monte Carlo approximation (25) with  $K = 50$  random directions. Along the experiments, the parameters  $(\boldsymbol{\mu}, \rho)$  are estimated using the moment estimators  $(\hat{\boldsymbol{\mu}}_{\text{MM}, k}, \hat{\rho}_{\text{MM}, k})$  due to its computational efficiency. We consider  $M = 500$  Monte Carlo replications for each scenario and  $B = 100$  bootstrap samples.

The first experiment evaluates the nominal size of the test under the null hypothesis. For that, we use  $C_k(\boldsymbol{\mu}, \rho)$  as data generating process with  $k \in \{1, 2\}$ ,  $\rho \in \{0.25, 0.5, 0.75\}$ ,  $d \in \{1, 2\}$ , and  $n = 100$ . Table 1 shows the rejection percentages at nominal level  $\alpha = 5\%$ . The results indicate that the test approximately maintains the nominal size across the explored configurations, with a variable performance likely due to the relatively small sample size and number of bootstrap replicates. At the scenario  $(k = 1, d = 2, \rho = 0.75)$  all the test show a conservative behavior, but this can be explained by the fact that the Monte Carlo samples are shared within each row.

$k$	$d$	$\rho$	$P_n^{\text{CvM, Unif}}$	$P_n^{\text{AD, Unif}}$	$P_n^{\text{CvM, } P_n}$	$P_n^{\text{AD, } P_n}$	$P_n^{\text{CvM, } C_k}$	$P_n^{\text{AD, } C_k}$
1	1	0.25		6.2	6.2	6.0	5.2	5.8
		0.50		5.0	5.2	5.4	4.0	5.0
		0.75		3.2	4.0	3.2	3.0	2.8
2	2	0.25		6.4	6.6	6.4	4.8	5.4
		0.50		4.4	4.8	4.4	4.2	5.4
		0.75		<u>1.6</u>	<u>2.0</u>	<u>1.8</u>	<u>2.6</u>	<u>1.4</u>
2	1	0.25		6.2	<u>7.6</u>	4.8	5.2	5.0
		0.50		4.0	<u>3.8</u>	4.6	5.0	4.2
		0.75		4.6	<u>4.8</u>	5.2	5.0	5.2
2	2	0.25		3.2	6.0	6.4	6.0	6.6
		0.50		<u>1.6</u>	4.0	5.0	4.2	4.4
		0.75		4.0	5.4	5.4	5.2	5.4

Table 1: Rejection percentages of the goodness-of-fit test for the null hypothesis of spherical cardiodness of order  $k$  at the significance level  $\alpha = 5\%$ . The null hypothesis holds: the generating process is  $C_k(\boldsymbol{\mu}, \rho)$ . Underlined values indicate empirical sizes outside the equal-tail 95% prediction interval for  $\text{Bin}(M, \alpha) \times 100/M$ .

The second experiment assesses the power of the test under a spherical cardioid alternative  $C_k(\boldsymbol{\mu}, \rho)$  with order  $k$  different from the order  $k_0$  of the family considered under the null hypothesis,  $\{C_{k_0}(\boldsymbol{\mu}, \rho) : (\boldsymbol{\mu}, \rho) \in \mathbb{S}^d \times [-1, 1]\}$ . We take  $(k, k_0) \in \{(1, 2), (2, 1)\}$ ,  $\rho \in \{0.10, 0.25, 0.5\}$ ,  $d \in \{1, 2\}$ , and  $n = 100$ . Table 2 shows the rejection percentages at nominal level  $\alpha = 5\%$ . The results show that all tests are able to detect the alternative, and that their powers increase with  $\rho$  (with  $\rho = 0$  the null hypothesis is satisfied). The explored tests have similar powers across the different configurations, with no test clearly outperforming the others.

## 7 Spherical cardiodness of comet orbits

Long-period comets are hypothesized to originate in the Oort cloud, a conjectured roughly spherical reservoir of icy planetesimals surrounding the Solar System, whereas short-period comets are associated with the flattened Kuiper belt. These different origins are reflected in orbital orientations: long-period comets exhibit an approximately isotropic distribution, in sharp contrast with the ecliptic-concentrated orientations of short-period comets (see, e.g., Dones et al. (2015, Sections 5 and 7.2)

and references therein). Orbital orientations can be represented by the directed unit normal vectors to the orbital planes on  $\mathbb{S}^2$ . An orbit with *inclination*  $i \in [0, \pi]$  and *longitude of the ascending node*  $\Omega \in [0, 2\pi)$  (see Jupp et al., 2003) has directed normal vector  $(\sin(i) \sin(\Omega), -\sin(i) \cos(\Omega), \cos(i))^\top$  to the orbit's plane (see the illustrative graphs in Figure 6). The sign encodes prograde (northern hemisphere) versus retrograde (southern hemisphere) motion.

$k$	$d$	$\rho$	$P_n^{\text{CvM, Unif}}$	$P_n^{\text{AD, Unif}}$	$P_n^{\text{CvM, P}_n}$	$P_n^{\text{AD, P}_n}$	$P_n^{\text{CvM, C}_k}$	$P_n^{\text{AD, C}_k}$
1	1	0.1	6.4	7.0	6.4	6.2	6.6	6.2
		0.2	29.2	30.0	28.6	28.2	30.2	29.2
		0.5	84.2	82.4	83.6	82.0	84.2	84.2
2	0.1	0.1	7.0	6.6	7.2	7.2	6.8	6.8
		0.2	31.6	31.2	31.0	30.0	31.2	31.6
		0.5	86.6	85.4	86.2	84.2	86.6	85.2
2	1	0.1	9.0	8.2	9.6	8.8	9.2	8.6
		0.2	31.2	31.0	32.2	30.2	32.2	32.0
		0.5	91.4	91.8	92.4	91.4	91.8	91.2
2	0.1	0.1	3.2	5.0	5.4	5.0	4.8	5.6
		0.2	11.4	15.8	16.0	15.2	14.8	14.6
		0.5	59.0	66.6	67.2	63.4	65.4	67.4

Table 2: Rejection percentages of the goodness-of-fit test for the null hypothesis of spherical cardiodidness of order  $k_0 = (k+1) \bmod 1$  at the significance level  $\alpha = 5\%$ . The null hypothesis is false: the data generating process is  $C_k(\boldsymbol{\mu}, \rho)$ , with  $k \neq k_0$ .

The **comets** object in the **sphunif** R package (García-Portugués and Verdebout, 2025) contains a dataset of comet orbits sourced from the JPL Small-Body Database Search. We analyze two subsets of comets with elliptical orbits: a set of  $n = 610$  long-period comets (orbital period exceeding 200 years) and a set of  $n = 784$  short-period comets (orbital period below 200 years). Records corresponding to comet fragments are excluded to avoid spurious clustering. Further details on data retrieval and preprocessing are given in García-Portugués et al. (2025, Section 7).

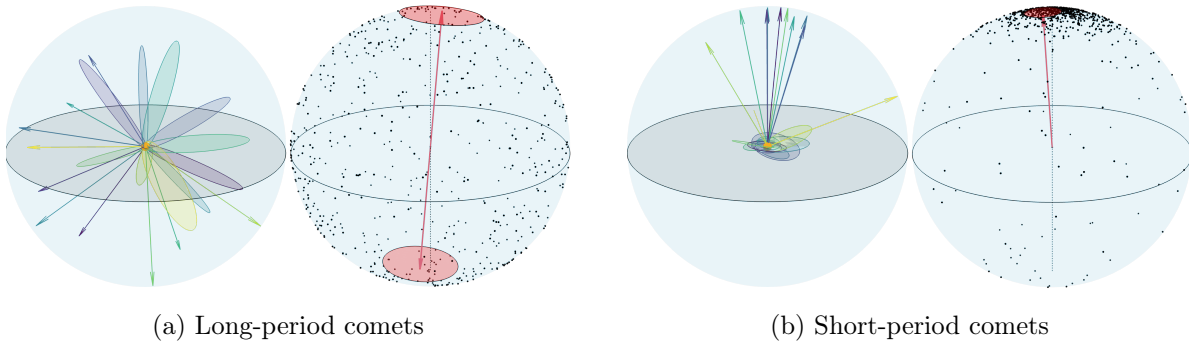


Figure 6: Orbits of long- and short-period comets and their normal vectors. Within each figure, the left plot displays ten illustrative elliptical orbits and their associated normal vectors, with the ecliptic plane shown in gray and the Sun represented as an orange sphere (one focus of the elliptical orbits). The right plot in each figure shows the full dataset of normal orbit vectors on  $\mathbb{S}^2$ . Red indicates the  $\hat{\boldsymbol{\mu}}_{\text{ML}}$  direction/axis and the bootstrap 95%-confidence spherical cap for  $\boldsymbol{\mu}$ . Figure adapted from García-Portugués et al. (2025).

Earlier symmetry diagnostics for these orbital normals suggested that long-period comets depart from uniformity mainly through a low-order axial effect, whereas rotational symmetry about an (unspecified) axis  $\boldsymbol{\mu}$  is not rejected at the 10% significance level (García-Portugués et al., 2025, Section 7). A plausible explanation for this combination of “non-uniform yet symmetric” behavior is observational selection: comet surveys concentrate a substantial fraction of their sky coverage

and cadence at small ecliptic latitudes (Jupp et al., 2003). This preferential sampling increases the incidence of near-ecliptic orbital planes, which translates into approximately antipodal (north–south) accumulations of the corresponding normal vectors on  $\mathbb{S}^2$ . These considerations motivate assessing the family  $C_k(\boldsymbol{\mu}, \rho)$  for small order  $k$  as a parsimonious model that retains rotational symmetry about  $\boldsymbol{\mu}$  while allowing moderate, low-order deviations from uniformity, particularly for long-period comets.

Table 3 reports the bootstrap  $p$ -values obtained by Algorithm 3 for testing the goodness-of-fit of  $C_k(\boldsymbol{\mu}, \rho)$ ,  $k = 1, 2, 3, 4$ , for long-period comets. We considered the statistics  $P_n^{W, \lambda}$ , for  $W \in \{\text{CvM}, \text{AD}\}$  and  $\lambda \in \{\text{Unif}, P_n, C_k\}$ , computed using closed-form expressions or the Monte Carlo approximation (25) with  $K = 10^4$  random directions. We used  $B = 10^4$  bootstrap samples and the ML estimates  $(\hat{\boldsymbol{\mu}}_{\text{ML}}, \hat{\rho}_{\text{ML}})$ . The test for the simple null hypothesis of uniformity was also conducted for reference.

$H_0$	$P_n^{\text{CvM, Unif}}$	$P_n^{\text{AD, Unif}}$	$P_n^{\text{CvM, } P_n}$	$P_n^{\text{AD, } P_n}$	$P_n^{\text{CvM, } C_k}$	$P_n^{\text{AD, } C_k}$
Unif	0.026	0.009	0.026	0.008	0.029	0.012
$C_1$	0.000	0.000	0.000	0.000	0.000	0.000
$C_2$	0.283	0.116	0.184	0.139	0.146	0.130
$C_3$	0.026	0.012	0.024	0.008	0.029	0.011
$C_4$	0.028	0.013	0.027	0.011	0.023	0.009

Table 3: Bootstrap  $p$ -values of the goodness-of-fit test of spherical cardioidness applied to the normal vectors of the orbits of long-period comets. The tests are conducted for the orders  $k = 1, 2, 3, 4$  and the simple null hypothesis of uniformity ( $\rho_0 = 0$ ).

The spherical cardioid model with  $k = 2$  is not rejected at the 10% significance level as the candidate model for the distribution of orbital normals of long-period comets, for all tests. Higher- and lower-order models, including uniformity, are found not compatible for long-period comets at the 5% significance level. This supports the suitability of the spherical cardioid family to capture the moderate non-uniformity of long-period comet orbits while accommodating their marked rotational symmetry. For short-period comets, all models are emphatically rejected with the minimal bootstrap  $p$ -values  $1/(B + 1) \approx 10^{-4}$ . The model with  $k = 1$  has the smallest test statistics for short-period comets.

Figure 7 gives additional insights on the outcomes of the goodness-of-fit tests. It displays the ecdf  $F_{n, \hat{\boldsymbol{\mu}}_{\text{ML}}}$  of the projected sample  $\{\hat{\boldsymbol{\mu}}_{\text{ML}}^\top \mathbf{X}_i\}_{i=1}^n$  versus the projected cdf  $\hat{F}_{\hat{\boldsymbol{\mu}}_{\text{ML}}}$  of the fitted  $C_k(\hat{\boldsymbol{\mu}}_{\text{ML}}, \hat{\rho}_{\text{ML}})$ , for long- ( $k = 2$ ) and short-period ( $k = 1$ ) comets. For long-period comets, the agreement between the ecdf and cdf is very remarkable. For short-period comets, the fitted cdf departs strongly from the ecdf, as the projected cdf is not able to capture the heavy concentration on the right tail of the ecdf, caused by the cluster near the north pole.

The fitted parameters for long-period orbits with  $k = 2$  are  $\hat{\boldsymbol{\mu}}_{\text{ML, long}} = (0.0804, -0.0067, 0.9967)^\top$  and  $\hat{\rho}_{\text{ML, long}} = 0.4727$ . The axis estimate  $\hat{\boldsymbol{\mu}}_{\text{ML, long}}$  is slightly tilted with respect to the normal axis of the ecliptic plane (north–south axis). The percentile bootstrap 95%-confidence interval for  $\rho_{\text{long}}$  is  $(0.3121, 0.6747)$ , coherent with the significant non-uniformity. The percentile bootstrap 95%-confidence region for  $\boldsymbol{\mu}_{\text{long}}$  is  $\{\boldsymbol{\mu} \in \mathbb{S}^2 : |\boldsymbol{\mu}^\top \hat{\boldsymbol{\mu}}_{\text{ML, long}}| \geq 0.9571\}$  (see Figure 6a). For short-period comets with  $k = 1$ ,  $\hat{\boldsymbol{\mu}}_{\text{ML, short}} = (-0.0626, -0.0662, 0.9958)^\top$  and  $\{\boldsymbol{\mu} \in \mathbb{S}^2 : \boldsymbol{\mu}^\top \hat{\boldsymbol{\mu}}_{\text{ML, short}} \geq 0.9922\}$  (Figure 6b). The concentration estimate  $\hat{\rho}_{\text{ML, short}} = 1$  and a percentile interval that collapses at the boundary indicate the lack of fit of the spherical cardioid model for the distribution of short-period orbits.

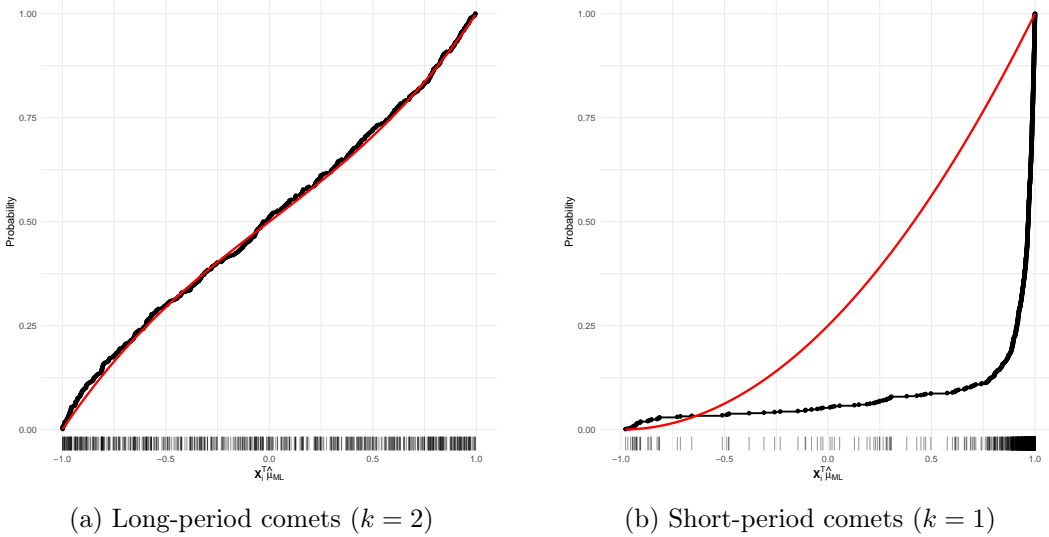


Figure 7: Comparison of the ecdf  $F_{n, \hat{\mu}_{ML}}$  of the projected sample  $\{\hat{\mu}_{ML}^\top \mathbf{X}_i\}_{i=1}^n$  (black curve) versus the projected cdf  $\hat{F}_{\hat{\mu}_{ML}}$  of the fitted  $C_k(\hat{\mu}_{ML}, \hat{\rho}_{ML})$  (red curve).

## 8 Discussion

We have studied a generalization of the well-known circular cardioid distribution that allows for spherical data and multimodality. Among its most attractive features, the spherical cardioid family has a tractable estimation and inference, simulation, projected distributions, and goodness-of-fit testing. The distribution is close to the uniform distribution on the sphere, as reflected in its moment structure, making it suitable for modeling mildly non-uniform spherical data. A good example of such data is provided by the orbital normals of long-period comets, for which the spherical cardioid distribution of order two provides an adequate fit.

Further research could focus on conducting numerical experiments to better compare the finite-sample performance of the different estimators in Section 4 across a variety of scenarios and edge cases. The finite-sample performance of the goodness-of-fit tests in Section 6 could also be more exhaustively investigated through simulations, especially to elucidate whether alternatives exist for which the choice of the distribution  $\lambda$  has a significant impact on the outcome of the test.

Generalizations of the spherical cardioid distribution to product spaces like the torus  $(\mathbb{S}^1)^d$  or the polysphere  $\mathbb{S}^{d_1} \times \dots \times \mathbb{S}^{d_r}$  seem possible based on (9) and could be relevant for constructing tractable dependence structures on these spaces. These extensions will be explored in future work.

## Acknowledgments

The author acknowledges support by grant PID2021-124051NB-I00, funded by MCIN/AEI/10.13039/-501100011033 and ERDF/EU.

## A Proofs of Section 3

### A.1 Proofs of Section 3.1

*Proof of Proposition 3.1.* A direct computation using (5) and (8) gives

$$\int_{\mathbb{S}^d} f_{C_{k_1}}(\mathbf{x}; \boldsymbol{\mu}_1, \rho_1) f_{C_{k_2}}(\mathbf{x}; \boldsymbol{\mu}_2, \rho_2) \sigma_d(d\mathbf{x})$$

$$\begin{aligned}
&= \frac{1}{\omega_d^2} \int_{\mathbb{S}^d} \left\{ 1 + \rho_1 \rho_2 \tilde{C}_{k_1}^{(d-1)/2}(\mathbf{x}^\top \boldsymbol{\mu}_1) \tilde{C}_{k_2}^{(d-1)/2}(\mathbf{x}^\top \boldsymbol{\mu}_2) \right\} \sigma_d(d\mathbf{x}) \\
&= \frac{1}{\omega_d} + \frac{\delta_{k_1, k_2} \rho_1 \rho_2}{\omega_d C_{k_1}^{(d-1)/2}(1)^2} \tau_{k_2, d}^{-1} C_{k_1}^{(d-1)/2}(\boldsymbol{\mu}_1^\top \boldsymbol{\mu}_2) \\
&= \frac{1}{\omega_d} + \frac{\delta_{k_1, k_2} \rho_1 \rho_2 / d_{k_1, d}}{\omega_d} \tilde{C}_{k_1}^{(d-1)/2}(\boldsymbol{\mu}_1^\top \boldsymbol{\mu}_2) \\
&= f_{C_{k_1}}(\boldsymbol{\mu}_1; \boldsymbol{\mu}_2, \delta_{k_1, k_2} \rho_1 \rho_2 / d_{k_1, d}).
\end{aligned}$$

An application of this result with  $\boldsymbol{\mu}_1 = \mathbf{x}$  yields

$$\int_{\mathbb{S}^d} f_{C_{k_1}}(\mathbf{x}; \mathbf{y}, \rho_1) f_{C_{k_2}}(\mathbf{y}; \boldsymbol{\mu}, \rho_2) \sigma_d(d\mathbf{y}) = f_{C_{k_1}}\left(\mathbf{x}; \boldsymbol{\mu}, \delta_{k_1, k_2} \frac{\rho_1 \rho_2}{d_{k_1, d}}\right),$$

thus giving the density of  $\mathbf{X}$  by the law of total probability.  $\square$

## A.2 Proofs of Section 3.3

*Proof of Theorem 3.1.* By construction,

$$\begin{aligned}
\mathbb{E}[\mathbf{X}^{\otimes m}] &= \mathbb{E}[\mathbf{U}^{\otimes m}] + \frac{\rho}{\omega_d C_k^{(d-1)/2}(1)} \int_{\mathbb{S}^d} \mathbf{x}^{\otimes m} C_k^{(d-1)/2}(\mathbf{x}^\top \boldsymbol{\mu}) \sigma_d(d\mathbf{x}) \\
&=: \boldsymbol{\mu}_{d+1, m} + \frac{\rho}{\omega_d C_k^{(d-1)/2}(1)} I_{m, k}(\boldsymbol{\mu}).
\end{aligned}$$

The uniform moments follow from Lemma 5 in Chacón et al. (2026):

$$\boldsymbol{\mu}_{d+1, m} = \mathbb{E}[\mathbf{U}^{\otimes m}] = \frac{(m-1)!!}{\prod_{r=0}^{m/2-1} (d+1+2r)} \mathbf{S}_{d+1, m}(\text{vec } \mathbf{I}_{d+1})^{\otimes m/2} \mathbf{1}_{\{m \text{ even}\}}.$$

We next focus on computing  $I_{m, k}(\boldsymbol{\mu})$ .

*Proof of (i).* The vectorized monomial  $\mathbf{x}^{\otimes m}$  is a homogeneous polynomial of order  $m$ . Its entries are not necessarily harmonic, i.e., such that the entrywise Laplacian  $\Delta \mathbf{x}^{\otimes m}$  is null. The projection of  $\mathbf{x}^{\otimes m}$  onto  $\mathcal{H}_k^d$ , the space of spherical harmonics of degree  $k$  on  $\mathbb{S}^d$  (i.e., homogeneous and harmonic polynomials) is carried out by the projection operator  $\text{proj}_k : L^2(\mathbb{S}^d) \rightarrow \mathcal{H}_k^d$ . For  $f \in L^2(\mathbb{S}^d)$ , this linear operator is

$$\text{proj}_k f(\mathbf{x}) = \frac{1}{\omega_d} \int_{\mathbb{S}^d} f(\mathbf{y}) Z_k(\mathbf{x}, \mathbf{y}) \sigma_d(d\mathbf{y}), \quad Z_k(\mathbf{x}, \mathbf{y}) = \tau_{k, d} C_k^{(d-1)/2}(\mathbf{x}^\top \mathbf{y}),$$

see Dai and Xu (2013, Lemma 1.2.4, Theorem 1.2.6) for  $d \geq 2$ .

When  $m < k$ ,  $\text{proj}_k \mathbf{x}^{\otimes m} = \mathbf{0}$  since  $\mathbf{x}^{\otimes m}$  decomposes into spherical harmonics of degree at most  $m$ , and hence the projection onto  $\mathcal{H}_k^d$  is null. Thus,

$$I_{m, k}(\boldsymbol{\mu}) = \tau_{k, d}^{-1} \int_{\mathbb{S}^d} \mathbf{x}^{\otimes m} Z_k(\mathbf{x}, \boldsymbol{\mu}) \sigma_d(d\mathbf{x}) = \tau_{k, d}^{-1} \omega_d \text{proj}_k(\mathbf{x}^{\otimes m})|_{\mathbf{x}=\boldsymbol{\mu}} = \mathbf{0}$$

and the result follows.

*Proof of (iii).* On the one hand,  $(-\mathbf{x})^{\otimes m} = (-1)^m \mathbf{x}^{\otimes m}$  because  $\mathbf{x}^{\otimes m}$  is a homogeneous polynomial of degree  $m$ . On the other hand,  $\text{proj}_k f(-\mathbf{x}) = (-1)^k \text{proj}_k f(\mathbf{x})$  for any  $f \in L^2(\mathbb{S}^d)$  since  $Z_k(-\mathbf{x}, \mathbf{y}) = (-1)^k Z_k(\mathbf{x}, \mathbf{y})$ . Therefore,  $\text{proj}_k(-\mathbf{x})^{\otimes m} = (-1)^m \text{proj}_k \mathbf{x}^{\otimes m}$  and  $\text{proj}_k(-\mathbf{x})^{\otimes m} = (-1)^k \text{proj}_k \mathbf{x}^{\otimes m}$ . When  $m > k$  and  $m - k$  is odd, then it must be that  $\text{proj}_k \mathbf{x}^{\otimes m} = \mathbf{0}$ .

*Proof of (ii).* The projection operator is relatively explicit for an homogeneous polynomial of degree  $k$  (Dai and Xu, 2013, Lemma 1.2.1), from which it follows that

$$\text{proj}_k \mathbf{x}^{\otimes k} = \sum_{j=0}^{\lfloor k/2 \rfloor} \frac{(-1)^j}{4^j j! (k + (d-1)/2 - j)_j} \Delta^j \mathbf{x}^{\otimes k}, \quad (29)$$

where  $(a)_j$  is the Pochhammer symbol and  $\Delta^j f = (\sum_{i=1}^{d+1} \partial_i^2)^j f$  is the iterated Laplacian operator with  $\Delta^0 f = f$ , and the operator is applied entrywise on  $\mathbf{x}^{\otimes k}$ . (Note this projection operator is given in Lemma 1.2.1 of Dai and Xu (2013) for  $d \geq 2$  but it extends to  $d = 1$ .) From the coordinate computation of the Laplacian, we have that

$$\Delta \mathbf{x}^{\otimes k} = k(k-1) \mathbf{S}_{d+1,k} (\text{vec } \mathbf{I}_{d+1} \otimes \mathbf{x}^{\otimes k-2}), \quad k \geq 2,$$

where  $\mathbf{S}_{d+1,k}$  is the symmetrizer matrix. More generally,

$$\Delta^j \mathbf{x}^{\otimes k} = \frac{k!}{(k-2j)!} \mathbf{S}_{d+1,k} ((\text{vec } \mathbf{I}_{d+1})^{\otimes j} \otimes \mathbf{x}^{\otimes k-2j}), \quad 0 \leq j \leq \lfloor k/2 \rfloor, \quad (30)$$

and  $\Delta^j \mathbf{x}^{\otimes k} = \mathbf{0}$  for  $j > \lfloor k/2 \rfloor$ . Replacing (30) into (29) leads to

$$\begin{aligned} \text{proj}_k \mathbf{x}^{\otimes k} &= \sum_{j=0}^{\lfloor k/2 \rfloor} \frac{(-1)^j}{4^j j! (k+(d-1)/2-j)_j} \left\{ \frac{k!}{(k-2j)!} \mathbf{S}_{d+1,k} ((\text{vec } \mathbf{I}_{d+1})^{\otimes j} \otimes \mathbf{x}^{\otimes k-2j}) \right\} \\ &= \mathbf{S}_{d+1,k} \sum_{j=0}^{\lfloor k/2 \rfloor} a_{k,j} (\text{vec } \mathbf{I}_{d+1})^{\otimes j} \otimes \mathbf{x}^{\otimes k-2j}, \end{aligned}$$

where

$$a_{k,j} = (-1)^j \frac{k!}{(k-2j)!} \frac{\Gamma(k+(d-1)/2-j)}{4^j j! \Gamma(k+(d-1)/2)} = (-1)^j \frac{k!}{2^j (k-2j)! j!} \frac{1}{\prod_{r=1}^j (2(k-r)+d-1)}$$

with the convention that  $a_{k,0} = 1$ . Therefore,

$$\begin{aligned} \frac{1}{\omega_d C_k^{(d-1)/2}(1)} I_{k,k}(\boldsymbol{\mu}) &= \frac{1}{\omega_d C_k^{(d-1)/2}(1)} \left( 1 + \frac{2k}{d-1} \right)^{-1} \omega_d \text{proj}_k(\mathbf{x}^{\otimes k})|_{\mathbf{x}=\boldsymbol{\mu}} \\ &= \frac{1}{d_{k,d}} \mathbf{S}_{d+1,k} \sum_{j=0}^{\lfloor k/2 \rfloor} a_{k,j} (\text{vec } \mathbf{I}_{d+1})^{\otimes j} \otimes \boldsymbol{\mu}^{\otimes k-2j}, \end{aligned}$$

proving the result.

*Proof of (iv).* For  $m > k$ , we follow a different approach, given the lack of an explicit expression for the projection of  $\mathbf{x}^{\otimes m}$  onto  $\mathcal{H}_k^d$ .

Let the tangent-normal change of variables  $\mathbf{x} = t\boldsymbol{\mu} + (1-t^2)^{1/2} \mathbf{B}_{\boldsymbol{\mu}} \boldsymbol{\xi}$ , with  $t = \mathbf{x}^\top \boldsymbol{\mu} \in [-1, 1]$ ,  $\boldsymbol{\xi} \in \mathbb{S}^{d-1}$ , and  $\mathbf{B}_{\boldsymbol{\mu}}$  a semi-orthogonal  $(d+1) \times d$  matrix such that  $\mathbf{B}_{\boldsymbol{\mu}} \mathbf{B}_{\boldsymbol{\mu}}^\top = \mathbf{I}_{d+1} - \boldsymbol{\mu} \boldsymbol{\mu}^\top$  and  $\mathbf{B}_{\boldsymbol{\mu}}^\top \mathbf{B}_{\boldsymbol{\mu}} = \mathbf{I}_d$ . Then,  $\sigma_d(d\mathbf{x}) = (1-t^2)^{d/2-1} dt \sigma_{d-1}(d\boldsymbol{\xi})$ . Using this change and the binomial theorem for the Kronecker product, we have

$$\begin{aligned} I_{m,k}(\boldsymbol{\mu}) &= \int_{\mathbb{S}^{d-1}} \int_{-1}^1 (t\boldsymbol{\mu} + (1-t^2)^{1/2} \mathbf{B}_{\boldsymbol{\mu}} \boldsymbol{\xi})^{\otimes m} C_k^{(d-1)/2}(t) (1-t^2)^{d/2-1} dt \sigma_{d-1}(d\boldsymbol{\xi}) \\ &= \mathbf{S}_{d+1,m} \int_{\mathbb{S}^{d-1}} \int_{-1}^1 \sum_{\ell=0}^m \binom{m}{\ell} \boldsymbol{\mu}^{\otimes \ell} \otimes (\mathbf{B}_{\boldsymbol{\mu}} \boldsymbol{\xi})^{\otimes m-\ell} \\ &\quad \times t^\ell (1-t^2)^{(m-\ell)/2} C_k^{(d-1)/2}(t) (1-t^2)^{d/2-1} dt \sigma_{d-1}(d\boldsymbol{\xi}) \\ &= \mathbf{S}_{d+1,m} \sum_{\ell=0}^m \binom{m}{\ell} \boldsymbol{\mu}^{\otimes \ell} \otimes \left\{ \mathbf{B}_{\boldsymbol{\mu}}^{\otimes m-\ell} \int_{\mathbb{S}^{d-1}} \boldsymbol{\xi}^{\otimes m-\ell} \sigma_{d-1}(d\boldsymbol{\xi}) \right\} \\ &\quad \times \int_{-1}^1 t^\ell (1-t^2)^{(d+m-\ell-2)/2} C_k^{(d-1)/2}(t) dt \end{aligned}$$

$$= \omega_{d-1} \mathbf{S}_{d+1,m} \sum_{\ell=0}^m c_{\ell,m,k} \binom{m}{\ell} \boldsymbol{\mu}^{\otimes \ell} \otimes \left\{ \mathbf{B}_{\boldsymbol{\mu}}^{\otimes m-\ell} \boldsymbol{\mu}_{d,m-\ell} \right\}, \quad (31)$$

where we have used (12) and

$$c_{\ell,m,k} = \int_{-1}^1 t^{\ell} (1-t^2)^{(d+m-\ell-2)/2} C_k^{(d-1)/2}(t) dt.$$

We replace (12) into (31) and apply Lemma D.1, using that the symmetrizer matrix commutes with the Kronecker powers, so

$$\mathbf{B}_{\boldsymbol{\mu}}^{\otimes p} \mathbf{S}_{d,p} = \mathbf{S}_{d+1,p} \mathbf{B}_{\boldsymbol{\mu}}^{\otimes p}.$$

This gives

$$\begin{aligned} I_{m,k}(\boldsymbol{\mu}) &= \omega_{d-1} \mathbf{S}_{d+1,m} \sum_{\ell=0}^m c_{\ell,m,k} \binom{m}{\ell} \frac{(m-\ell-1)!!}{\prod_{r=0}^{(m-\ell)/2-1} (d+2r)} \\ &\quad \times \boldsymbol{\mu}^{\otimes \ell} \otimes \left\{ \mathbf{B}_{\boldsymbol{\mu}}^{\otimes m-\ell} \left[ \mathbf{S}_{d,m-\ell} (\text{vec } \mathbf{I}_d)^{\otimes (m-\ell)/2} \mathbf{1}_{\{m-\ell \text{ even}\}} \right] \right\} \\ &= \omega_{d-1} \mathbf{S}_{d+1,m} \sum_{\ell=0}^m c_{\ell,m,k} \binom{m}{\ell} \frac{(m-\ell-1)!!}{\prod_{r=0}^{(m-\ell)/2-1} (d+2r)} \\ &\quad \times \boldsymbol{\mu}^{\otimes \ell} \otimes \left\{ \mathbf{S}_{d+1,m-\ell} (\text{vec} [\mathbf{I}_{d+1} - \boldsymbol{\mu} \boldsymbol{\mu}^{\top}])^{\otimes (m-\ell)/2} \right\} \mathbf{1}_{\{m-\ell \text{ even}\}}. \end{aligned}$$

The inner symmetrizer can be absorbed into the outer one, yielding

$$\begin{aligned} I_{m,k}(\boldsymbol{\mu}) &= \omega_{d-1} \mathbf{S}_{d+1,m} \sum_{\substack{\ell=0 \\ m-\ell \text{ even}}}^m c_{\ell,m,k} \binom{m}{\ell} \frac{(m-\ell-1)!!}{\prod_{r=0}^{(m-\ell)/2-1} (d+2r)} \\ &\quad \times \boldsymbol{\mu}^{\otimes \ell} \otimes \left\{ (\text{vec } \mathbf{I}_{d+1} - \boldsymbol{\mu}^{\otimes 2})^{\otimes (m-\ell)/2} \right\} \end{aligned}$$

and then the parity of the indexes can be enforced with the summation index  $j = (m-\ell)/2$ ,  $j = 0, \dots, \lfloor m/2 \rfloor$ , leading to

$$\begin{aligned} I_{m,k}(\boldsymbol{\mu}) &= \omega_{d-1} \mathbf{S}_{d+1,m} \sum_{j=0}^{\lfloor m/2 \rfloor} c_{m-2j,m,k} \binom{m}{2j} \frac{(2j-1)!!}{\prod_{r=0}^{j-1} (d+2r)} \\ &\quad \times \boldsymbol{\mu}^{\otimes (m-2j)} \otimes \left\{ (\text{vec } \mathbf{I}_{d+1} - \boldsymbol{\mu}^{\otimes 2})^{\otimes j} \right\}. \end{aligned} \quad (32)$$

It remains only to compute the coefficients

$$\begin{aligned} c_{m-2j,m,k} &= \int_{-1}^1 t^{m-2j} (1-t^2)^{d/2-1+j} C_k^{(d-1)/2}(t) dt \\ &= \int_{-1}^1 t^{m-2j} (1-t^2)^b C_k^{(d-1)/2}(t) dt \end{aligned}$$

where  $b := d/2 - 1 + j$ . We use the series expansion of the Gegenbauer and Chebyshev polynomials (see DLMF, 2025, Eqs. 18.5.10 and 18.5.11\_1), unified for  $d \geq 1$  as

$$C_k^{(d-1)/2}(x) = g_{k,d} \sum_{s=0}^{\lfloor k/2 \rfloor} (-1)^s \frac{\Gamma((d-1)/2 + k - s)}{s!(k-2s)!} (2x)^{k-2s}, \quad (33)$$

$$g_{k,d} := \begin{cases} k/2, & d = 1, \\ [\Gamma((d-1)/2)]^{-1}, & d \geq 2. \end{cases}$$

Substituting (33) into the definition of  $c_{m-2j,m,k}$  gives

$$\begin{aligned} c_{m-2j,m,k} &= g_{k,d} \int_{-1}^1 t^{m-2j} (1-t^2)^b \sum_{s=0}^{\lfloor k/2 \rfloor} (-1)^s \frac{\Gamma((d-1)/2+k-s)}{s!(k-2s)!} (2t)^{k-2s} dt \\ &= g_{k,d} \sum_{s=0}^{\lfloor k/2 \rfloor} (-1)^s \frac{2^{k-2s} \Gamma((d-1)/2+k-s)}{s!(k-2s)!} \int_{-1}^1 t^{a_s} (1-t^2)^b dt \end{aligned} \quad (34)$$

with  $a_s := m-2j+k-2s = m+k-2(j+s)$ .

The parity of the integrands in (34) depends on  $a_s$ , which in turn depends on  $m+k$ . If  $m+k$  is odd, then all  $a_s$  are odd and  $c_{m-2j,m,k} = 0$ . If  $m+k$  is even, then all  $a_s$  are even and the integrals are beta-type integrals that can be computed explicitly. Assume henceforth that  $m+k$  is even and write  $a_s = 2r_s$  with  $r_s := (m+k)/2 - (j+s)$ . Then

$$\int_{-1}^1 t^{2r_s} (1-t^2)^b dt = B(r_s + 1/2, b+1) = \frac{\Gamma(r_s + 1/2) \Gamma(b+1)}{\Gamma(r_s + b + 3/2)}. \quad (35)$$

Substituting this expression back into (34), and recalling the definitions of  $b$  and  $r_s$ , we obtain

$$\begin{aligned} c_{m-2j,m,k} &= g_{k,d} \sum_{s=0}^{\lfloor k/2 \rfloor} (-1)^s \frac{2^{k-2s} \Gamma((d-1)/2+k-s)}{\Gamma((d-1)/2) s!(k-2s)!} \frac{\Gamma(r_s + 1/2) \Gamma(b+1)}{\Gamma(r_s + b + 3/2)} \\ &= \frac{\Gamma(d/2+j)}{g_{k,d}} \sum_{s=0}^{\lfloor k/2 \rfloor} (-1)^s \frac{2^{k-2s} \Gamma((d-1)/2+k-s)}{s!(k-2s)!} \frac{\Gamma((m+k+1)/2-j-s)}{\Gamma((d+k+m+1)/2-s)} \end{aligned}$$

Coming back to (32), we have proved that

$$\begin{aligned} &\frac{1}{\omega_d C_k^{(d-1)/2}(1)} I_{m,k}(\boldsymbol{\mu}) \\ &= \frac{\omega_{d-1}}{\omega_d} \frac{1}{C_k^{(d-1)/2}(1)} S_{d+1,m} \sum_{j=0}^{\lfloor m/2 \rfloor} e_{j,k,m} \boldsymbol{\mu}^{\otimes(m-2j)} \otimes \left\{ (\text{vec } \mathbf{I}_{d+1} - \boldsymbol{\mu}^{\otimes 2})^{\otimes j} \right\}, \end{aligned}$$

where

$$e_{j,k,m} := \binom{m}{2j} \frac{(2j-1)!!}{\prod_{r=0}^{j-1} (d+2r)} f_{j,m,k} \mathbf{1}_{\{m+k \text{ even}\}}$$

and

$$\begin{aligned} f_{j,m,k} &:= \int_{-1}^1 t^{m-2j} (1-t^2)^{d/2-1+j} C_k^{(d-1)/2}(t) dt \\ &= \frac{\Gamma(d/2+j)}{g_{k,d}} \sum_{s=0}^{\lfloor k/2 \rfloor} (-1)^s \frac{2^{k-2s} \Gamma((d-1)/2+k-s)}{s!(k-2s)!} \frac{\Gamma((m+k+1)/2-j-s)}{\Gamma((d+k+m+1)/2-s)}. \end{aligned}$$

□

*Proof of Corollary 3.1.* We derive the moments using Theorem 3.1(ii). First, we need the coefficients  $a_{k,j}$ ,  $j = 0, \dots, \lfloor k/2 \rfloor$ , for  $k = 1, \dots, 4$ :

$$a_{1,0} = 1, \quad a_{2,0} = 1, \quad a_{2,1} = -\frac{1}{d+1}; \quad a_{3,0} = 1, \quad a_{3,1} = -\frac{3}{d+3};$$

$$a_{4,0} = 1, \quad a_{4,1} = -\frac{6}{d+5}, \quad a_{4,2} = \frac{3}{(d+3)(d+5)}.$$

Second, we compute  $\boldsymbol{\mu}_{d+1,k}$  for  $k = 1, \dots, 4$  using (12):

$$\begin{aligned} \boldsymbol{\mu}_{d+1,1} &= \mathbf{0}, \quad \boldsymbol{\mu}_{d+1,2} = \frac{1}{d+1} \operatorname{vec} \mathbf{I}_{d+1}, \quad \boldsymbol{\mu}_{d+1,3} = \mathbf{0}, \\ \boldsymbol{\mu}_{d+1,4} &= \frac{3}{(d+1)(d+3)} \mathbf{S}_{d+1,4} (\operatorname{vec} \mathbf{I}_{d+1})^{\otimes 2}. \end{aligned}$$

Third, we obtain  $d_{k,d}$  using (3):

$$\begin{aligned} d_{1,d} &= d+1, \quad d_{2,d} = \frac{d(d+3)}{2}, \quad d_{3,d} = \frac{d(d+1)(d+5)}{6}, \\ d_{4,d} &= \frac{d(d+1)(d+2)(d+7)}{24}. \end{aligned}$$

We can now plug in these values into Theorem 3.1(ii) to obtain the desired results:

$$\begin{aligned} \operatorname{E}[\mathbf{X}_1] &= \frac{\rho}{d_{1,d}} \mathbf{S}_{d+1,1} \boldsymbol{\mu} = \frac{\rho}{d+1} \boldsymbol{\mu}, \\ \operatorname{E}[\mathbf{X}^{\otimes 2}] &= \boldsymbol{\mu}_{d+1,2} + \frac{\rho}{d_{2,d}} \mathbf{S}_{d+1,2} \{ \boldsymbol{\mu}^{\otimes 2} + a_{2,1} \operatorname{vec} \mathbf{I}_{d+1} \} \\ &= \frac{1}{d+1} \operatorname{vec} \mathbf{I}_{d+1} + \frac{2\rho}{d(d+3)} \left\{ \boldsymbol{\mu}^{\otimes 2} - \frac{1}{d+1} \operatorname{vec} \mathbf{I}_{d+1} \right\} \\ \operatorname{E}[\mathbf{X}^{\otimes 3}] &= \frac{\rho}{d_{3,d}} \mathbf{S}_{d+1,3} \{ \boldsymbol{\mu}^{\otimes 3} + a_{3,1} (\operatorname{vec} \mathbf{I}_{d+1}) \otimes \boldsymbol{\mu} \} \\ &= \frac{6\rho}{d(d+1)(d+5)} \mathbf{S}_{d+1,3} \left\{ \boldsymbol{\mu}^{\otimes 3} - \frac{3}{d+3} (\operatorname{vec} \mathbf{I}_{d+1}) \otimes \boldsymbol{\mu} \right\} \\ \operatorname{E}[\mathbf{X}^{\otimes 4}] &= \boldsymbol{\mu}_{d+1,4} + \frac{\rho}{d_{4,d}} \mathbf{S}_{d+1,4} \{ \boldsymbol{\mu}^{\otimes 4} + a_{4,1} (\operatorname{vec} \mathbf{I}_{d+1}) \otimes \boldsymbol{\mu}^{\otimes 2} + a_{4,2} (\operatorname{vec} \mathbf{I}_{d+1})^{\otimes 2} \} \\ &= \frac{3}{(d+1)(d+3)} \mathbf{S}_{d+1,4} (\operatorname{vec} \mathbf{I}_{d+1})^{\otimes 2} \\ &\quad + \frac{24\rho}{d(d+1)(d+2)(d+7)} \mathbf{S}_{d+1,4} \left\{ \boldsymbol{\mu}^{\otimes 4} - \frac{6}{d+5} (\operatorname{vec} \mathbf{I}_{d+1}) \otimes \boldsymbol{\mu}^{\otimes 2} \right. \\ &\quad \left. + \frac{3}{(d+3)(d+5)} (\operatorname{vec} \mathbf{I}_{d+1})^{\otimes 2} \right\}. \end{aligned}$$

□

*Proof of Corollary 3.2.* Using that  $\operatorname{vec}(\mathbf{a}\mathbf{b}^\top) = \mathbf{a} \otimes \mathbf{b}$ , we have

$$\begin{aligned} \operatorname{Var}[\mathbf{X}^{\otimes m}] &= \operatorname{vec}_{(d+1)^m, (d+1)^m}^{-1} \left( \operatorname{E}[\operatorname{vec}(\mathbf{X}^{\otimes m} \mathbf{X}^{\otimes m \top})] - \operatorname{vec}(\operatorname{E}[\mathbf{X}^{\otimes m}] \operatorname{E}[\mathbf{X}^{\otimes m}]^\top) \right) \\ &= \operatorname{vec}_{(d+1)^m, (d+1)^m}^{-1} \left( \operatorname{E}[\mathbf{X}^{\otimes 2m}] - \operatorname{E}[\mathbf{X}^{\otimes m}]^{\otimes 2} \right). \end{aligned}$$

Hence, covariance matrices follow from Theorem 3.1. In particular, Theorem 3.1(iii) leads to  $\operatorname{E}[\mathbf{X}^{\otimes 2m}] = \boldsymbol{\mu}_{d+1,2m}$  when  $2m+k$  is odd, i.e., when  $k$  is odd. For  $k=1$ , the result follows from  $\boldsymbol{\mu}_{d+1,2} = (d+1)^{-1} \operatorname{vec} \mathbf{I}_{d+1}$  and Corollary 3.1. □

### A.3 Proofs of Section 3.4

*Proof of Proposition 3.2.* To derive the moment generating function, we consider the second equation in Magnus et al. (1966, p. 227) and the arguments from the proof of Proposition 3 in Fernández-de-Marcos and García-Portugués (2023) to obtain

$$e^{\kappa x} = \left( \frac{2}{\kappa} \right)^{(d-1)/2} \sum_{\ell=0}^{\infty} e_{\ell,d} \mathcal{I}_{(2\ell+d-1)/2}(\kappa) C_\ell^{(d-1)/2}(x), \quad x \in (-1, 1), \quad \kappa > 0, \quad (36)$$

where

$$e_{\ell,d} = \begin{cases} \Gamma((d-1)/2)(\ell + (d-1)/2), & d \geq 2, \\ 2 - \delta_{\ell,0}, & d = 1. \end{cases}$$

Plugging (36) into the definition of the moment generating function and using (8), we have

$$\begin{aligned} M_{\mathbf{X}}(\mathbf{t}) &= \frac{1}{\omega_d} \int_{\mathbb{S}^d} e^{\|\mathbf{t}\| \mathbf{x}^\top (\mathbf{t}/\|\mathbf{t}\|)} \left\{ 1 + \frac{\rho}{C_k^{(d-1)/2}(1)} C_k^{(d-1)/2}(\mathbf{x}^\top \boldsymbol{\mu}) \right\} \sigma_d(d\mathbf{x}) \\ &= \frac{1}{\omega_d} \left( \frac{2}{\|\mathbf{t}\|} \right)^{(d-1)/2} \sum_{\ell=0}^{\infty} e_{\ell,d} \mathcal{I}_{(2\ell+d-1)/2}(\|\mathbf{t}\|) \\ &\quad \times \int_{\mathbb{S}^d} C_\ell^{(d-1)/2} \left( \frac{\mathbf{x}^\top \mathbf{t}}{\|\mathbf{t}\|} \right) \left\{ 1 + \frac{\rho}{C_k^{(d-1)/2}(1)} C_k^{(d-1)/2}(\mathbf{x}^\top \boldsymbol{\mu}) \right\} \sigma_d(d\mathbf{x}) \\ &= \left( \frac{2}{\|\mathbf{t}\|} \right)^{(d-1)/2} \left\{ e_{0,d} \mathcal{I}_{(d-1)/2}(\|\mathbf{t}\|) \right. \\ &\quad \left. + \frac{\rho}{d_{k,d}} e_{k,d} \mathcal{I}_{(2k+d-1)/2}(\|\mathbf{t}\|) C_k^{(d-1)/2} \left( \frac{\boldsymbol{\mu}^\top \mathbf{t}}{\|\mathbf{t}\|} \right) \right\}. \end{aligned} \quad (37)$$

To derive the characteristic function, we use an analogous argument as in (36) but now using the third equation in Magnus et al. (1966, p. 227) to obtain

$$e^{i\kappa x} = \left( \frac{2}{\kappa} \right)^{(d-1)/2} \sum_{\ell=0}^{\infty} e_{\ell,d} i^\ell \mathcal{J}_{(2\ell+d-1)/2}(\kappa) C_\ell^{(d-1)/2}(x), \quad x \in (-1, 1), \quad \kappa > 0.$$

Then,

$$\begin{aligned} \varphi_{\mathbf{X}}(\mathbf{t}) &= \frac{1}{\omega_d} \int_{\mathbb{S}^d} e^{i\|\mathbf{t}\| \mathbf{x}^\top (\mathbf{t}/\|\mathbf{t}\|)} \left\{ 1 + \frac{\rho}{C_k^{(d-1)/2}(1)} C_k^{(d-1)/2}(\mathbf{x}^\top \boldsymbol{\mu}) \right\} \sigma_d(d\mathbf{x}) \\ &= \left( \frac{2}{\|\mathbf{t}\|} \right)^{(d-1)/2} \left\{ e_{0,d} \mathcal{J}_{(d-1)/2}(\|\mathbf{t}\|) \right. \\ &\quad \left. + \frac{\rho}{d_{k,d}} e_{k,d} i^k \mathcal{J}_{(2k+d-1)/2}(\|\mathbf{t}\|) C_k^{(d-1)/2} \left( \frac{\boldsymbol{\mu}^\top \mathbf{t}}{\|\mathbf{t}\|} \right) \right\}. \end{aligned} \quad (38)$$

For  $\mathbf{t} = \mathbf{0}$ , both (37) and (38) reduce to 1 by continuity using that, for any  $\mathbf{t} \in \mathbb{R}^{d+1}$ ,

$$\left| C_k^{(d-1)/2} \left( \frac{\boldsymbol{\mu}^\top \mathbf{t}}{\|\mathbf{t}\|} \right) \right| \leq C_k^{(d-1)/2}(1)$$

and that, as  $x \rightarrow 0$ ,  $\mathcal{I}_{(d-1)/2}(x) \sim \mathcal{J}_{(d-1)/2}(x) \sim (x/2)^{(d-1)/2}/\Gamma((d+1)/2)$  (DLMF, 2025, Eqs. 10.30.1 and 10.7.3).  $\square$

#### A.4 Proofs of Section 3.5

*Proof of Proposition 3.3.* We show that the density of  $T = SR$  is  $f_{\boldsymbol{\mu}}(t) = f_d(t) \{1 + \rho \tilde{C}_k^{(d-1)/2}(t)\}$ , as given in (19).

By construction, the density of  $T$  is

$$\begin{aligned} f_T(t) &= 1_{\{t \in [-1,0]\}} f_R(|t|) \mathbb{P}\{S = -1 \mid R = |t|\} + 1_{\{t \in [0,1]\}} f_R(|t|) \mathbb{P}\{S = 1 \mid R = |t|\} \\ &= f_R(|t|) \left\{ 1_{\{t \in [-1,0]\}} \frac{1 + \rho \tilde{C}_k^{(d-1)/2}(t)}{2} + 1_{\{t \in [0,1]\}} \frac{1 + \rho \tilde{C}_k^{(d-1)/2}(t)}{2} \right\} \end{aligned}$$

$$= f_R(|t|) \frac{1 + \rho \tilde{C}_k^{(d-1)/2}(t)}{2},$$

where we have used the oddness of  $\tilde{C}_k^{(d-1)/2}$ .

Since  $X = \mathbf{U}^\top \mathbf{e}_1 \sim F_d$  is symmetric,  $f_d$  is even and the density of  $R = |X|$  is  $f_R(r) = f_d(r) + f_d(-r) = 2f_d(r)$ ,  $r \in [0, 1]$ . Therefore,

$$f_T(t) = f_d(|t|) \left\{ 1 + \rho \tilde{C}_k^{(d-1)/2}(t) \right\} = f_{\boldsymbol{\mu}}(t),$$

proving the result.  $\square$

## B Proofs of Section 4

*Proof of Theorem 4.1.* Let us denote  $\boldsymbol{\xi} = \rho \boldsymbol{\mu}$ . Then,

$$\mathbb{E}[\mathbf{X}] = \frac{1}{d+1} \boldsymbol{\xi}, \quad \text{Var}[\mathbf{X}] = \frac{1}{d+1} \mathbf{I}_{d+1} - \frac{1}{(d+1)^2} \boldsymbol{\xi} \boldsymbol{\xi}^\top.$$

*Proof of (i).* By Strong Law of Large Numbers (SLLN),  $\bar{\mathbf{X}} \xrightarrow{\text{a.s.}} (d+1)^{-1} \boldsymbol{\xi}$ . The continuous mapping theorem applied to  $\mathbf{x} \mapsto ((d+1)\|\mathbf{x}\|, \mathbf{x}/\|\mathbf{x}\|)$ ,  $\mathbf{x} \neq \mathbf{0}$ , gives the almost sure convergence of the estimators.

*Proof of (ii).* By the multivariate CLT,

$$\sqrt{n} (\bar{\mathbf{X}} - \mathbb{E}[\mathbf{X}]) \rightsquigarrow \mathcal{N}_{d+1} \left( \mathbf{0}, \frac{1}{(d+1)^2} ((d+1)\mathbf{I}_{d+1} - \boldsymbol{\xi} \boldsymbol{\xi}^\top) \right).$$

We consider the transformation  $g : \mathbb{R}^{d+1} \rightarrow \mathbb{R} \times \mathbb{S}^d$  defined by  $g(\mathbf{x}) := (\|\mathbf{x}\|, \mathbf{x}/\|\mathbf{x}\|)$  to apply the delta method:

$$\sqrt{n}(g(\bar{\mathbf{X}}) - g(\mathbb{E}[\mathbf{X}])) \rightsquigarrow \mathcal{N}_{d+2} \left( \mathbf{0}, \mathbb{D}g(\mathbb{E}[\mathbf{X}]) \text{Var}[\mathbf{X}] \mathbb{D}g(\mathbb{E}[\mathbf{X}])^\top \right).$$

The function  $g$  is differentiable at all  $\mathbf{x} \neq \mathbf{0}$ , with Jacobian matrix

$$\mathbb{D}g(\mathbf{x}) = \begin{pmatrix} \|\mathbf{x}\|^{-1} \mathbf{x}^\top \\ \|\mathbf{x}\|^{-1} (\mathbf{I}_{d+1} - \|\mathbf{x}\|^{-2} \mathbf{x} \mathbf{x}^\top) \end{pmatrix}_{(d+2) \times (d+1)}$$

that, when applied at  $\mathbb{E}[\mathbf{X}] = [\rho/(d+1)] \boldsymbol{\mu}$ , becomes

$$\mathbb{D}g(\mathbb{E}[\mathbf{X}]) = \begin{pmatrix} \boldsymbol{\mu}^\top \\ \frac{d+1}{\rho} (\mathbf{I}_{d+1} - \boldsymbol{\mu} \boldsymbol{\mu}^\top) \end{pmatrix}_{(d+2) \times (d+1)}.$$

The asymptotic covariance matrix becomes

$$\begin{aligned} & \mathbb{D}g(\mathbb{E}[\mathbf{X}]) \text{Var}[\mathbf{X}] \mathbb{D}g(\mathbb{E}[\mathbf{X}])^\top \\ &= \frac{1}{(d+1)^2} \mathbb{D}g(\mathbb{E}[\mathbf{X}]) \left[ (d+1)\mathbf{I}_{d+1} - \rho^2 \boldsymbol{\mu} \boldsymbol{\mu}^\top \right] \mathbb{D}g(\mathbb{E}[\mathbf{X}])^\top \\ &= \frac{1}{(d+1)^2} \left( \frac{d+1}{\rho} (\mathbf{I}_{d+1} - \boldsymbol{\mu} \boldsymbol{\mu}^\top) \left[ (d+1)\mathbf{I}_{d+1} - \rho^2 \boldsymbol{\mu} \boldsymbol{\mu}^\top \right] \right) \mathbb{D}g(\mathbb{E}[\mathbf{X}])^\top \\ &= \frac{1}{(d+1)^2} \begin{pmatrix} d+1 - \rho^2 & \mathbf{0}^\top \\ \mathbf{0} & (d+1)^3 \rho^{-2} (\mathbf{I}_{d+1} - \boldsymbol{\mu} \boldsymbol{\mu}^\top) \end{pmatrix}. \end{aligned}$$

Since  $g(\mathbb{E}[\mathbf{X}]) = (\|\mathbb{E}[\mathbf{X}]\|, \mathbb{E}[\mathbf{X}]/\|\mathbb{E}[\mathbf{X}]\|) = (\rho/(d+1), \boldsymbol{\mu})$ , then

$$\sqrt{n} \left( \frac{\|\bar{\mathbf{X}}\| - \frac{\rho}{d+1}}{\|\bar{\mathbf{X}}\|} - \boldsymbol{\mu} \right) \rightsquigarrow \mathcal{N}_{d+2} \left( \mathbf{0}, \frac{1}{(d+1)^2} \begin{pmatrix} d+1 - \rho^2 & \mathbf{0}^\top \\ \mathbf{0} & (d+1)^3 \rho^{-2} (\mathbf{I}_{d+1} - \boldsymbol{\mu} \boldsymbol{\mu}^\top) \end{pmatrix} \right)$$

and therefore

$$\sqrt{n} \begin{pmatrix} \hat{\rho}_{\text{MM},1} - \rho \\ \hat{\boldsymbol{\mu}}_{\text{MM},1} - \boldsymbol{\mu} \end{pmatrix} \rightsquigarrow \mathcal{N}_{d+2} \left( \mathbf{0}, \begin{pmatrix} d+1-\rho^2 & \mathbf{0}^\top \\ \mathbf{0} & (d+1)\rho^{-2}(\mathbf{I}_{d+1} - \boldsymbol{\mu}\boldsymbol{\mu}^\top) \end{pmatrix} \right).$$

Reordering the components of this statement concludes the proof.  $\square$

*Proof of Theorem 4.2.* We assume without loss of generality that  $\rho > 0$  and therefore  $\mathbf{u}(\cdot) = \mathbf{u}_+(\cdot)$  and  $\lambda(\cdot) = \lambda_-(\cdot)$  represent the first eigenpair.

The multivariate CLT

$$\sqrt{n} (\text{vec}(\mathbf{S}) - \mathbb{E}[\mathbf{X}^{\otimes 2}]) \rightsquigarrow \mathcal{N}_{(d+1)^2} (\mathbf{0}, \text{Var}[\mathbf{X}^{\otimes 2}])$$

readily follows. We seek to apply the multivariate delta method to the map

$$g : \text{vec}(\mathbf{S}) \in \mathbb{R}^{(d+1)^2} \mapsto (\lambda(\mathbf{S}), \mathbf{u}(\mathbf{S})) \in \mathbb{R}_+ \times \mathbb{S}^d.$$

Note that  $g$  is differentiable at any  $\text{vec}(\mathbf{S})$  such that  $\lambda(\mathbf{S})$  is a simple eigenvalue of  $\mathbf{S}$ , which is guaranteed as long as  $\rho \neq 0$ .

Theorem 7 in Magnus and Neudecker (1999, p. 158) states that the differentials of a simple eigenpair  $(\lambda, \mathbf{u})$  of a real symmetric matrix  $\mathbf{S}$  with respect to its entries are

$$d\lambda = \mathbf{u}^\top (d\mathbf{S}) \mathbf{u}, \quad d\mathbf{u} = (\lambda \mathbf{I}_{d+1} - \mathbf{S})^+ (d\mathbf{S}) \mathbf{u}.$$

where  $(\cdot)^+$  denotes the Moore–Penrose pseudoinverse. These differentials can be expressed as gradients/Jacobians with respect to  $\text{vec}(\mathbf{S})$ . For that, we use  $\text{tr}(\mathbf{A}^\top \mathbf{B}) = \text{vec}(\mathbf{A})^\top \text{vec}(\mathbf{B})$  in  $d\lambda$  and (55) in  $d\mathbf{u}$ , to obtain

$$\begin{aligned} d\lambda &= \text{tr}(\mathbf{u} \mathbf{u}^\top d\mathbf{S}) = \text{vec}(\mathbf{u} \mathbf{u}^\top)^\top \text{vec}(d\mathbf{S}) = \mathbf{u}^{\otimes 2\top} \text{vec}(d\mathbf{S}), \\ d\mathbf{u} &= (\lambda \mathbf{I}_{d+1} - \mathbf{S})^+ [(d\mathbf{S}) \mathbf{u}] = (\lambda \mathbf{I}_{d+1} - \mathbf{S})^+ [(\mathbf{u}^\top \otimes \mathbf{I}_{d+1}) \text{vec}(d\mathbf{S})]. \end{aligned}$$

These differentials yield the Jacobian matrix

$$\mathbb{D}g(\text{vec}(\mathbf{S})) = \begin{pmatrix} \mathbf{u}^{\otimes 2\top} \\ (\lambda \mathbf{I}_{d+1} - \mathbf{S})^+ (\mathbf{u}^\top \otimes \mathbf{I}_{d+1}) \end{pmatrix}_{(1+(d+1)) \times (d+1)^2}.$$

We specialize the Jacobian at  $\boldsymbol{\Sigma} = a(\rho)\boldsymbol{\mu}\boldsymbol{\mu}^\top + b(\rho)(\mathbf{I}_{d+1} - \boldsymbol{\mu}\boldsymbol{\mu}^\top)$ . First, note that

$$\begin{aligned} a(\rho)\mathbf{I}_{d+1} - \boldsymbol{\Sigma} &= a(\rho)\mathbf{I}_{d+1} - [b(\rho)\mathbf{I}_{d+1} + (a(\rho) - b(\rho))\boldsymbol{\mu}\boldsymbol{\mu}^\top] \\ &= (a(\rho) - b(\rho))(\mathbf{I}_{d+1} - \boldsymbol{\mu}\boldsymbol{\mu}^\top) \\ &= \frac{2\rho}{d(d+3)}(\mathbf{I}_{d+1} - \boldsymbol{\mu}\boldsymbol{\mu}^\top) \end{aligned}$$

so the Moore–Penrose pseudoinverse is

$$(a(\rho)\mathbf{I}_{d+1} - \boldsymbol{\Sigma})^+ = \frac{d(d+3)}{2\rho}(\mathbf{I}_{d+1} - \boldsymbol{\mu}\boldsymbol{\mu}^\top).$$

Therefore,

$$\mathbb{D}g(\text{vec}(\boldsymbol{\Sigma})) = \begin{pmatrix} \partial_{\lambda} g^\top \\ \partial_{\mathbf{u}} g \end{pmatrix} = \begin{pmatrix} \mathbf{u}^{\otimes 2\top} \\ \frac{d(d+3)}{2\rho}(\mathbf{I}_{d+1} - \boldsymbol{\mu}\boldsymbol{\mu}^\top)(\boldsymbol{\mu}^\top \otimes \mathbf{I}_{d+1}) \end{pmatrix}_{(1+(d+1)) \times (d+1)^2}$$

and

$$\sqrt{n} \begin{pmatrix} \lambda(\mathbf{S}) - a(\rho) \\ \mathbf{u}(\mathbf{S}) - \boldsymbol{\mu} \end{pmatrix} \rightsquigarrow \mathcal{N}_{d+2} \left( \mathbf{0}, \mathbb{D}g(\text{vec}(\boldsymbol{\Sigma})) \text{Var}[\mathbf{X}^{\otimes 2}] \mathbb{D}g(\text{vec}(\boldsymbol{\Sigma}))^\top \right).$$

The asymptotic covariance matrix has the following block structure

$$\text{Dg}(\text{vec}(\boldsymbol{\Sigma}))\text{Var}[\mathbf{X}^{\otimes 2}]\text{Dg}(\text{vec}(\boldsymbol{\Sigma}))^\top = \begin{pmatrix} \boldsymbol{\partial}_{\lambda} g^\top \text{Var}[\mathbf{X}^{\otimes 2}] \boldsymbol{\partial}_{\lambda} g & \boldsymbol{\partial}_{\lambda} g^\top \text{Var}[\mathbf{X}^{\otimes 2}] \boldsymbol{\partial}_{\mathbf{u}} g^\top \\ \boldsymbol{\partial}_{\mathbf{u}} g \text{Var}[\mathbf{X}^{\otimes 2}] \boldsymbol{\partial}_{\lambda} g & \boldsymbol{\partial}_{\mathbf{u}} g \text{Var}[\mathbf{X}^{\otimes 2}] \boldsymbol{\partial}_{\mathbf{u}} g^\top \end{pmatrix}.$$

We proceed to evaluate each block separately.

*Block  $\boldsymbol{\partial}_{\lambda} g^\top \text{Var}[\mathbf{X}^{\otimes 2}] \boldsymbol{\partial}_{\lambda} g$ .*

We will use that, for a  $(d+1) \times (d+1)$  matrix  $\mathbf{A}$  and the random vector  $\mathbf{X}$ , due to

$$\mathbf{X}^\top \mathbf{A} \mathbf{X} = \text{tr}(\mathbf{A} \mathbf{X} \mathbf{X}^\top) = \text{vec}(\mathbf{A})^\top \text{vec}(\mathbf{X} \mathbf{X}^\top) = \text{vec}(\mathbf{A})^\top \mathbf{X}^{\otimes 2},$$

we have that

$$\text{vec}(\mathbf{A})^\top \text{Var}[\mathbf{X}^{\otimes 2}] \text{vec}(\mathbf{B}) = \text{Cov}[\mathbf{X}^\top \mathbf{A} \mathbf{X}, \mathbf{X}^\top \mathbf{B} \mathbf{X}].$$

We also use unvectorization operator  $\text{vec}^{-1}(\cdot)$  mapping to  $(d+1) \times (d+1)$  matrices:

$$\text{vec}^{-1}(\boldsymbol{\partial}_{\lambda} g) = \text{vec}^{-1}(\boldsymbol{\mu}^{\otimes 2\top}) = \boldsymbol{\mu} \boldsymbol{\mu}^\top.$$

Using these facts, we compute

$$\begin{aligned} \boldsymbol{\partial}_{\lambda} g^\top \text{Var}[\mathbf{X}^{\otimes 2}] \boldsymbol{\partial}_{\lambda} g &= \text{Cov}[\mathbf{X}^\top \text{vec}^{-1}(\boldsymbol{\partial}_{\lambda} g) \mathbf{X}, \mathbf{X}^\top \text{vec}^{-1}(\boldsymbol{\partial}_{\lambda} g) \mathbf{X}] \\ &= \text{Cov}[\mathbf{X}^\top \boldsymbol{\mu} \boldsymbol{\mu}^\top \mathbf{X}, \mathbf{X}^\top \boldsymbol{\mu} \boldsymbol{\mu}^\top \mathbf{X}] \\ &= \text{Var}[(\boldsymbol{\mu}^\top \mathbf{X})^2] = \mathbb{E}[(\boldsymbol{\mu}^\top \mathbf{X})^4] - \mathbb{E}[(\boldsymbol{\mu}^\top \mathbf{X})^2]^2 \\ &=: v_1(\rho). \end{aligned}$$

We compute these projected moments using  $\tilde{C}_2^{(d-1)/2}(t) = d^{-1}((d+1)t^2 - 1)$  and (35):

$$\begin{aligned} \mathbb{E}[(\boldsymbol{\mu}^\top \mathbf{X})^{2m}] &= \frac{\omega_{d-1}}{\omega_d} \int_{-1}^1 t^{2m} \left\{ 1 + \rho \tilde{C}_2^{(d-1)/2}(t) \right\} (1-t^2)^{d/2-1} dt \\ &= \frac{\omega_{d-1}}{\omega_d} \left\{ \frac{d-\rho}{d} \int_{-1}^1 t^{2m} (1-t^2)^{d/2-1} dt + \frac{\rho(d+1)}{d} \int_{-1}^1 t^{2m+2} (1-t^2)^{d/2-1} dt \right\} \\ &= \frac{\omega_{d-1}}{\omega_d d} \left\{ (d-\rho) \text{B}(m+1/2, d/2) + \rho(d+1) \text{B}(m+3/2, d/2) \right\}. \end{aligned}$$

Specializing for  $m=1$  yields

$$\mathbb{E}[(\boldsymbol{\mu}^\top \mathbf{X})^2] = \frac{d+3+2\rho}{(d+1)(d+3)}$$

and

$$\begin{aligned} \mathbb{E}[(\boldsymbol{\mu}^\top \mathbf{X})^4] &= \frac{\omega_{d-1}}{\omega_d d} \left\{ (d-\rho) \frac{\Gamma(5/2)\Gamma(d/2)}{\Gamma(d/2+5/2)} + \rho(d+1) \frac{\Gamma(7/2)\Gamma(d/2)}{\Gamma(d/2+7/2)} \right\} \\ &= \frac{3(d+5+4\rho)}{(d+1)(d+3)(d+5)}. \end{aligned}$$

Then

$$\begin{aligned} v_1(\rho) &= \mathbb{E}[(\boldsymbol{\mu}^\top \mathbf{X})^4] - \mathbb{E}[(\boldsymbol{\mu}^\top \mathbf{X})^2]^2 \\ &= \frac{3(d+5+4\rho)}{(d+1)(d+3)(d+5)} - \left\{ \frac{d+3+2\rho}{(d+1)(d+3)} \right\}^2 \\ &= 2 \frac{d(d+3)(d+5) + 4(d-1)(d+3)\rho - 2(d+5)\rho^2}{(d+1)^2(d+3)^2(d+5)}. \end{aligned}$$

Blocks  $\partial_\lambda g^\top \text{Var}[\mathbf{X}^{\otimes 2}] \partial_{ug}^\top$  and  $\partial_{ug} \text{Var}[\mathbf{X}^{\otimes 2}] \partial_\lambda g$ .

We show that these two blocks are zero matrices. By symmetry, it suffices to consider  $\partial_\lambda g^\top \text{Var}[\mathbf{X}^{\otimes 2}] \partial_{ug}^\top$ . We check that

$$(\partial_\lambda g^\top \text{Var}[\mathbf{X}^{\otimes 2}] \partial_{ug}^\top) \mathbf{w} = \mathbf{0}, \quad \text{for all } \mathbf{w} \in \mathbb{R}^{d+1}.$$

First, we unvectorize to  $(d+1) \times (d+1)$  matrices:

$$\begin{aligned} \text{vec}^{-1}(\partial_{ug}^\top \mathbf{w}) &= \frac{d(d+3)}{2\rho} \text{vec}^{-1}\left([(I_{d+1} - \boldsymbol{\mu}\boldsymbol{\mu}^\top)(\boldsymbol{\mu}^\top \otimes I_{d+1})]^\top \mathbf{w}\right) \\ &= \frac{d(d+3)}{2\rho} \text{vec}^{-1}\left((\boldsymbol{\mu} \otimes I_{d+1})[(I_{d+1} - \boldsymbol{\mu}\boldsymbol{\mu}^\top)\mathbf{w}]\right) \\ &= \frac{d(d+3)}{2\rho} [(I_{d+1} - \boldsymbol{\mu}\boldsymbol{\mu}^\top)\mathbf{w}] \boldsymbol{\mu}^\top \end{aligned}$$

where we used that  $\text{vec}(\mathbf{a}\mathbf{b}^\top) = (\mathbf{b} \otimes I_{d+1})\mathbf{a}$ .

Joining these results, we have

$$\begin{aligned} &(\partial_\lambda g)^\top \text{Var}[\mathbf{X}^{\otimes 2}] (\partial_{ug}^\top \mathbf{w}) \\ &= \text{Cov}[\mathbf{X}^\top \text{vec}^{-1}(\partial_\lambda g) \mathbf{X}, \mathbf{X}^\top \text{vec}^{-1}(\partial_{ug}^\top \mathbf{w}) \mathbf{X}] \\ &= \text{Cov}[(\boldsymbol{\mu}^\top \mathbf{X})^2, \mathbf{X}^\top \text{vec}^{-1}(\partial_{ug}^\top \mathbf{w}) \mathbf{X}] \\ &= \frac{d(d+3)}{2\rho} \text{Cov}[(\boldsymbol{\mu}^\top \mathbf{X})^2, [\mathbf{X}^\top (I_{d+1} - \boldsymbol{\mu}\boldsymbol{\mu}^\top)\mathbf{w}] (\boldsymbol{\mu}^\top \mathbf{X})]. \end{aligned}$$

Using the tangent-normal decomposition  $\mathbf{X} = \boldsymbol{\mu}T + \mathbf{B}_\mu \sqrt{1-T^2} \boldsymbol{\Xi}$  with  $T = \boldsymbol{\mu}^\top \mathbf{X}$  and  $\boldsymbol{\Xi} \sim \text{Unif}(\mathbb{S}^{d-1})$  independent, it follows that

$$\mathbb{E}[(\boldsymbol{\mu}^\top \mathbf{X})^3 [\mathbf{X}^\top (I_{d+1} - \boldsymbol{\mu}\boldsymbol{\mu}^\top)\mathbf{w}]] = \mathbb{E}[T^3 \sqrt{1-T^2}] \mathbb{E}[\boldsymbol{\Xi}^\top (\mathbf{B}_\mu^\top \mathbf{w})] = \mathbf{0} \quad (39)$$

and hence the covariance is null. Consequently,  $\partial_\lambda g^\top \text{Var}[\mathbf{X}^{\otimes 2}] \partial_{ug}^\top = \mathbf{0}^\top$ .

*Block  $\partial_{ug} \text{Var}[\mathbf{X}^{\otimes 2}] \partial_{ug}^\top$ .*

We compute the  $ij$ th element of this block, for  $i, j = 1, \dots, d+1$ . First, note that

$$\text{vec}^{-1}(\partial_{ug}^\top \mathbf{e}_i) = \frac{d(d+3)}{2\rho} [(I_{d+1} - \boldsymbol{\mu}\boldsymbol{\mu}^\top) \mathbf{e}_i] \boldsymbol{\mu}^\top.$$

We have

$$\begin{aligned} &\mathbf{e}_i^\top \partial_{ug} \text{Var}[\mathbf{X}^{\otimes 2}] \partial_{ug}^\top \mathbf{e}_j \\ &= (\partial_{ug}^\top \mathbf{e}_i)^\top \text{Var}[\mathbf{X}^{\otimes 2}] (\partial_{ug}^\top \mathbf{e}_j) \\ &= \text{Cov}[\mathbf{X}^\top \text{vec}^{-1}(\partial_{ug}^\top \mathbf{e}_i) \mathbf{X}, \mathbf{X}^\top \text{vec}^{-1}(\partial_{ug}^\top \mathbf{e}_j) \mathbf{X}] \\ &= \frac{d^2(d+3)^2}{4\rho^2} \text{Cov}[(\boldsymbol{\mu}^\top \mathbf{X})[\mathbf{e}_i^\top (I_{d+1} - \boldsymbol{\mu}\boldsymbol{\mu}^\top) \mathbf{X}], (\boldsymbol{\mu}^\top \mathbf{X})[\mathbf{X}^\top (I_{d+1} - \boldsymbol{\mu}\boldsymbol{\mu}^\top) \mathbf{e}_j]] \\ &= \frac{d^2(d+3)^2}{4\rho^2} \mathbf{e}_i^\top \left\{ \mathbb{E}[(\boldsymbol{\mu}^\top \mathbf{X})^2 [(I_{d+1} - \boldsymbol{\mu}\boldsymbol{\mu}^\top) \mathbf{X}] [\mathbf{X}^\top (I_{d+1} - \boldsymbol{\mu}\boldsymbol{\mu}^\top)]] \right. \\ &\quad \left. - (I_{d+1} - \boldsymbol{\mu}\boldsymbol{\mu}^\top) \mathbb{E}[(\boldsymbol{\mu}^\top \mathbf{X}) \mathbf{X}] \mathbb{E}[(\boldsymbol{\mu}^\top \mathbf{X}) \mathbf{X}^\top] (I_{d+1} - \boldsymbol{\mu}\boldsymbol{\mu}^\top) \right\} \mathbf{e}_j \\ &= \frac{d^2(d+3)^2}{4\rho^2} \mathbf{e}_i^\top (I_{d+1} - \boldsymbol{\mu}\boldsymbol{\mu}^\top) \mathbb{E}[(\boldsymbol{\mu}^\top \mathbf{X})^2 \mathbf{X} \mathbf{X}^\top] (I_{d+1} - \boldsymbol{\mu}\boldsymbol{\mu}^\top) \mathbf{e}_j, \end{aligned} \quad (40)$$

where we used that  $(I_{d+1} - \boldsymbol{\mu}\boldsymbol{\mu}^\top) \mathbb{E}[(\boldsymbol{\mu}^\top \mathbf{X}) \mathbf{X}] = \mathbf{0}$  due to an analogous argument as in (39).

Thus, it remains to compute the following matrix:

$$\begin{aligned}
& (\mathbf{I}_{d+1} - \boldsymbol{\mu}\boldsymbol{\mu}^\top) \mathbb{E}[(\boldsymbol{\mu}^\top \mathbf{X})^2 \mathbf{X} \mathbf{X}^\top] \\
&= (\mathbf{I}_{d+1} - \boldsymbol{\mu}\boldsymbol{\mu}^\top) \frac{\omega_{d-1}}{\omega_d} \int_{-1}^1 t^2 \left[ t^2 \boldsymbol{\mu}\boldsymbol{\mu}^\top + \frac{1-t^2}{d} (\mathbf{I}_{d+1} - \boldsymbol{\mu}\boldsymbol{\mu}^\top) \right] \left\{ 1 + \frac{\rho}{d} ((d+1)t^2 - 1) \right\} \\
&\quad \times (1-t^2)^{d/2-1} dt \\
&= (\mathbf{I}_{d+1} - \boldsymbol{\mu}\boldsymbol{\mu}^\top) \frac{\omega_{d-1}}{\omega_d d^2} \left\{ \rho(d+1) \int_{-1}^1 t^4 (1-t^2)^{d/2} dt + (d-\rho) \int_{-1}^1 t^2 (1-t^2)^{d/2} dt \right\} \\
&= (\mathbf{I}_{d+1} - \boldsymbol{\mu}\boldsymbol{\mu}^\top) \frac{\omega_{d-1}}{\omega_d d^2} \{ \rho(d+1) B(5/2, d/2+1) + (d-\rho) B(3/2, d/2+1) \},
\end{aligned}$$

where the last line used (35). Further simplification gives

$$\begin{aligned}
& (\mathbf{I}_{d+1} - \boldsymbol{\mu}\boldsymbol{\mu}^\top) \mathbb{E}[(\boldsymbol{\mu}^\top \mathbf{X})^2 \mathbf{X} \mathbf{X}^\top] \\
&= (\mathbf{I}_{d+1} - \boldsymbol{\mu}\boldsymbol{\mu}^\top) \frac{\omega_{d-1}}{\omega_d d^2} \left\{ \rho(d+1) \frac{\Gamma(5/2)\Gamma(d/2+1)}{\Gamma(d/2+7/2)} + (d-\rho) \frac{\Gamma(3/2)\Gamma(d/2+1)}{\Gamma(d/2+5/2)} \right\} \\
&= (\mathbf{I}_{d+1} - \boldsymbol{\mu}\boldsymbol{\mu}^\top) \frac{d(d+5) + 2(d-1)\rho}{d(d+1)(d+3)(d+5)}. \tag{41}
\end{aligned}$$

Replacing (41) into (40) gives

$$\begin{aligned}
& \mathbf{e}_i^\top \partial_{\mathbf{u}g} \text{Var}[\mathbf{X}^{\otimes 2}] \partial_{\mathbf{u}g}^\top \mathbf{e}_j \\
&= \frac{d^2(d+3)^2}{4\rho^2} \mathbf{e}_i^\top (\mathbf{I}_{d+1} - \boldsymbol{\mu}\boldsymbol{\mu}^\top) \frac{d(d+5) + 2(d-1)\rho}{d(d+1)(d+3)(d+5)} \mathbf{e}_j \\
&= \frac{d(d+3)[d(d+5) + 2(d-1)\rho]}{4\rho^2(d+1)(d+5)} \mathbf{e}_i^\top (\mathbf{I}_{d+1} - \boldsymbol{\mu}\boldsymbol{\mu}^\top) \mathbf{e}_j \\
&=: v_2(\rho) \mathbf{e}_i^\top (\mathbf{I}_{d+1} - \boldsymbol{\mu}\boldsymbol{\mu}^\top) \mathbf{e}_j,
\end{aligned}$$

in turn providing  $\partial_{\mathbf{u}g} \text{Var}[\mathbf{X}^{\otimes 2}] \partial_{\mathbf{u}g}^\top = v_2(\rho) (\mathbf{I}_{d+1} - \boldsymbol{\mu}\boldsymbol{\mu}^\top)$ .

Putting together the three asymptotic covariance blocks gives

$$\sqrt{n} \begin{pmatrix} \lambda(\mathbf{S}) - a(\rho) \\ \mathbf{u}(\mathbf{S}) - \boldsymbol{\mu} \end{pmatrix} \rightsquigarrow \mathcal{N}_{d+2} \left( \mathbf{0}, \begin{pmatrix} v_1(\rho) & \mathbf{0}^\top \\ \mathbf{0} & v_2(\rho) (\mathbf{I}_{d+1} - \boldsymbol{\mu}\boldsymbol{\mu}^\top) \end{pmatrix} \right).$$

Finally, we apply the linear map  $h(x) = ((d+3)/2)((d+1)x - 1)$  to the first entry, for which  $h(\lambda(\mathbf{S})) = \hat{\rho}_{\text{MM},2}$  and  $h(a(\rho)) = \rho$ . Another application of the delta method yields the stated result:

$$\sqrt{n} \begin{pmatrix} \hat{\rho}_{\text{MM},2} - \rho \\ \hat{\boldsymbol{\mu}}_{\text{MM},2} - \boldsymbol{\mu} \end{pmatrix} \rightsquigarrow \mathcal{N}_{d+2} \left( \mathbf{0}, \begin{pmatrix} \sigma_{\text{MM},2}^2(\rho) & \mathbf{0}^\top \\ \mathbf{0} & \sigma_{\text{MM},2}^2(\boldsymbol{\mu}) (\mathbf{I}_{d+1} - \boldsymbol{\mu}\boldsymbol{\mu}^\top) \end{pmatrix} \right), \tag{42}$$

where  $\sigma_{\text{MM},2}^2(\boldsymbol{\mu}) = v_2(\rho)$  and

$$\sigma_{\text{MM},2}^2(\rho) = \left( \frac{(d+3)(d+1)}{2} \right)^2 v_1(\rho) = \frac{d(d+3)}{2} + \frac{2(d-1)(d+3)}{d+5} \rho - \rho^2.$$

For  $d = 1$ ,  $\sigma_{\text{MM},2}^2(\boldsymbol{\mu}) = 2\rho^{-2} = \sigma_{\text{MM},1}^2(\boldsymbol{\mu})$  and  $\sigma_{\text{MM},2}^2(\rho) = 2 - \rho^2 = \sigma_{\text{MM},1}^2(\rho)$ .

Reordering the components of (42) concludes the proof.  $\square$

*Proof of Theorem 4.3.* The estimator is motivated by the expectation of the Gegenbauer moment:

$$\mathbb{E}[C_k^{(d-1)/2}(\mathbf{X}^\top \boldsymbol{\mu})] = \frac{1}{\omega_d} \int_{\mathbb{S}^d} C_k^{(d-1)/2}(\mathbf{x}^\top \boldsymbol{\mu}) \{1 + \rho \tilde{C}_k^{(d-1)/2}(\mathbf{x}^\top \boldsymbol{\mu})\} \sigma_d(d\mathbf{x})$$

$$\begin{aligned}
&= \rho \frac{\omega_{d-1}}{\omega_d C_k^{(d-1)/2}(1)} \int_{-1}^1 [C_k^{(d-1)/2}(t)]^2 (1-t^2)^{d/2-1} dt \\
&= \rho \frac{\omega_{d-1}}{\omega_d C_k^{(d-1)/2}(1)} c_{k,d} \\
&= \frac{\rho}{\tau_{k,d}},
\end{aligned}$$

where we have used the orthogonality of the Gegenbauer polynomials and (5). Consequently, the unbiasedness (i) follows immediately. Strong consistency (ii) follows from the SLLN.

The CLT readily entails the asymptotic normality (iii). The variance of  $\hat{\rho}_{GM}$  follows from

$$\begin{aligned}
&E[\{C_k^{(d-1)/2}(\mathbf{X}^\top \boldsymbol{\mu})\}^2] \\
&= \frac{\omega_{d-1}}{\omega_d} \int_{-1}^1 [C_k^{(d-1)/2}(t)]^2 \{1 + \rho \tilde{C}_k^{(d-1)/2}(t)\} (1-t^2)^{d/2-1} dt \\
&= \tau_{k,d}^{-2} \left\{ d_{k,d} + \rho \tau_{k,d} \frac{I_3(k)}{c_{k,d}} \right\},
\end{aligned}$$

where

$$I_3(k) := \int_{-1}^1 [C_k^{(d-1)/2}(t)]^3 (1-t^2)^{d/2-1} dt.$$

We then have

$$\begin{aligned}
\text{Var}[C_k^{(d-1)/2}(\mathbf{X}^\top \boldsymbol{\mu})] &= E[\{C_k^{(d-1)/2}(\mathbf{X}^\top \boldsymbol{\mu})\}^2] - E[C_k^{(d-1)/2}(\mathbf{X}^\top \boldsymbol{\mu})]^2 \\
&= \tau_{k,d}^{-2} \left\{ d_{k,d} + \rho \tau_{k,d} \frac{I_3(k)}{c_{k,d}} - \rho^2 \right\}.
\end{aligned}$$

For  $k$  odd,  $I_3(k) = 0$  by symmetry. Using Lemma 2 in Fernández-de-Marcos and García-Portugués (2023), we can compute  $I_3(k)$  for  $k$  even. For  $d \geq 2$ ,  $I_3(k)$  is given as the term  $a_{k/2,k,k,(d-1)/2}$  defined therein:

$$\begin{aligned}
\left(1 + \frac{2k}{d-1}\right) \frac{I_3(k)}{c_{k,d}} &= \left(1 + \frac{2k}{d-1}\right) a_{k/2,k,k,(d-1)/2} \\
&= \left(1 + \frac{2k}{d-1}\right) \frac{2k+d-1}{3k+d-1} \frac{1}{(k/2)!} \binom{k}{k/2} \\
&\quad \times \frac{\Gamma((d+k-1)/2)B((d+k-1)/2, (d+k-1)/2)}{\Gamma((d-1)/2)B((d+3k-1)/2, (d-1)/2)} \\
&= \frac{(2k+d-1)^2}{(3k+d-1)(d-1)} \frac{k!}{((k/2)!)^3} \\
&\quad \times \frac{\Gamma((d+k-1)/2)^3 \Gamma(d+3k/2-1)}{\Gamma(d+k-1) \Gamma((d-1)/2)^2 \Gamma((d+3k-1)/2)} \\
&=: \eta_{k,d}.
\end{aligned} \tag{43}$$

For  $d = 1$ ,  $I_3(k) = 0 =: \eta_{k,1}$  for  $k$  even.

The variance of  $\hat{\rho}_{GM}$  is then

$$\sigma_{GM,k}^2(\rho) = \tau_{k,d}^2 \text{Var}[C_k^{(d-1)/2}(\mathbf{X}^\top \boldsymbol{\mu})] = d_{k,d} + \rho \eta_{k,d} \mathbf{1}_{\{k \text{ even}\}} - \rho^2 \tag{44}$$

That  $\sigma_{GM,1}^2(\rho) = \sigma_{MM,1}^2(\rho)$  follows immediately from (44) and (43). For  $k = 2$  and  $d \geq 2$ ,

$$\eta_{2,d} = \frac{8(d+3)}{(d+5)(d+1)(d-1)} \frac{\Gamma((d+1)/2)^2 (d+1)}{\Gamma((d-1)/2)^2} = \frac{2(d-1)(d+3)}{(d+5)},$$

so that  $\sigma_{GM,2}^2(\rho) = \sigma_{MM,2}^2(\rho)$  for  $d \geq 2$ .  $\square$

*Proof of Theorem 4.4.* The proof is split in computing the Fisher information matrix  $\mathcal{I}(\boldsymbol{\xi})$ , obtaining the asymptotic covariance matrix of  $(\hat{\rho}_{\text{MLE}}, \hat{\boldsymbol{\mu}}_{\text{MLE}})$ , and finally verifying conditions for the ML estimation asymptotics that ensure statements 4.4(i)–4.4(iii).

*Computation of  $\mathcal{I}(\boldsymbol{\xi})$  for  $d \geq 2$ .*

We begin by deriving the score function  $\mathbf{x} \mapsto \dot{\ell}(\boldsymbol{\xi}) := \frac{\partial}{\partial \boldsymbol{\xi}} \ell(\boldsymbol{\xi})$ , where

$$\ell(\boldsymbol{\xi}) := \log f_{C_k}(\mathbf{x}; \boldsymbol{\xi}) = -\log(\omega_d) + \log \left\{ 1 + \|\boldsymbol{\xi}\| \tilde{C}_k^{(d-1)/2}(\mathbf{x}^\top \boldsymbol{\xi} / \|\boldsymbol{\xi}\|) \right\}$$

We proceed to differentiate with respect to  $\boldsymbol{\xi}$ , use that  $[C_k^{(d-1)/2}(x)]' = (d-1)C_{k-1}^{(d+1)/2}(x)$ , and rearrange terms:

$$\begin{aligned} \dot{\ell}(\boldsymbol{\xi}) &= \frac{1}{C_k^{(d-1)/2}(1) + \|\boldsymbol{\xi}\| C_k^{(d-1)/2}(\mathbf{x}^\top \boldsymbol{\xi} / \|\boldsymbol{\xi}\|)} \\ &\quad \times \left\{ \|\boldsymbol{\xi}\|^{-1} \boldsymbol{\xi} C_k^{(d-1)/2}(\mathbf{x}^\top \boldsymbol{\xi} / \|\boldsymbol{\xi}\|) + (d-1) C_{k-1}^{(d+1)/2}(\mathbf{x}^\top \boldsymbol{\xi} / \|\boldsymbol{\xi}\|) (\mathbf{I}_{d+1} - \|\boldsymbol{\xi}\|^{-2} \boldsymbol{\xi} \boldsymbol{\xi}^\top) \mathbf{x} \right\} \\ &= \frac{1}{C_k^{(d-1)/2}(1) + \rho C_k^{(d-1)/2}(\mathbf{x}^\top \boldsymbol{\mu})} \\ &\quad \times \left\{ \left[ C_k^{(d-1)/2}(\mathbf{x}^\top \boldsymbol{\mu}) - (d-1) C_{k-1}^{(d+1)/2}(\mathbf{x}^\top \boldsymbol{\mu}) (\mathbf{x}^\top \boldsymbol{\mu}) \right] \boldsymbol{\mu} + \left[ (d-1) C_{k-1}^{(d+1)/2}(\mathbf{x}^\top \boldsymbol{\mu}) \right] \mathbf{x} \right\}. \end{aligned}$$

Let us consider the tangent-normal change of variables  $t = \mathbf{x}^\top \boldsymbol{\mu}$ , so that  $\mathbf{x} = t\boldsymbol{\mu} + (1-t^2)^{1/2} \mathbf{B}_\boldsymbol{\mu} \boldsymbol{\gamma}$  for some  $\boldsymbol{\gamma} \in \mathbb{S}^{d-1}$  (see the proof of Theorem 3.1(iv)). Then,

$$\begin{aligned} \dot{\ell}(\boldsymbol{\xi}) &= \frac{1}{C_k^{(d-1)/2}(1) + \rho C_k^{(d-1)/2}(t)} \\ &\quad \times \left\{ C_k^{(d-1)/2}(t) \boldsymbol{\mu} + \left[ (d-1) C_{k-1}^{(d+1)/2}(t) (1-t^2)^{1/2} \right] \mathbf{B}_\boldsymbol{\mu} \boldsymbol{\gamma} \right\}. \end{aligned}$$

From this expression we proceed to obtain the Fisher information matrix  $\mathcal{I}(\boldsymbol{\xi})$ . First,

$$\begin{aligned} \dot{\ell}(\boldsymbol{\xi}) \dot{\ell}(\boldsymbol{\xi})^\top &= \frac{1}{(C_k^{(d-1)/2}(1) + \rho C_k^{(d-1)/2}(t))^2} \\ &\quad \times \left\{ C_k^{(d-1)/2}(t)^2 \boldsymbol{\mu} \boldsymbol{\mu}^\top + (d-1)^2 C_{k-1}^{(d+1)/2}(t)^2 (1-t^2)^2 \mathbf{B}_\boldsymbol{\mu} \boldsymbol{\gamma} \boldsymbol{\gamma}^\top \mathbf{B}_\boldsymbol{\mu}^\top \right. \\ &\quad \left. + C_k^{(d-1)/2}(t) \left[ (d-1) C_{k-1}^{(d+1)/2}(t) (1-t^2)^{1/2} \right] \left[ \boldsymbol{\mu} (\mathbf{B}_\boldsymbol{\mu} \boldsymbol{\gamma})^\top + (\mathbf{B}_\boldsymbol{\mu} \boldsymbol{\gamma}) \boldsymbol{\mu}^\top \right] \right\}. \end{aligned} \quad (45)$$

Second, using  $\int_{\mathbb{S}^{d-1}} \boldsymbol{\gamma} \sigma_{d-1}(d\boldsymbol{\gamma}) = \mathbf{0}$ ,  $\int_{\mathbb{S}^{d-1}} \boldsymbol{\gamma} \boldsymbol{\gamma}^\top \sigma_{d-1}(d\boldsymbol{\gamma}) = (\omega_{d-1}/d) \mathbf{I}_d$ ,  $\boldsymbol{\mu}^\top \mathbf{B}_\boldsymbol{\mu} = \mathbf{0}$ , and also  $\mathbf{B}_\boldsymbol{\mu} \mathbf{B}_\boldsymbol{\mu}^\top = \mathbf{I}_{d+1} - \boldsymbol{\mu} \boldsymbol{\mu}^\top$ , we have

$$\begin{aligned} \mathcal{I}(\boldsymbol{\xi}) &= \mathbb{E}[\dot{\ell}(\boldsymbol{\xi}) \dot{\ell}(\boldsymbol{\xi})^\top] \\ &= \int_{\mathbb{S}^{d-1}} \int_{-1}^1 \frac{1}{(C_k^{(d-1)/2}(1) + \rho C_k^{(d-1)/2}(t))^2} \\ &\quad \times \left\{ C_k^{(d-1)/2}(t)^2 \boldsymbol{\mu} \boldsymbol{\mu}^\top + (d-1)^2 C_{k-1}^{(d+1)/2}(t)^2 (1-t^2)^2 \mathbf{B}_\boldsymbol{\mu} \boldsymbol{\gamma} \boldsymbol{\gamma}^\top \mathbf{B}_\boldsymbol{\mu}^\top \right\} \\ &\quad \times \frac{1}{\omega_d} \left\{ 1 + \rho \tilde{C}_k^{(d-1)/2}(t) \right\} (1-t^2)^{d/2-1} dt \sigma_{d-1}(d\boldsymbol{\gamma}) \\ &= \frac{\omega_{d-1}}{\omega_d C_k^{(d-1)/2}(1)} \int_{-1}^1 \frac{\{C_k^{(d-1)/2}(1) + \rho C_k^{(d-1)/2}(t)\}}{(C_k^{(d-1)/2}(1) + \rho C_k^{(d-1)/2}(t))^2} \end{aligned}$$

$$\begin{aligned}
& \times \left[ C_k^{(d-1)/2}(t)^2 \boldsymbol{\mu} \boldsymbol{\mu}^\top + (d-1)^2 C_{k-1}^{(d+1)/2}(t)^2 \frac{1-t^2}{d} (\mathbf{I}_{d+1} - \boldsymbol{\mu} \boldsymbol{\mu}^\top) \right] \\
& \times (1-t^2)^{d/2-1} dt \\
& = A_k(\rho) \boldsymbol{\mu} \boldsymbol{\mu}^\top + B_k(\rho) (\mathbf{I}_{d+1} - \boldsymbol{\mu} \boldsymbol{\mu}^\top),
\end{aligned}$$

where

$$\begin{aligned}
A_k(\rho) &= \frac{\omega_{d-1}}{\omega_d C_k^{(d-1)/2}(1)} \int_{-1}^1 \frac{C_k^{(d-1)/2}(t)^2 (1-t^2)^{d/2-1}}{C_k^{(d-1)/2}(1) + \rho C_k^{(d-1)/2}(t)} dt, \\
B_k(\rho) &= \frac{\omega_{d-1}}{\omega_d C_k^{(d-1)/2}(1)} \frac{(d-1)^2}{d} \int_{-1}^1 \frac{C_{k-1}^{(d+1)/2}(t)^2 (1-t^2)^{d/2}}{C_k^{(d-1)/2}(1) + \rho C_k^{(d-1)/2}(t)} dt.
\end{aligned}$$

For  $d = 2$  and  $k = 1$ ,

$$\begin{aligned}
A_1(\rho) &= \frac{1}{2} \int_{-1}^1 \frac{t^2}{1+\rho t} dt = \frac{\tanh^{-1}(\rho) - \rho}{\rho^3}, \\
B_1(\rho) &= \frac{1}{4} \int_{-1}^1 \frac{1-t^2}{1+\rho t} dt = \frac{\rho - (1-\rho^2) \tanh^{-1}(\rho)}{2\rho^3}.
\end{aligned}$$

The matrix  $\mathcal{I}(\boldsymbol{\xi})$  is positive definite since  $A_k(\rho) > 0$  and  $B_k(\rho) > 0$  for the specified ranges of  $\rho$  (the integrands are positive). Its inverse follows straightforwardly by the spectral theorem:

$$\mathcal{I}(\boldsymbol{\xi})^{-1} = \frac{1}{A_k(\rho)} \boldsymbol{\mu} \boldsymbol{\mu}^\top + \frac{1}{B_k(\rho)} (\mathbf{I}_{d+1} - \boldsymbol{\mu} \boldsymbol{\mu}^\top).$$

*Computation of  $\mathcal{I}(\boldsymbol{\xi})$  for  $d = 1$ .*

When  $d = 1$  the derivation of  $\dot{\ell}(\boldsymbol{\xi})$  is analogous but using that  $[T_k(x)]' = kU_{k-1}(x)$ , with  $U_k(x) = \sin((k+1)\cos^{-1}(x))/\sqrt{1-x^2}$  the Chebyshev polynomial of the second kind. We can directly replace in (45)  $C_k^{(d-1)/2}(t)$  with  $T_k(t)$  and  $(d-1)C_{k-1}^{(d+1)/2}(t)$  with  $kU_{k-1}(t)$ , giving

$$\begin{aligned}
\dot{\ell}(\boldsymbol{\xi}) \dot{\ell}(\boldsymbol{\xi})^\top &= \frac{1}{(1+\rho T_k(t))^2} \left\{ T_k(t)^2 \boldsymbol{\mu} \boldsymbol{\mu}^\top + k^2 U_{k-1}(t)^2 (1-t^2) \mathbf{B}_\mu \boldsymbol{\gamma} \boldsymbol{\gamma}^\top \mathbf{B}_\mu^\top \right. \\
&\quad \left. + T_k(t) \left[ kU_{k-1}(t)(1-t^2)^{1/2} \right] \left[ \boldsymbol{\mu} (\mathbf{B}_\mu \boldsymbol{\gamma})^\top + (\mathbf{B}_\mu \boldsymbol{\gamma}) \boldsymbol{\mu}^\top \right] \right\},
\end{aligned}$$

with the tangent-normal change of variables  $t = \mathbf{x}^\top \boldsymbol{\mu}$  now with  $\boldsymbol{\gamma} \in \mathbb{S}^0 = \{-1, 1\}$  and  $\mathbf{B}_\mu = (\mu_2, -\mu_1)^\top$ . Clearly,  $\int_{\mathbb{S}^0} \gamma \sigma_0(d\gamma) = 0$ ,  $\int_{\mathbb{S}^0} \gamma^2 \sigma_0(d\gamma) = 2$ ,  $\boldsymbol{\mu}^\top \mathbf{B}_\mu = \mathbf{0}$ , and also  $\mathbf{B}_\mu \mathbf{B}_\mu^\top = \mathbf{I}_2 - \boldsymbol{\mu} \boldsymbol{\mu}^\top$ . Using these, we have

$$\begin{aligned}
\mathcal{I}(\boldsymbol{\xi}) &= \mathbb{E}[\dot{\ell}(\boldsymbol{\xi}) \dot{\ell}(\boldsymbol{\xi})^\top] \\
&= \frac{1}{\pi} \int_{-1}^1 \frac{1+\rho T_k(t)}{\{1+\rho T_k(t)\}^2} \left[ T_k(t)^2 \boldsymbol{\mu} \boldsymbol{\mu}^\top + k^2 U_{k-1}(t)^2 (1-t^2) (\mathbf{I}_2 - \boldsymbol{\mu} \boldsymbol{\mu}^\top) \right] (1-t^2)^{-1/2} dt \\
&= \frac{1}{\pi} \int_{-1}^1 \frac{1}{1+\rho T_k(t)} \left[ T_k(t)^2 \boldsymbol{\mu} \boldsymbol{\mu}^\top + k^2 U_{k-1}(t)^2 (1-t^2) (\mathbf{I}_2 - \boldsymbol{\mu} \boldsymbol{\mu}^\top) \right] (1-t^2)^{-1/2} dt \\
&= A_k(\rho) \boldsymbol{\mu} \boldsymbol{\mu}^\top + B_k(\rho) (\mathbf{I}_2 - \boldsymbol{\mu} \boldsymbol{\mu}^\top),
\end{aligned}$$

where

$$A_k(\rho) = \frac{1}{\pi} \int_{-1}^1 \frac{T_k(t)^2 (1-t^2)^{-1/2}}{1+\rho T_k(t)} dt = \frac{1}{\pi} \int_0^\pi \frac{\cos(k\theta)^2}{1+\rho \cos(k\theta)} d\theta = \frac{1-\sqrt{1-\rho^2}}{\rho^2 \sqrt{1-\rho^2}},$$

$$B_k(\rho) = \frac{k^2}{\pi} \int_{-1}^1 \frac{U_{k-1}(t)^2(1-t^2)^{1/2}}{1+\rho T_k(t)} dt = \frac{k^2}{\pi} \int_0^\pi \frac{\sin(k\theta)^2}{1+\rho \cos(k\theta)} d\theta = k^2 \frac{1-\sqrt{1-\rho^2}}{\rho^2}.$$

The matrix  $\mathcal{I}(\xi)$  is also positive definite since  $A_k(\rho) > 0$  and  $B_k(\rho) > 0$  for the specified ranges of  $\rho$ .

*Asymptotic covariance matrix of  $(\hat{\rho}_{\text{ML}}, \hat{\mu}_{\text{ML}})$ .*

As in the proof of Theorem 4.1(i), we apply the delta method for  $g(\mathbf{x}) := (\|\mathbf{x}\|, \mathbf{x}/\|\mathbf{x}\|)$ ,  $\mathbf{x} \neq \mathbf{0}$ , now on (47). The resulting asymptotic covariance matrix is

$$\begin{aligned} \mathbb{D}g(\xi)\mathcal{I}(\xi)^{-1}\mathbb{D}g(\xi)^\top &= \begin{pmatrix} A_k(\rho)^{-1}\mu^\top \\ [B_k(\rho)\rho]^{-1}(\mathbf{I}_{d+1} - \mu\mu^\top) \end{pmatrix} (\mu \quad \rho^{-1}(\mathbf{I}_{d+1} - \mu\mu^\top)) \\ &= \begin{pmatrix} A_k(\rho)^{-1} & \mathbf{0}^\top \\ \mathbf{0} & [B_k(\rho)\rho^2]^{-1}(\mathbf{I}_{d+1} - \mu\mu^\top) \end{pmatrix}. \end{aligned}$$

The statement in 4.4(iii) follows after rearranging the components:

$$\sqrt{n} \begin{pmatrix} \hat{\rho}_n - \rho \\ \hat{\mu}_n - \mu \end{pmatrix} \rightsquigarrow \mathcal{N}_{d+2} \left( \mathbf{0}, \begin{pmatrix} \sigma_{\text{ML}}^2(\rho) & \mathbf{0}^\top \\ \mathbf{0} & \sigma_{\text{ML}}^2(\mu)(\mathbf{I}_{d+1} - \mu\mu^\top) \end{pmatrix} \right),$$

where  $\sigma_{\text{ML}}^2(\rho) = A_k(\rho)^{-1}$  and  $\sigma_{\text{ML}}^2(\mu) = [B_k(\rho)\rho^2]^{-1}$ .

*Conditions for ML estimation asymptotics.*

We verify the ‘‘classical conditions’’ for asymptotic normality of  $Z$ -estimators, as given in van der Vaart (1998, Theorems 5.41 and 5.42). These conditions are straightforward to check due to the smoothness of the spherical cardioid in the  $\xi$ -parametrization (14) and the compactness of  $\mathbb{S}^d$ . We provide them here for the sake of completeness.

Let  $\xi_0$  denote the true parameter. In the  $\xi$ -parametrization, the open parameter space (15) is  $\Xi \subset \{\xi \in \mathbb{R}^{d+1} : 0 < \|\xi\| < \rho_\star\}$  for  $0 < \rho_\star < 1$ , and  $\xi_0 \in \Xi$ . Denote  $\psi_\xi(\mathbf{x}) := \dot{\ell}(\xi) = \frac{\partial}{\partial \xi} \log f_{C_k}(\mathbf{x}; \xi)$ , with  $\mathbf{x} \in \mathbb{S}^d$  and  $\xi \in \Xi$ . The function  $\xi \mapsto \psi_\xi(\mathbf{x})$  is twice continuously differentiable for every  $\mathbf{x} \in \mathbb{S}^d$  because of the (infinite) smoothness of  $f_{C_k}(\mathbf{x}; \xi) = \omega_d^{-1}\{1 + \|\xi\|\tilde{C}_k^{(d-1)/2}(\mathbf{x}^\top \xi / \|\xi\|)\}$  for  $(\mathbf{x}, \xi) \in \mathbb{S}^d \times \Xi$ . Due to the boundedness of  $\mathbf{x} \mapsto \psi_\xi(\mathbf{x})$ , the dominated convergence theorem guarantees interchangeability of derivatives and integral sign, giving

$$\mathbb{E}_{\xi_0}[\psi_{\xi_0}(\mathbf{X})] = \int_{\mathbb{S}^d} \frac{\partial}{\partial \xi} \Big|_{\xi=\xi_0} f_{C_k}(\mathbf{x}; \xi) \sigma_d(d\mathbf{x}) = \frac{\partial}{\partial \xi} \Big|_{\xi=\xi_0} \int_{\mathbb{S}^d} f_{C_k}(\mathbf{x}; \xi) \sigma_d(d\mathbf{x}) = \mathbf{0}. \quad (46)$$

Also, trivially,  $\mathbb{E}_{\xi_0}[\|\psi_{\xi_0}(\mathbf{X})\|^2] \leq \sup_{\mathbf{x} \in \mathbb{S}^d} \|\psi_{\xi_0}(\mathbf{x})\|^2 < \infty$ . The Fisher information matrix  $\mathcal{I}(\xi_0) = \mathbb{E}_{\xi_0}[\dot{\ell}(\xi_0)\dot{\ell}(\xi_0)^\top]$  exists and is positive definite for  $0 < \|\xi_0\| < 1$  by previous derivations. The smoothness of  $\xi \mapsto \ell(\xi)$ ,

$$\frac{\partial^2}{\partial \xi_i \partial \xi_j} \ell(\xi) = -\frac{\partial}{\partial \xi_i} \ell(\xi) \frac{\partial}{\partial \xi_j} \ell(\xi) + \frac{1}{f_{C_k}(\mathbf{x}; \xi)} \frac{\partial^2}{\partial \xi_i \partial \xi_j} f_{C_k}(\mathbf{x}; \xi),$$

the dominated convergence theorem, and an argument as in (46) imply that  $\mathbb{E}_{\xi_0}[\ddot{\ell}(\xi_0)] = -\mathbb{E}_{\xi_0}[\dot{\ell}(\xi_0)\dot{\ell}(\xi_0)^\top]$ . Therefore,  $\mathbb{E}_{\xi_0}[\dot{\ell}(\xi_0)]^{-1} \mathbb{E}_{\xi_0}[\dot{\ell}(\xi_0)\dot{\ell}(\xi_0)^\top] \mathbb{E}_{\xi_0}[\ddot{\ell}(\xi_0)]^{-1} = \mathcal{I}(\xi_0)^{-1}$ . Finally, in a closed neighborhood  $V_{\xi_0}$  of  $\xi_0$ , the second partial derivatives  $\mathbf{x} \mapsto \ddot{\psi}_\xi(\mathbf{x})$  are dominated by  $\mathbf{x} \mapsto \sup_{\xi \in V_{\xi_0}} \|\ddot{\psi}_\xi(\mathbf{x})\|$ , for every  $\xi \in V_{\xi_0}$ , which is finitely integrable on  $\mathbb{S}^d$ , since  $\omega_d^{-1}(1 - \rho_\star) \leq f_{C_k}(\mathbf{x}; \xi) \leq \omega_d^{-1}(1 + \rho_\star)$  uniformly in  $(\mathbf{x}, \xi)$ . The conditions of Theorem 5.41 in van der Vaart (1998) are therefore satisfied.

The conditions of Theorem 5.42 are the same, plus an additional one stating that  $\xi_0$  is a local maximizer of  $\xi \mapsto \mathbb{E}_{\xi_0}[\log f_{C_k}(\mathbf{X}; \xi)]$ . This is true by a Kullback–Leibler divergence argument:  $\mathbb{E}_{\xi_0}[\log f_{C_k}(\mathbf{X}; \xi)] - \mathbb{E}_{\xi_0}[\log f_{C_k}(\mathbf{X}; \xi_0)] = -\text{KL}(f_{C_k}(\cdot; \xi_0) \| f_{C_k}(\cdot; \xi)) \leq 0$ .

Theorems 5.41 and 5.42 in van der Vaart (1998) imply that:

- i. The probability that  $\xi \mapsto \ell_n(\xi)$  has at least one local maximum tends to one as  $n \rightarrow \infty$ .

ii. There exists a sequence of local maxima  $\hat{\boldsymbol{\xi}}_n$  such that  $\hat{\boldsymbol{\xi}}_n \rightarrow \boldsymbol{\xi}_0$  in probability.

iii. The sequence  $\hat{\boldsymbol{\xi}}_n$  is asymptotically normal:

$$\sqrt{n}(\hat{\boldsymbol{\xi}}_n - \boldsymbol{\xi}_0) \rightsquigarrow \mathcal{N}_{d+1}(\mathbf{0}, \mathcal{I}(\boldsymbol{\xi}_0)^{-1}) \quad (47)$$

as  $n \rightarrow \infty$ .

In addition, by Theorem 5.41 in ibid,

$$\sqrt{n}(\hat{\boldsymbol{\xi}}_n - \boldsymbol{\xi}_0) = \mathcal{I}(\boldsymbol{\xi}_0)^{-1} \frac{1}{\sqrt{n}} \sum_{i=1}^n \psi_{\boldsymbol{\xi}_0}(\mathbf{X}_i) + o_P(1).$$

These statements conclude the proof.  $\square$

## C Proofs of Section 5

### C.1 Proofs of Section 5.1

*Proof of Theorem 5.1.* Let us consider a rotationally symmetric density on  $\mathbb{S}^d$  about  $\boldsymbol{\mu}$ ,  $\mathbf{x} \mapsto c_d(g)g(\mathbf{x}^\top \boldsymbol{\mu})$ , where  $g : [-1, 1] \rightarrow \mathbb{R}_{\geq 0}$  is an angular function and  $c_d(g)$  the normalizing constant. Note (9) belongs to this setup.

Consider the tangent-normal decomposition  $\mathbf{x} = t\boldsymbol{\gamma} + (1-t^2)^{1/2}\mathbf{B}_{\boldsymbol{\gamma}}\boldsymbol{\xi}$ , where  $t = \mathbf{x}^\top \boldsymbol{\gamma}$ ,  $\boldsymbol{\xi} \in \mathbb{S}^{d-1}$ , and  $\mathbf{B}_{\boldsymbol{\gamma}}^\top \mathbf{B}_{\boldsymbol{\gamma}} = \mathbf{I}_d$  and  $\mathbf{B}_{\boldsymbol{\gamma}}\mathbf{B}_{\boldsymbol{\gamma}}^\top = \mathbf{I}_{d+1} - \boldsymbol{\gamma}\boldsymbol{\gamma}^\top$ . Then

$$\begin{aligned} & \int_{\mathbb{S}^d} c_d(g)g(\mathbf{x}^\top \boldsymbol{\mu}) \sigma_d(d\mathbf{x}) \\ &= \int_{\mathbb{S}^{d-1}} \int_{-1}^1 c_d(g)g([t\boldsymbol{\gamma} + (1-t^2)^{1/2}\mathbf{B}_{\boldsymbol{\gamma}}\boldsymbol{\xi}]^\top \boldsymbol{\mu})(1-t^2)^{d/2-1} dt \sigma_{d-1}(d\boldsymbol{\xi}) \\ &= \int_{-1}^1 c_d(g)(1-t^2)^{d/2-1} \left\{ \int_{\mathbb{S}^{d-1}} g([t\boldsymbol{\gamma} + (1-t^2)^{1/2}\mathbf{B}_{\boldsymbol{\gamma}}\boldsymbol{\xi}]^\top \boldsymbol{\mu}) \sigma_{d-1}(d\boldsymbol{\xi}) \right\} dt \\ &=: \int_{-1}^1 c_d(g)(1-t^2)^{d/2-1} g_{\boldsymbol{\gamma}, \boldsymbol{\mu}}(t) dt \end{aligned}$$

and  $T = \boldsymbol{\gamma}^\top \mathbf{X}$  has density  $c_d(g)(1-t^2)^{d/2-1} g_{\boldsymbol{\gamma}, \boldsymbol{\mu}}(t)$  on  $[-1, 1]$ . Let us compute  $g_{\boldsymbol{\gamma}, \boldsymbol{\mu}}$  in a simpler form under (9) (in this case  $c_d(g) = 1$ ) to obtain the density (19).

We tackle first the case  $d = 1$ , where  $\boldsymbol{\xi} \in \mathbb{S}^0 = \{-1, 1\}$  and  $\mathbf{B}_{\boldsymbol{\gamma}} = (\gamma_2, -\gamma_1)^\top$ . Thus,

$$\begin{aligned} g_{\boldsymbol{\gamma}, \boldsymbol{\mu}}(t) &= \frac{1}{2} \left\{ g([t\boldsymbol{\gamma} + (1-t^2)^{1/2}\mathbf{B}_{\boldsymbol{\gamma}}]^\top \boldsymbol{\mu}) + g([t\boldsymbol{\gamma} - (1-t^2)^{1/2}\mathbf{B}_{\boldsymbol{\gamma}}]^\top \boldsymbol{\mu}) \right\} \\ &= \frac{1}{4\pi} \left\{ 2 + \rho T_k([t\boldsymbol{\gamma} + (1-t^2)^{1/2}\mathbf{B}_{\boldsymbol{\gamma}}]^\top \boldsymbol{\mu}) + \rho T_k([t\boldsymbol{\gamma} - (1-t^2)^{1/2}\mathbf{B}_{\boldsymbol{\gamma}}]^\top \boldsymbol{\mu}) \right\}. \end{aligned}$$

Denote  $t = \cos \alpha$  and  $\boldsymbol{\gamma}^\top \boldsymbol{\mu} = \cos \beta$ , so that

$$[t\boldsymbol{\gamma} \pm (1-t^2)^{1/2}\mathbf{B}_{\boldsymbol{\gamma}}]^\top \boldsymbol{\mu} = \cos \alpha \cos \beta \pm \sin \alpha \sin \beta = \cos(\alpha \mp \beta).$$

Then

$$\begin{aligned} g_{\boldsymbol{\gamma}, \boldsymbol{\mu}}(t) &= \frac{1}{4\pi} \{ 2 + \rho T_k(\cos(\alpha - \beta)) + \rho T_k(\cos(\alpha + \beta)) \} \\ &= \frac{1}{4\pi} \{ 2 + 2\rho \cos(k\beta) \cos(k\alpha) \} \\ &= \frac{1}{2\pi} \left\{ 1 + \rho T_k(\boldsymbol{\gamma}^\top \boldsymbol{\mu}) T_k(t) \right\}. \end{aligned}$$

The density of  $T = \boldsymbol{\gamma}^\top \boldsymbol{\mu}$  for  $d = 1$  is then

$$\begin{aligned} f_{\boldsymbol{\gamma}}(t) &= \frac{1}{2\pi} \left\{ 1 + \rho T_k(\boldsymbol{\gamma}^\top \boldsymbol{\mu}) T_k(t) \right\} (1-t^2)^{-1/2} \\ &= f_1(t) \left\{ 1 + \rho \tilde{C}_k^0(\boldsymbol{\gamma}^\top \boldsymbol{\mu}) \tilde{C}_k^0(t) \right\}. \end{aligned} \quad (48)$$

We now tackle the case  $d \geq 2$ :

$$\begin{aligned} g_{\boldsymbol{\gamma}, \boldsymbol{\mu}}(t) &= \int_{\mathbb{S}^{d-1}} g([t\boldsymbol{\gamma} + (1-t^2)^{1/2} \mathbf{B}_{\boldsymbol{\gamma}} \boldsymbol{\xi}]^\top \boldsymbol{\mu}) \sigma_{d-1}(\mathrm{d}\boldsymbol{\xi}) \\ &= \int_{\mathbb{S}^{d-1}} \frac{1}{\omega_d} \left\{ 1 + \rho \tilde{C}_k^{(d-1)/2}([t\boldsymbol{\gamma} + (1-t^2)^{1/2} \mathbf{B}_{\boldsymbol{\gamma}} \boldsymbol{\xi}]^\top \boldsymbol{\mu}) \right\} \sigma_{d-1}(\mathrm{d}\boldsymbol{\xi}) \\ &= \frac{\omega_{d-1}}{\omega_d} + \frac{\rho}{\omega_d C_k^{(d-1)/2}(1)} \\ &\quad \times \int_{\mathbb{S}^{d-1}} C_k^{(d-1)/2} \left( t[\boldsymbol{\gamma}^\top \boldsymbol{\mu}] + (1-t^2)^{1/2}(1 - [\boldsymbol{\gamma}^\top \boldsymbol{\mu}]^2)^{1/2} \boldsymbol{\xi}^\top \left[ \frac{\mathbf{B}_{\boldsymbol{\gamma}}^\top \boldsymbol{\mu}}{\|\mathbf{B}_{\boldsymbol{\gamma}}^\top \boldsymbol{\mu}\|} \right] \right) \sigma_{d-1}(\mathrm{d}\boldsymbol{\xi}) \\ &= \frac{\omega_{d-1}}{\omega_d} + \frac{\rho \omega_{d-2}}{\omega_d C_k^{(d-1)/2}(1)} \\ &\quad \times \int_{-1}^1 C_k^{(d-1)/2} \left( t[\boldsymbol{\gamma}^\top \boldsymbol{\mu}] + (1-t^2)^{1/2}(1 - [\boldsymbol{\gamma}^\top \boldsymbol{\mu}]^2)^{1/2} s \right) (1-s^2)^{(d-3)/2} \mathrm{d}s. \end{aligned}$$

Denote  $t = \cos \alpha$  and  $\boldsymbol{\gamma}^\top \boldsymbol{\mu} = \cos \beta$  and use Eq. ET II 283(20) in Gradshteyn and Ryzhik (2014):

$$\begin{aligned} &\int_{-1}^1 (1-x^2)^{\nu-1} C_k^\nu(\cos \alpha \cos \beta + x \sin \alpha \sin \beta) \mathrm{d}x \\ &= \frac{2^{2\nu-1} k! [\Gamma(\nu)]^2}{\Gamma(2\nu+k)} C_k^\nu(\cos \alpha) C_k^\nu(\cos \beta). \end{aligned}$$

Then,

$$\begin{aligned} g_{\boldsymbol{\gamma}, \boldsymbol{\mu}}(t) &= \frac{\omega_{d-1}}{\omega_d} + \frac{\rho \omega_{d-2}}{\omega_d C_k^{(d-1)/2}(1)} \int_{-1}^1 C_k^{(d-1)/2}(\cos \alpha \cos \beta + \sin \alpha \sin \beta s) (1-s^2)^{(d-3)/2} \mathrm{d}s \\ &= \frac{\omega_{d-1}}{\omega_d} + \frac{\rho \omega_{d-2}}{\omega_d C_k^{(d-1)/2}(1)} \frac{2^{d-2} k! [\Gamma((d-1)/2)]^2}{\Gamma(d-1+k)} C_k^{(d-1)/2}(t) C_k^{(d-1)/2}(\boldsymbol{\gamma}^\top \boldsymbol{\mu}) \\ &= \frac{\omega_{d-1}}{\omega_d} \left\{ 1 + \rho \frac{\omega_{d-2} 2^{d-2} [\Gamma((d-1)/2)]^2}{\omega_{d-1} \Gamma(d-1)} \frac{C_k^{(d-1)/2}(\boldsymbol{\gamma}^\top \boldsymbol{\mu})}{[C_k^{(d-1)/2}(1)]^2} C_k^{(d-1)/2}(t) \right\}, \end{aligned}$$

since  $C_k^{(d-1)/2}(1) = \Gamma(d-1+k)/(\Gamma(d-1)k!)$ . Using the expression for  $\omega_d$  and the Legendre duplication formula  $\Gamma((d-1)/2) \Gamma(d/2) = 2^{2-d} \sqrt{\pi} \Gamma(d-1)$ , we have

$$\frac{\omega_{d-2} 2^{d-2} [\Gamma((d-1)/2)]^2}{\omega_{d-1} \Gamma(d-1)} = \frac{\pi^{-1/2} 2^{d-2} \Gamma((d-1)/2)}{\Gamma(d-1)/\Gamma(d/2)} = 1.$$

The density of  $T = \boldsymbol{\gamma}^\top \boldsymbol{\mu}$  for  $d \geq 2$  is then

$$\begin{aligned} f_{\boldsymbol{\gamma}}(t) &= \frac{\omega_{d-1}}{\omega_d} \left\{ 1 + \rho \frac{C_k^{(d-1)/2}(\boldsymbol{\gamma}^\top \boldsymbol{\mu})}{[C_k^{(d-1)/2}(1)]^2} C_k^{(d-1)/2}(t) \right\} (1-t^2)^{d/2-1} \\ &= f_d(t) \left\{ 1 + \rho \tilde{C}_k^{(d-1)/2}(\boldsymbol{\gamma}^\top \boldsymbol{\mu}) \tilde{C}_k^{(d-1)/2}(t) \right\}. \end{aligned} \quad (49)$$

Expressions (48) and (49) prove (19) for  $d \geq 1$ .

To obtain the cdf (20) we use

$$\begin{aligned} G_k(x) &:= - \int_{-1}^x C_k^{(d-1)/2}(t)(1-t^2)^{d/2-1} dt \\ &= \begin{cases} \frac{1}{k} \sin(k \cos^{-1}(x)), & d = 1, \\ \frac{d-1}{k(k+d-1)} C_{k-1}^{(d+1)/2}(x)(1-x^2)^{d/2}, & d \geq 2. \end{cases} \end{aligned}$$

(Lemma B.5 in García-Portugués et al. (2023)), and (48) and (49):

$$\begin{aligned} F_{\gamma}(x) &= \int_{-1}^x f_d(t) + \left\{ \rho \frac{\omega_{d-1}}{\omega_d} \frac{C_k^{(d-1)/2}(\gamma^\top \mu)}{[C_k^{(d-1)/2}(1)]^2} \right\} C_k^{(d-1)/2}(t)(1-t^2)^{d/2-1} dt \\ &= F_d(x) + \rho \eta_k(\gamma^\top \mu) \int_{-1}^x C_k^{(d-1)/2}(t)(1-t^2)^{d/2-1} dt \\ &= F_d(x) - \rho \eta_k(\gamma^\top \mu) G_k(x). \end{aligned}$$

□

## C.2 Proofs of Section 5.2

*Proof of Theorem 5.2.* We compute each of the following terms separately:

$$\begin{aligned} n^{-1} P_n^{W,\lambda} &= \mathbb{E}_{\gamma} \left[ \int_{-1}^1 \{F_{\gamma}(x)\}^2 dW(F_{\gamma}(x)) \right] - 2 \mathbb{E}_{\gamma} \left[ \int_{-1}^1 F_{n,\gamma}(x) F_{\gamma}(x) dW(F_{\gamma}(x)) \right] \\ &\quad + \mathbb{E}_{\gamma} \left[ \int_{-1}^1 \{F_{n,\gamma}(x)\}^2 dW(F_{\gamma}(x)) \right] \\ &=: P_n^{(1)} - 2P_n^{(2)} + P_n^{(3)}. \end{aligned}$$

*Computation of  $P_n^{(1)}$ .* Considering the change of variables  $u = F_{\gamma}(x)$ , it readily follows that

$$P_n^{(1)} = \mathbb{E}_{\gamma} \left[ \int_0^1 u^2 dW(u) \right] = W_2(1) - W_2(0),$$

where  $W_2(x) := \int_0^x u^2 dW(u)$ .

*Computation of  $P_n^{(2)}$ .* Using the same change of variables as before,

$$\begin{aligned} P_n^{(2)} &= \frac{1}{n} \sum_{i=1}^n \mathbb{E}_{\gamma} \left[ \int_{-1}^1 \mathbb{1}_{\{\gamma^\top \mathbf{X}_i \leq x\}} F_{\gamma}(x) dW(F_{\gamma}(x)) \right] \\ &= \frac{1}{n} \sum_{i=1}^n \mathbb{E}_{\gamma} \left[ \int_{\gamma^\top \mathbf{X}_i}^1 F_{\gamma}(x) dW(F_{\gamma}(x)) \right] \\ &= \frac{1}{n} \sum_{i=1}^n \mathbb{E}_{\gamma} \left[ \int_{F_{\gamma}(\gamma^\top \mathbf{X}_i)}^1 u dW(u) \right] \\ &= W_1(1) - \frac{1}{n} \sum_{i=1}^n \mathbb{E}_{\gamma} \left[ W_1(F_{\gamma}(\gamma^\top \mathbf{X}_i)) \right], \end{aligned}$$

where  $W_1(x) := \int_0^x u dW(u)$ .

Computation of  $P_n^{(3)}$ . Similar as before,

$$\begin{aligned} P_n^{(3)} &= \frac{1}{n^2} \sum_{i=1}^n \mathbb{E}_{\gamma} \left[ \int_{-1}^1 1_{\{\gamma^\top \mathbf{X}_i \leq x\}} dW(F_{\gamma}(x)) \right] \\ &\quad + \frac{1}{n^2} \sum_{i \neq j} \mathbb{E}_{\gamma} \left[ \int_{-1}^1 1_{\{\gamma^\top \mathbf{X}_i \leq x, \gamma^\top \mathbf{X}_j \leq x\}} dW(F_{\gamma}(x)) \right] \\ &=: P_n^{(3,1)} + P_n^{(3,2)}. \end{aligned}$$

Therefore,

$$\begin{aligned} P_n^{(3,1)} &= \frac{1}{n^2} \sum_{i=1}^n \mathbb{E}_{\gamma} \left[ \int_0^1 1_{\{F_{\gamma}(\gamma^\top \mathbf{X}_i) \leq u\}} dW(u) \right] \\ &= \frac{W(1)}{n} - \frac{1}{n^2} \sum_{i=1}^n \mathbb{E}_{\gamma} \left[ W(F_{\gamma}(\gamma^\top \mathbf{X}_i)) \right] \end{aligned}$$

and

$$\begin{aligned} P_n^{(3,2)} &= \frac{1}{n^2} \sum_{i \neq j} \mathbb{E}_{\gamma} \left[ \int_0^1 1_{\{F_{\gamma}(\gamma^\top \mathbf{X}_i) \leq u, F_{\gamma}(\gamma^\top \mathbf{X}_j) \leq u\}} dW(u) \right] \\ &= \frac{1}{n^2} \sum_{i \neq j} \mathbb{E}_{\gamma} \left[ \int_0^1 1_{\{F_{\gamma}(\max(\gamma^\top \mathbf{X}_i, \gamma^\top \mathbf{X}_j)) \leq u\}} dW(u) \right] \\ &= \frac{(n-1)}{n} W(1) - \frac{1}{n^2} \sum_{i \neq j} \mathbb{E}_{\gamma} \left[ W(F_{\gamma}(\max(\gamma^\top \mathbf{X}_i, \gamma^\top \mathbf{X}_j))) \right]. \end{aligned}$$

Putting together all terms:

$$\begin{aligned} n^{-1} P_n^{W,\lambda} &= P_n^{(1)} - 2P_n^{(2)} + P_n^{(3,1)} + P_n^{(3,2)} \\ &= W_2(1) - W_2(0) - 2W_1(1) + \frac{2}{n} \sum_{i=1}^n \mathbb{E}_{\gamma} \left[ W_1(F_{\gamma}(\gamma^\top \mathbf{X}_i)) \right] \\ &\quad + \frac{W(1)}{n} - \frac{1}{n^2} \sum_{i=1}^n \mathbb{E}_{\gamma} \left[ W(F_{\gamma}(\gamma^\top \mathbf{X}_i)) \right] \\ &\quad + \frac{(n-1)}{n} W(1) - \frac{1}{n^2} \sum_{i \neq j} \mathbb{E}_{\gamma} \left[ W(F_{\gamma}(\max(\gamma^\top \mathbf{X}_i, \gamma^\top \mathbf{X}_j))) \right], \\ &= W(1) + W_2(1) - W_2(0) - 2W_1(1) \\ &\quad + \frac{2}{n} \sum_{i=1}^n \mathbb{E}_{\gamma} \left[ W_1(F_{\gamma}(\gamma^\top \mathbf{X}_i)) \right] - \frac{1}{n^2} \sum_{i,j=1}^n \mathbb{E}_{\gamma} \left[ W(F_{\gamma}(\max(\gamma^\top \mathbf{X}_i, \gamma^\top \mathbf{X}_j))) \right], \end{aligned}$$

proving the result.  $\square$

*Proof of Corollary 5.1.* To derive  $P_n^{\text{AD},\lambda}$ , we consider the truncated weight  $dW^{\text{AD},\varepsilon}(x) := [x(1-x)]^{-1} 1_{\{\varepsilon < x < 1-\varepsilon\}} dx$ ,  $\varepsilon \in (0, 1/2)$ , obtain  $P_n^{\text{AD},\varepsilon,\lambda}$  and compute  $\lim_{\varepsilon \rightarrow 0} P_n^{\text{AD},\varepsilon,\lambda} = P_n^{\text{AD},\lambda}$ .

Let  $L_{\varepsilon} := \log((1-\varepsilon)/\varepsilon)$ . Direct calculations give

$$W^{\text{AD},\varepsilon}(x) = \begin{cases} 0, & x \leq \varepsilon, \\ L_{\varepsilon} + \log(x/(1-x)), & \varepsilon < x < 1-\varepsilon, \\ 2L_{\varepsilon}, & x \geq 1-\varepsilon, \end{cases}$$

$$W_1^{\text{AD}\varepsilon}(x) = \begin{cases} 0, & x \leq \varepsilon, \\ \log((1-\varepsilon)/(1-x)), & \varepsilon < x < 1-\varepsilon, \\ L_\varepsilon, & x \geq 1-\varepsilon, \end{cases}$$

$$W_2^{\text{AD}\varepsilon}(x) = \begin{cases} 0, & x \leq \varepsilon, \\ \varepsilon - x + \log((1-\varepsilon)/(1-x)), & \varepsilon < x < 1-\varepsilon, \\ L_\varepsilon + 2\varepsilon - 1, & x \geq 1-\varepsilon. \end{cases}$$

Denote  $t_{i,\gamma} := \gamma^\top \mathbf{X}_i$  and  $m_{ij,\gamma} = \max(\gamma^\top \mathbf{X}_i, \gamma^\top \mathbf{X}_j)$ . Theorem 5.2 gives

$$\begin{aligned} P_n^{\text{AD}\varepsilon, \lambda} &= n(W^{\text{AD}\varepsilon}(1) + W_2^{\text{AD}\varepsilon}(1) - W_2^{\text{AD}\varepsilon}(0) - 2W_1^{\text{AD}\varepsilon}(1)) \\ &\quad + 2 \sum_{i=1}^n \mathbb{E}_\gamma \left[ W_1^{\text{AD}\varepsilon}(F_\gamma(t_{i,\gamma})) \right] - \frac{1}{n} \sum_{i,j=1}^n \mathbb{E}_\gamma \left[ W^{\text{AD}\varepsilon}(F_\gamma(m_{ij,\gamma})) \right] \\ &= n(L_\varepsilon + 2\varepsilon - 1) \\ &\quad + 2 \sum_{i=1}^n \mathbb{E}_\gamma \left[ \log \left( \frac{1-\varepsilon}{1-F_\gamma(t_{i,\gamma})} \right) \mathbf{1}_{\{F_\gamma(t_{i,\gamma}) \in (\varepsilon, 1-\varepsilon)\}} \right] \\ &\quad + 2L_\varepsilon \sum_{i=1}^n \mathbb{P}[F_\gamma(t_{i,\gamma}) \geq 1-\varepsilon] \\ &\quad - \frac{1}{n} \sum_{i,j=1}^n \mathbb{E}_\gamma \left[ \left\{ L_\varepsilon + \log \left( \frac{F_\gamma(m_{ij,\gamma})}{1-F_\gamma(m_{ij,\gamma})} \right) \right\} \mathbf{1}_{\{F_\gamma(m_{ij,\gamma}) \in (\varepsilon, 1-\varepsilon)\}} \right] \\ &\quad - \frac{2L_\varepsilon}{n} \sum_{i,j=1}^n \mathbb{P}[F_\gamma(m_{ij,\gamma}) \geq 1-\varepsilon] \\ &= -n(1-2\varepsilon) \\ &\quad + 2 \sum_{i=1}^n \mathbb{E}_\gamma \left[ \log \left( \frac{1-\varepsilon}{1-F_\gamma(t_{i,\gamma})} \right) \mathbf{1}_{\{F_\gamma(t_{i,\gamma}) \in (\varepsilon, 1-\varepsilon)\}} \right] \\ &\quad - \frac{1}{n} \sum_{i,j=1}^n \mathbb{E}_\gamma \left[ \log \left( \frac{F_\gamma(m_{ij,\gamma})}{1-F_\gamma(m_{ij,\gamma})} \right) \mathbf{1}_{\{F_\gamma(m_{ij,\gamma}) \in (\varepsilon, 1-\varepsilon)\}} \right] \\ &\quad + L_\varepsilon R_\varepsilon, \end{aligned} \tag{50}$$

where

$$\begin{aligned} R_\varepsilon &= n + 2 \sum_{i=1}^n \mathbb{P}[F_\gamma(t_{i,\gamma}) \geq 1-\varepsilon] - \frac{1}{n} \sum_{i,j=1}^n \mathbb{P}[F_\gamma(m_{ij,\gamma}) \in (\varepsilon, 1-\varepsilon)] \\ &\quad - \frac{2}{n} \sum_{i,j=1}^n \mathbb{P}[F_\gamma(m_{ij,\gamma}) \geq 1-\varepsilon] \\ &= 2 \sum_{i=1}^n \mathbb{P}[F_\gamma(t_{i,\gamma}) \geq 1-\varepsilon] + \frac{1}{n} \sum_{i,j=1}^n \mathbb{P}[F_\gamma(m_{ij,\gamma}) \leq \varepsilon] \\ &\quad - \frac{1}{n} \sum_{i,j=1}^n \mathbb{P}[F_\gamma(m_{ij,\gamma}) \geq 1-\varepsilon]. \end{aligned}$$

As  $\varepsilon \rightarrow 0$ , the dominated convergence theorem applied to (50) readily gives the statement of the corollary, provided that  $L_\varepsilon R_\varepsilon \rightarrow 0$  as  $\varepsilon \rightarrow 0$ . Since  $L_\varepsilon \sim -\log(\varepsilon)$  as  $\varepsilon \rightarrow 0$ , it suffices to show that the probabilities in  $R_\varepsilon$  are  $O(\varepsilon)$  as  $\varepsilon \rightarrow 0$ .

Set  $m := 1 - |\rho| > 0$ . By Theorem 5.1,  $f_{\gamma}(x) \geq m f_d(x)$  for any  $x \in [-1, 1]$ . Hence,

$$F_{\gamma}(x) = \int_{-1}^x f_{\gamma}(u) du \geq m F_d(x) \quad \text{and} \quad 1 - F_{\gamma}(x) = \int_x^1 f_{\gamma}(u) du \geq m(1 - F_d(x)).$$

Therefore, for  $x_{\gamma} = t_{i,\gamma}$  or  $x_{\gamma} = m_{ij,\gamma}$ ,

$$\{F_{\gamma}(x_{\gamma}) \leq \varepsilon\} \subset \{F_d(x_{\gamma}) \leq \varepsilon/m\} \quad \text{and} \quad \{F_{\gamma}(x_{\gamma}) \geq 1 - \varepsilon\} \subset \{F_d(x_{\gamma}) \geq 1 - \varepsilon/m\}.$$

These inclusions allow us to bound the probabilities in  $R_{\varepsilon}$  through those involving  $F_d$ , which are easier to handle.

Let  $\lambda$  denote the bounded density of  $\gamma$  with respect to the surface area measure  $\sigma_d$ , bounded by  $M > 0$ . Then

$$P[\gamma \in A] = \int_A \lambda(\gamma) \sigma_d(d\gamma) \leq M \sigma_d(A) = M \omega_d P[U \in A]$$

where  $\mathbf{U} \sim \text{Unif}(\mathbb{S}^d)$ . Then,

$$\begin{aligned} P[F_{\gamma}(\gamma^{\top} \mathbf{X}_i) \geq 1 - \varepsilon] &\leq P[F_d(\gamma^{\top} \mathbf{X}_i) \geq 1 - \varepsilon/m] \\ &\leq M \omega_d P[F_d(\mathbf{U}^{\top} \mathbf{X}_i) \geq 1 - \varepsilon/m] \\ &= M \omega_d \frac{\varepsilon}{m}, \end{aligned}$$

with the last equality following from  $F_d(\mathbf{U}^{\top} \mathbf{X}_i) \sim \text{Unif}(0, 1)$ .

For  $m_{ij,\gamma} = \max(\gamma^{\top} \mathbf{X}_i, \gamma^{\top} \mathbf{X}_j)$ , recall that

$$\{F_d(m_{ij,\gamma}) \geq 1 - \varepsilon/m\} \subset \{F_d(t_{i,\gamma}) \geq 1 - \varepsilon/m\} \cup \{F_d(t_{j,\gamma}) \geq 1 - \varepsilon/m\},$$

implying

$$P[F_{\gamma}(m_{ij,\gamma}) \geq 1 - \varepsilon] \leq 2M \omega_d \frac{\varepsilon}{m}.$$

Finally, since  $\{F_d(m_{ij,\gamma}) \leq \varepsilon/m\} \subset \{F_d(t_{i,\gamma}) \leq \varepsilon/m\}$ , then

$$P[F_{\gamma}(m_{ij,\gamma}) \leq \varepsilon] \leq M \omega_d \frac{\varepsilon}{m}.$$

This shows that  $R_{\varepsilon} = O(\varepsilon)$  as  $\varepsilon \rightarrow 0$ .  $\square$

*Proof of Theorem 5.3.* For the CvM weight,  $W(x) = x$ , we have  $W_1(x) = x^2/2$  and  $W_2(x) = x^3/3$ . Hence, the bias term is  $W(1) + W_2(1) - W_2(0) - 2W_1(1) = 1/3$ . We also define the two kernels

$$\tilde{\varphi}(\mathbf{X}_1) := 2E_{\gamma}[W_1(F_{\gamma}(\gamma^{\top} \mathbf{X}_1))] - \frac{1}{3}, \quad \tilde{\psi}(\mathbf{X}_1, \mathbf{X}_2) := E_{\gamma}[W(F_{\gamma}(\max(\gamma^{\top} \mathbf{X}_1, \gamma^{\top} \mathbf{X}_2)))].$$

This yields the  $V$ -statistic expression

$$n^{-1} P_n^{\text{CvM, Unif}} = \frac{1}{3} + \frac{1}{n} \sum_{i=1}^n \left[ \tilde{\varphi}(\mathbf{X}_i) + \frac{1}{3} \right] - \frac{1}{n^2} \sum_{i,j=1}^n \tilde{\psi}(\mathbf{X}_i, \mathbf{X}_j). \quad (51)$$

We obtain the forms of  $\tilde{\varphi}$  and  $\tilde{\psi}$  next.

*Computation of  $\tilde{\varphi}(\mathbf{X}_1)$ .*

The first kernel is

$$\tilde{\varphi}(\mathbf{X}_1) = \frac{1}{\omega_d} \int_{\mathbb{S}^d} [F_d(\gamma^{\top} \mathbf{X}_1)]^2 \sigma_d(d\gamma) - \frac{1}{3}$$

$$\begin{aligned}
& -\frac{2\rho}{\omega_d} \int_{\mathbb{S}^d} F_d(\boldsymbol{\gamma}^\top \mathbf{X}_1) \eta_k(\boldsymbol{\gamma}^\top \boldsymbol{\mu}) G_k(\boldsymbol{\gamma}^\top \mathbf{X}_1) \sigma_d(d\boldsymbol{\gamma}) \\
& + \frac{\rho^2}{\omega_d} \int_{\mathbb{S}^d} [\eta_k(\boldsymbol{\gamma}^\top \boldsymbol{\mu}) G_k(\boldsymbol{\gamma}^\top \mathbf{X}_1)]^2 \sigma_d(d\boldsymbol{\gamma}) \\
& = \int_{-1}^1 F_d(x)^2 f_d(x) dx - \frac{1}{3} \\
& - \frac{2\rho}{\omega_d} \int_{\mathbb{S}^d} F_d(\boldsymbol{\gamma}^\top \mathbf{X}_1) G_k(\boldsymbol{\gamma}^\top \mathbf{X}_1) \eta_k(\boldsymbol{\gamma}^\top \boldsymbol{\mu}) \sigma_d(d\boldsymbol{\gamma}) \\
& + \frac{\rho^2}{\omega_d} \int_{\mathbb{S}^d} [G_k(\boldsymbol{\gamma}^\top \mathbf{X}_1) \eta_k(\boldsymbol{\gamma}^\top \boldsymbol{\mu})]^2 \sigma_d(d\boldsymbol{\gamma}) \\
& = -2\rho \frac{\omega_{d-1}}{\omega_d^2} \frac{1}{[C_k^{(d-1)/2}(1)]^2} \int_{\mathbb{S}^d} F_d(\boldsymbol{\gamma}^\top \mathbf{X}_1) G_k(\boldsymbol{\gamma}^\top \mathbf{X}_1) C_k^{(d-1)/2}(\boldsymbol{\gamma}^\top \boldsymbol{\mu}) \sigma_d(d\boldsymbol{\gamma}) \\
& + \rho^2 \frac{\omega_{d-1}^2}{\omega_d^3} \frac{1}{[C_k^{(d-1)/2}(1)]^4} \int_{\mathbb{S}^d} [G_k(\boldsymbol{\gamma}^\top \mathbf{X}_1) C_k^{(d-1)/2}(\boldsymbol{\gamma}^\top \boldsymbol{\mu})]^2 \sigma_d(d\boldsymbol{\gamma}) \\
& =: -2\rho \frac{\omega_{d-1}}{\omega_d^2} \frac{1}{[C_k^{(d-1)/2}(1)]^2} \tilde{\varphi}^{(1)}(\mathbf{X}_1) + \rho^2 \frac{\omega_{d-1}^2}{\omega_d^3} \frac{1}{[C_k^{(d-1)/2}(1)]^4} \tilde{\varphi}^{(2)}(\mathbf{X}_1). \tag{52}
\end{aligned}$$

We compute now

$$\begin{aligned}
\tilde{\varphi}^{(1)}(\mathbf{X}_1) &= \int_{\mathbb{S}^d} F_d(\boldsymbol{\gamma}^\top \mathbf{X}_1) G_k(\boldsymbol{\gamma}^\top \mathbf{X}_1) C_k^{(d-1)/2}(\boldsymbol{\gamma}^\top \boldsymbol{\mu}) \sigma_d(d\boldsymbol{\gamma}), \\
\tilde{\varphi}^{(2)}(\mathbf{X}_1) &= \int_{\mathbb{S}^d} [G_k(\boldsymbol{\gamma}^\top \mathbf{X}_1) C_k^{(d-1)/2}(\boldsymbol{\gamma}^\top \boldsymbol{\mu})]^2 \sigma_d(d\boldsymbol{\gamma})
\end{aligned}$$

for the cases  $d = 1$ ,  $(d = 2, k = 1)$  and  $(d = 2, k = 2)$ . The evaluation of these integrals has been done with the help of Mathematica (Wolfram Research, Inc., 2021).

For  $d = 1$ ,

$$\begin{aligned}
\tilde{\varphi}^{(1)}(\mathbf{X}_1) &= \frac{1}{k} \int_{\mathbb{S}^1} \frac{\pi - \cos^{-1}(\boldsymbol{\gamma}^\top \mathbf{X}_1)}{\pi} \sin(k \cos^{-1}(\boldsymbol{\gamma}^\top \mathbf{X}_1)) \cos(k \cos^{-1}(\boldsymbol{\gamma}^\top \boldsymbol{\mu})) \sigma_1(d\boldsymbol{\gamma}) \\
&= \frac{1}{k} \int_0^{2\pi} \frac{\pi - \cos^{-1}(\cos(\gamma - \theta_1))}{\pi} \sin(k \cos^{-1}(\cos(\gamma - \theta_1))) \cos(k \cos^{-1}(\cos(\gamma - \mu))) d\gamma \\
&= \frac{1}{2k^2} T_k(\mathbf{X}_1^\top \boldsymbol{\mu})
\end{aligned}$$

and

$$\begin{aligned}
\tilde{\varphi}^{(2)}(\mathbf{X}_1) &= \frac{1}{k^2} \int_{\mathbb{S}^1} [\sin(k \cos^{-1}(\boldsymbol{\gamma}^\top \mathbf{X}_1)) \cos(k \cos^{-1}(\boldsymbol{\gamma}^\top \boldsymbol{\mu}))]^2 \sigma_1(d\boldsymbol{\gamma}) \\
&= \frac{1}{k^2} \int_0^{2\pi} [\sin(k \cos^{-1}(\cos(\gamma - \theta_1))) \cos(k \cos^{-1}(\cos(\gamma - \mu)))]^2 d\gamma \\
&= \frac{\pi}{4k^2} (2 - T_{2k}(\mathbf{X}_1^\top \boldsymbol{\mu})).
\end{aligned}$$

For  $d = 2$ ,

$$\begin{aligned}
\tilde{\varphi}^{(1)}(\mathbf{X}_1) &= \frac{1}{2k(k+1)} \int_{\mathbb{S}^2} (\boldsymbol{\gamma}^\top \mathbf{X}_1 + 1) C_{k-1}^{3/2}(\boldsymbol{\gamma}^\top \mathbf{X}_1) C_k^{1/2}(\boldsymbol{\gamma}^\top \boldsymbol{\mu}) (1 - (\boldsymbol{\gamma}^\top \mathbf{X}_1)^2) \sigma_2(d\boldsymbol{\gamma}), \\
\tilde{\varphi}^{(2)}(\mathbf{X}_1) &= \frac{1}{k^2(k+1)^2} \int_{\mathbb{S}^2} [C_{k-1}^{3/2}(\boldsymbol{\gamma}^\top \mathbf{X}_1) C_k^{1/2}(\boldsymbol{\gamma}^\top \boldsymbol{\mu}) (1 - (\boldsymbol{\gamma}^\top \mathbf{X}_1)^2)]^2 \sigma_2(d\boldsymbol{\gamma}).
\end{aligned}$$

For  $k = 1$ ,

$$\tilde{\varphi}^{(1)}(\mathbf{X}_1) = 4\pi \frac{\mathbf{X}_1^\top \boldsymbol{\mu}}{30}, \quad \tilde{\varphi}^{(2)}(\mathbf{X}_1) = 4\pi \left\{ \frac{2}{35} - \frac{4(\mathbf{X}_1^\top \boldsymbol{\mu})^2}{105} \right\}.$$

For  $k = 2$ ,

$$\tilde{\varphi}^{(1)}(\mathbf{X}_1) = 4\pi \frac{3(\mathbf{X}_1^\top \boldsymbol{\mu})^2 - 1}{420}, \quad \tilde{\varphi}^{(2)}(\mathbf{X}_1) = 4\pi \left\{ \frac{1}{330} + \frac{3(\mathbf{X}_1^\top \boldsymbol{\mu})^2}{385} - \frac{(\mathbf{X}_1^\top \boldsymbol{\mu})^4}{110} \right\}.$$

We can now substitute these expressions into (52) to obtain the final forms of  $\tilde{\varphi}(\mathbf{X}_1)$  in each case:

- For  $d = 1$  and  $k \geq 1$ :

$$\begin{aligned} \tilde{\varphi}(\mathbf{X}_1) &= -\frac{\rho}{\pi^2} \tilde{\varphi}^{(1)}(\mathbf{X}_1) + \frac{\rho^2}{2\pi^3} \tilde{\varphi}^{(2)}(\mathbf{X}_1) \\ &= -\frac{\rho}{2\pi^2 k^2} \left\{ T_k(\mathbf{X}_1^\top \boldsymbol{\mu}) - \frac{\rho}{4}(2 - T_{2k}(\mathbf{X}_1^\top \boldsymbol{\mu})) \right\}. \end{aligned}$$

- For  $d = 2$ :

$$\begin{aligned} \tilde{\varphi}(\mathbf{X}_1) &= -\frac{\rho}{4\pi [C_k^{1/2}(1)]^2} \tilde{\varphi}^{(1)}(\mathbf{X}_1) + \frac{\rho^2}{16\pi [C_k^{1/2}(1)]^4} \tilde{\varphi}^{(2)}(\mathbf{X}_1) \\ &= -\frac{\rho}{4\pi} \tilde{\varphi}^{(1)}(\mathbf{X}_1) + \frac{\rho^2}{16\pi} \tilde{\varphi}^{(2)}(\mathbf{X}_1). \end{aligned}$$

For  $k = 1$ ,

$$\begin{aligned} \tilde{\varphi}(\mathbf{X}_1) &= -\frac{\rho}{4\pi} 4\pi \frac{\mathbf{X}_1^\top \boldsymbol{\mu}}{30} + \frac{\rho^2}{16\pi} 4\pi \left\{ \frac{2}{35} - \frac{4(\mathbf{X}_1^\top \boldsymbol{\mu})^2}{105} \right\} \\ &= -\frac{\rho}{30} \mathbf{X}_1^\top \boldsymbol{\mu} + \frac{\rho^2}{4} \left\{ \frac{2}{35} - \frac{4(\mathbf{X}_1^\top \boldsymbol{\mu})^2}{105} \right\}. \end{aligned}$$

For  $k = 2$ ,

$$\begin{aligned} \tilde{\varphi}(\mathbf{X}_1) &= -\frac{\rho}{4\pi} 4\pi \frac{3(\mathbf{X}_1^\top \boldsymbol{\mu})^2 - 1}{420} + \frac{\rho^2}{16\pi} 4\pi \left\{ \frac{1}{330} + \frac{3(\mathbf{X}_1^\top \boldsymbol{\mu})^2}{385} - \frac{(\mathbf{X}_1^\top \boldsymbol{\mu})^4}{110} \right\} \\ &= -\frac{\rho}{420} (3(\mathbf{X}_1^\top \boldsymbol{\mu})^2 - 1) + \frac{\rho^2}{4} \left\{ \frac{1}{330} + \frac{3(\mathbf{X}_1^\top \boldsymbol{\mu})^2}{385} - \frac{(\mathbf{X}_1^\top \boldsymbol{\mu})^4}{110} \right\}. \end{aligned}$$

*Computation of  $\tilde{\psi}(\mathbf{X}_1, \mathbf{X}_2)$ .*

Denote  $m_{12,\gamma} := \max(\gamma^\top \mathbf{X}_1, \gamma^\top \mathbf{X}_2)$ . The second kernel is

$$\begin{aligned} \tilde{\psi}(\mathbf{X}_1, \mathbf{X}_2) &= \mathbb{E}_\gamma [F_\gamma(m_{12,\gamma})] \\ &= \mathbb{E}_\gamma [F_d(m_{12,\gamma})] - \rho \mathbb{E}_\gamma \left[ \eta_k(\gamma^\top \boldsymbol{\mu}) G_k(m_{12,\gamma}) \right] \\ &= \mathbb{E}_\gamma [F_d(m_{12,\gamma})] - \rho \frac{\omega_{d-1}}{\omega_d} \frac{1}{[C_k^{(d-1)/2}(1)]^2} \mathbb{E}_\gamma \left[ C_k^{(d-1)/2}(\gamma^\top \boldsymbol{\mu}) G_k(m_{12,\gamma}) \right] \\ &=: \tilde{\psi}^{(1)}(\mathbf{X}_1, \mathbf{X}_2) - \rho \frac{\omega_{d-1}}{\omega_d} \frac{1}{[C_k^{(d-1)/2}(1)]^2} \tilde{\psi}^{(2)}(\mathbf{X}_1, \mathbf{X}_2). \end{aligned} \tag{53}$$

By Propositions 2.3 and 2.4 in García-Portugués et al. (2023),

$$\tilde{\psi}^{(1)}(\mathbf{X}_1, \mathbf{X}_2) = \mathbb{E}_\gamma [F_d(m_{12,\gamma})]$$

$$\begin{aligned}
&= 1 - \mathbb{E}_{\boldsymbol{\gamma}} [1 - F_d(m_{12,\boldsymbol{\gamma}})] \\
&= 1 - \mathbb{E}_{\boldsymbol{\gamma}} \left[ \int_{-1}^1 1_{\{m_{12,\boldsymbol{\gamma}} \leq x\}} f_d(x) \, dx \right] \\
&= 1 - \int_{-1}^1 \mathbb{E}_{\boldsymbol{\gamma}} \left[ 1_{\{\boldsymbol{\gamma}^\top \mathbf{X}_1 \leq x, \boldsymbol{\gamma}^\top \mathbf{X}_2 \leq x\}} \right] f_d(x) \, dx
\end{aligned}$$

equals  $1 - \psi_d^{\text{CvM}}(\theta_{12})$ , the CvM kernel for testing uniformity on  $\mathbb{S}^d$  given in García-Portugués et al. (2023), with  $\theta_{12} = \cos^{-1}(\mathbf{X}_1^\top \mathbf{X}_2)$ . For  $d = 1, 2$ , this gives

$$1 - \tilde{\psi}^{(1)}(\mathbf{X}_1, \mathbf{X}_2) = \psi_d^{\text{CvM}}(\theta_{12}) = \begin{cases} \frac{1}{2} + \frac{\theta_{12}}{2\pi} \left( \frac{\theta_{12}}{2\pi} - 1 \right), & d = 1, \\ \frac{1}{2} - \frac{1}{4} \sin \left( \frac{\theta_{12}}{2} \right), & d = 2. \end{cases}$$

We specialize next the kernels for the cases  $d = 1$ ,  $(d = 2, k = 1)$  and  $(d = 2, k = 2)$ . We used Mathematica (Wolfram Research, Inc., 2021) to evaluate parts of the integrals involved.

For  $d = 1$ ,

$$\begin{aligned}
\tilde{\psi}^{(2)}(\mathbf{X}_1, \mathbf{X}_2) &= \frac{1}{k} \mathbb{E}_{\boldsymbol{\gamma}} \left[ C_k^0(\boldsymbol{\gamma}^\top \boldsymbol{\mu}) \sin(k \cos^{-1}(m_{12,\boldsymbol{\gamma}})) \right] \\
&= \frac{1}{2k\pi} \int_{\mathbb{S}^1} \cos(k \cos^{-1}(\boldsymbol{\gamma}^\top \boldsymbol{\mu})) \sin(k \cos^{-1}(m_{12,\boldsymbol{\gamma}})) \sigma_1(d\boldsymbol{\gamma}) \\
&= \frac{1}{2k\pi} \int_0^{2\pi} \cos(k(\cos^{-1}(\cos(\gamma - \mu)))) \sin(k \cos^{-1}(\max(\cos(\gamma - \theta_1), \cos(\gamma - \theta_2)))) \, d\gamma \\
&= \frac{1}{k} \left\{ -\frac{\pi - \cos^{-1}(\mathbf{X}_1^\top \mathbf{X}_2)}{2\pi} T_k \left( \frac{(\mathbf{X}_1 + \mathbf{X}_2)^\top \boldsymbol{\mu}}{\sqrt{2(1 + \mathbf{X}_1^\top \mathbf{X}_2)}} \right) \sin \left( \frac{k \cos^{-1}(\mathbf{X}_1^\top \mathbf{X}_2)}{2} \right) \right\}.
\end{aligned}$$

For  $d \geq 2$ ,

$$\tilde{\psi}^{(2)}(\mathbf{X}_1, \mathbf{X}_2) = \frac{d-1}{k(k+d-1)} \mathbb{E}_{\boldsymbol{\gamma}} \left[ C_k^{(d-1)/2}(\boldsymbol{\gamma}^\top \boldsymbol{\mu}) C_{k-1}^{(d+1)/2}(m_{12,\boldsymbol{\gamma}}) (1 - m_{12,\boldsymbol{\gamma}}^2)^{d/2} \right]. \quad (54)$$

If  $k = 1$ , (54) simplifies to

$$\tilde{\psi}^{(2)}(\mathbf{X}_1, \mathbf{X}_2) = \frac{(d-1)^2}{d} \mathbb{E}_{\boldsymbol{\gamma}} \left[ (\boldsymbol{\gamma}^\top \boldsymbol{\mu}) (1 - m_{12,\boldsymbol{\gamma}}^2)^{d/2} \right]$$

and, if  $d = 2$ , to

$$\begin{aligned}
\tilde{\psi}^{(2)}(\mathbf{X}_1, \mathbf{X}_2) &= \frac{1}{2} \mathbb{E}_{\boldsymbol{\gamma}} \left[ (\boldsymbol{\gamma}^\top \boldsymbol{\mu}) (1 - m_{12,\boldsymbol{\gamma}}^2) \right] \\
&= -\frac{1}{16} \sqrt{\frac{1 - \mathbf{X}_1^\top \mathbf{X}_2}{2}} (\mathbf{X}_1 + \mathbf{X}_2)^\top \boldsymbol{\mu}.
\end{aligned}$$

If  $k = 2$ , (54) simplifies to

$$\begin{aligned}
\tilde{\psi}^{(2)}(\mathbf{X}_1, \mathbf{X}_2) &= \frac{(d-1)(d+1)}{2(d+1)} \frac{d-1}{2} \mathbb{E}_{\boldsymbol{\gamma}} \left[ [(d+1)(\boldsymbol{\gamma}^\top \boldsymbol{\mu})^2 - 1] m_{12,\boldsymbol{\gamma}} (1 - m_{12,\boldsymbol{\gamma}}^2)^{d/2} \right] \\
&= \frac{(d-1)^2}{4} \mathbb{E}_{\boldsymbol{\gamma}} \left[ [(d+1)(\boldsymbol{\gamma}^\top \boldsymbol{\mu})^2 - 1] m_{12,\boldsymbol{\gamma}} (1 - m_{12,\boldsymbol{\gamma}}^2)^{d/2} \right]
\end{aligned}$$

and, if  $d = 2$ , to

$$\tilde{\psi}^{(2)}(\mathbf{X}_1, \mathbf{X}_2) = \frac{1}{4} \mathbb{E}_{\boldsymbol{\gamma}} \left[ [3(\boldsymbol{\gamma}^\top \boldsymbol{\mu})^2 - 1] m_{12,\boldsymbol{\gamma}} (1 - m_{12,\boldsymbol{\gamma}}^2) \right]$$

$$\begin{aligned}
&= \frac{\sqrt{(1 - \mathbf{X}_1^\top \mathbf{X}_2)/2}}{64} \left\{ \frac{1 + \mathbf{X}_1^\top \mathbf{X}_2}{2} + \frac{3(3\mathbf{X}_1^\top \mathbf{X}_2 - 1)}{4(1 - \mathbf{X}_1^\top \mathbf{X}_2)} [(\mathbf{X}_1^\top \boldsymbol{\mu})^2 + (\mathbf{X}_2^\top \boldsymbol{\mu})^2] \right. \\
&\quad \left. + \frac{3(\mathbf{X}_1^\top \mathbf{X}_2 - 3)}{2(1 - \mathbf{X}_1^\top \mathbf{X}_2)} (\mathbf{X}_1^\top \boldsymbol{\mu})(\mathbf{X}_2^\top \boldsymbol{\mu}) \right\}.
\end{aligned}$$

We can now substitute these expressions into (53) to obtain the final forms of  $\psi(\mathbf{X}_1, \mathbf{X}_2)$  in each case:

- For  $d = 1$  and  $k \geq 1$ :

$$\begin{aligned}
\tilde{\psi}(\mathbf{X}_1, \mathbf{X}_2) &= \tilde{\psi}^{(1)}(\mathbf{X}_1, \mathbf{X}_2) - \frac{\rho}{\pi} \tilde{\psi}^{(2)}(\mathbf{X}_1, \mathbf{X}_2) \\
&= 1 - \psi_d^{\text{CvM}}(\cos^{-1}(\mathbf{X}_1^\top \mathbf{X}_2)) \\
&\quad + \rho \left\{ \frac{\pi - \cos^{-1}(\mathbf{X}_1^\top \mathbf{X}_2)}{2\pi^2 k} T_k \left( \frac{(\mathbf{X}_1 + \mathbf{X}_2)^\top \boldsymbol{\mu}}{\|\mathbf{X}_1 + \mathbf{X}_2\|} \right) \sin \left( \frac{k \cos^{-1}(\mathbf{X}_1^\top \mathbf{X}_2)}{2} \right) \right\}.
\end{aligned}$$

- For  $d = 2$  and  $k = 1$ :

$$\begin{aligned}
\tilde{\psi}(\mathbf{X}_1, \mathbf{X}_2) &= \tilde{\psi}^{(1)}(\mathbf{X}_1, \mathbf{X}_2) - \frac{\rho}{2} \tilde{\psi}^{(2)}(\mathbf{X}_1, \mathbf{X}_2) \\
&= 1 - \psi_2^{\text{CvM}}(\cos^{-1}(\mathbf{X}_1^\top \mathbf{X}_2)) + \frac{\rho}{32} \sqrt{\frac{1 - \mathbf{X}_1^\top \mathbf{X}_2}{2}} (\mathbf{X}_1 + \mathbf{X}_2)^\top \boldsymbol{\mu}.
\end{aligned}$$

- For  $d = 2$  and  $k = 2$ :

$$\begin{aligned}
\tilde{\psi}(\mathbf{X}_1, \mathbf{X}_2) &= \tilde{\psi}^{(1)}(\mathbf{X}_1, \mathbf{X}_2) - \frac{\rho}{2} \tilde{\psi}^{(2)}(\mathbf{X}_1, \mathbf{X}_2) \\
&= 1 - \psi_2^{\text{CvM}}(\cos^{-1}(\mathbf{X}_1^\top \mathbf{X}_2)) \\
&\quad + \frac{\rho}{128} \sqrt{\frac{1 - \mathbf{X}_1^\top \mathbf{X}_2}{2}} \left\{ \frac{1 + \mathbf{X}_1^\top \mathbf{X}_2}{2} + \frac{3(3\mathbf{X}_1^\top \mathbf{X}_2 - 1)}{4(1 - \mathbf{X}_1^\top \mathbf{X}_2)} [(\mathbf{X}_1^\top \boldsymbol{\mu})^2 + (\mathbf{X}_2^\top \boldsymbol{\mu})^2] \right. \\
&\quad \left. + \frac{3(\mathbf{X}_1^\top \mathbf{X}_2 - 3)}{2(1 - \mathbf{X}_1^\top \mathbf{X}_2)} (\mathbf{X}_1^\top \boldsymbol{\mu})(\mathbf{X}_2^\top \boldsymbol{\mu}) \right\}.
\end{aligned}$$

Since  $\psi_1^{\text{CvM}}(0) = \psi_2^{\text{CvM}}(0) = 1/2$ , it is easy to check that  $\tilde{\psi}(\mathbf{X}_1, \mathbf{X}_1) = 1/2$ .

*Final expression.*

We get back to the  $V$ -statistic expression (51) and rearrange it:

$$\begin{aligned}
n^{-1} P_n^{\text{CvM, Unif}} &= \frac{1}{3} + \frac{1}{n} \sum_{i=1}^n \left[ \tilde{\varphi}(\mathbf{X}_i) + \frac{1}{3} \right] - \frac{1}{n^2} \sum_{i,j=1}^n \tilde{\psi}(\mathbf{X}_i, \mathbf{X}_j) \\
&= \frac{2}{3} - 1 - \frac{1}{n} \sum_{i=1}^n [-\tilde{\varphi}(\mathbf{X}_i)] + \frac{1}{n^2} \sum_{i,j=1}^n [1 - \tilde{\psi}(\mathbf{X}_i, \mathbf{X}_j)] \\
&= -\frac{1}{3} - \frac{1}{n} \sum_{i=1}^n [-\tilde{\varphi}(\mathbf{X}_i)] + \frac{2}{n^2} \sum_{i,j=1}^n [1 - \tilde{\psi}(\mathbf{X}_i, \mathbf{X}_j)] + \frac{1}{2n} \\
&= \frac{3 - 2n}{6n} - \frac{1}{n} \sum_{i=1}^n [-\tilde{\varphi}(\mathbf{X}_i)] + \frac{2}{n^2} \sum_{i < j} [1 - \tilde{\psi}(\mathbf{X}_i, \mathbf{X}_j)].
\end{aligned}$$

We set  $\varphi(\mathbf{X}_i) = -\tilde{\varphi}(\mathbf{X}_i)$  and  $\psi(\mathbf{X}_i, \mathbf{X}_j) = 1 - \tilde{\psi}(\mathbf{X}_i, \mathbf{X}_j)$  to obtain (28).  $\square$

## D Auxiliary results

**Lemma D.1.** *Let  $d \geq 1$  and let  $\mathbf{B}_\mu \in \mathcal{M}_{d+1,d}$  be a semi-orthogonal matrix such that*

$$\mathbf{B}_\mu \mathbf{B}_\mu^\top = \mathbf{I}_{d+1} - \mu \mu^\top =: \mathbf{P}_\mu \quad \text{and} \quad \mathbf{B}_\mu^\top \mathbf{B}_\mu = \mathbf{I}_d.$$

*Then, for any  $p \geq 0$ ,*

$$\mathbf{B}_\mu^{\otimes 2p} (\text{vec } \mathbf{I}_d)^{\otimes p} = (\text{vec } \mathbf{P}_\mu)^{\otimes p}.$$

*Proof of Lemma D.1.* We use two standard equalities for the Kronecker product: the vec-operator identity

$$\text{vec}(\mathbf{A} \mathbf{X} \mathbf{B}^\top) = (\mathbf{B} \otimes \mathbf{A}) \text{ vec } \mathbf{X} \quad (55)$$

and the mixed-product property  $(\mathbf{A} \otimes \mathbf{B})(\mathbf{C} \otimes \mathbf{D}) = (\mathbf{A}\mathbf{C}) \otimes (\mathbf{B}\mathbf{D})$ , both for conformable matrices. The latter can be inductively extended to

$$\mathbf{A}^{\otimes p} \mathbf{B}^{\otimes p} = (\mathbf{A}\mathbf{B})^{\otimes p}, \quad p \geq 0. \quad (56)$$

Applying (55),

$$(\mathbf{B}_\mu \otimes \mathbf{B}_\mu) \text{ vec } \mathbf{I}_d = \text{vec}(\mathbf{B}_\mu \mathbf{I}_d \mathbf{B}_\mu^\top) = \text{vec}(\mathbf{B}_\mu \mathbf{B}_\mu^\top) = \text{vec } \mathbf{P}_\mu$$

while, due to the associativity of the Kronecker product,

$$\mathbf{B}_\mu^{\otimes 2p} = (\mathbf{B}_\mu \otimes \mathbf{B}_\mu)^{\otimes p}$$

Using these results and (56), we obtain

$$\mathbf{B}_\mu^{\otimes 2p} (\text{vec } \mathbf{I}_d)^{\otimes p} = (\mathbf{B}_\mu \otimes \mathbf{B}_\mu)^{\otimes p} (\text{vec } \mathbf{I}_d)^{\otimes p} = [(\mathbf{B}_\mu \otimes \mathbf{B}_\mu) \text{ vec } \mathbf{I}_d]^{\otimes p} = (\text{vec } \mathbf{P}_\mu)^{\otimes p},$$

proving the claimed result.  $\square$

## References

Azzalini, A. and Capitanio, A. (2014). *The Skew-Normal and Related Families*, volume 3 of *Institute of Mathematical Statistics Monographs*. Cambridge University Press, Cambridge.

Banerjee, B. and Biswas, S. (2024). Intrinsic geometry-inspired dependent toroidal distribution: Application to regression model for astigmatism data. *arXiv preprint*, arXiv:2409.06229.

Baringhaus, L. and Grübel, R. (2024). Discrete mixture representations of spherical distributions. *Stat. Pap.*, 65(2):557–596.

Borodavka, J. and Ebner, B. (2026). A general maximal projection approach to uniformity testing on the hypersphere. *Bernoulli*, to appear.

Chacón, J. E. and Duong, T. (2018). *Multivariate Kernel Smoothing and its Applications*, volume 160 of *Monographs on Statistics and Applied Probability*. CRC Press, Boca Raton.

Chacón, J. E., García-Portugués, E., and Meilán-Vila, A. (2026). Blessing of dimensionality in cross-validated bandwidth selection on the sphere. *Submitted*.

Dai, F. and Xu, Y. (2013). *Approximation Theory and Harmonic Analysis on Spheres and Balls*. Springer Monographs in Mathematics. Springer, New York.

DLMF (2025). *NIST Digital Library of Mathematical Functions*. F. W. J. Olver, A. B. Olde Daalhuis, D. W. Lozier, B. I. Schneider, R. F. Boisvert, C. W. Clark, B. R. Miller and B. V. Saunders, eds.

Dones, L., Brasser, R., Kaib, N., and Rickman, H. (2015). Origin and evolution of the cometary reservoirs. *Space Sci. Rev.*, 197(1):191–269.

Ebner, B., Henze, N., and Meintanis, S. (2024). A unified approach to goodness-of-fit testing for spherical and hyperspherical data. *Statistical Papers*, 65(6):3447–3475.

Fernández-de-Marcos, A. and García-Portugués, E. (2023). On new omnibus tests of uniformity on the hypersphere. *Test*, 32(4):1508–1529.

Fernández-Durán, J. J. (2004). Circular distributions based on nonnegative trigonometric sums. *Biometrics*, 60(2):499–503.

Fernández-Durán, J. J. (2007). Models for circular-linear and circular-circular data constructed from circular distributions based on nonnegative trigonometric sums. *Biometrics*, 63(2):579–585.

García-Portugués, E., Navarro-Esteban, P., and Cuesta-Albertos, J. A. (2023). On a projection-based class of uniformity tests on the hypersphere. *Bernoulli*, 29(1):181–204.

García-Portugués, E., Paindaveine, D., and Verdebout, T. (2025). On a class of Sobolev tests for symmetry, their detection thresholds, and asymptotic powers. *J. Am. Stat. Assoc.*, to appear.

García-Portugués, E. and Verdebout, T. (2025). *sphunif: Uniformity Tests on the Circle, Sphere, and Hypersphere*. R package version 1.4.4.

Giné, E. (1975). Invariant tests for uniformity on compact Riemannian manifolds based on Sobolev norms. *Ann. Stat.*, 3(6):1243–1266.

Gradshteyn, I. S. and Ryzhik, I. M. (2014). *Table of Integrals, Series, and Products*. Academic Press, Amsterdam, eighth edition.

Jammalamadaka, S. R. and SenGupta, A. (2001). *Topics in Circular Statistics*, volume 5 of *Series on Multivariate Analysis*. World Scientific, Singapore.

Jeffreys, H. (2003). *Theory of Probability*. Oxford University Press, Oxford, third edition.

Jones, M. C. and Pewsey, A. (2005). A family of symmetric distributions on the circle. *J. Am. Stat. Assoc.*, 100(472):1422–1428.

Jupp, P. E., Kim, P. T., Koo, J.-Y., and Wiegert, P. (2003). The intrinsic distribution and selection bias of long-period cometary orbits. *J. Am. Stat. Assoc.*, 98(463):515–521.

Kalf, H. (1995). On the expansion of a function in terms of spherical harmonics in arbitrary dimensions. *Bull. Belg. Math. Soc. Simon Stevin*, 2(4):361–380.

Kato, S. and Jones, M. C. (2015). A tractable and interpretable four-parameter family of unimodal distributions on the circle. *Biometrika*, 102(1):181–190.

Klemelä, J. (2000). Estimation of densities and derivatives of densities with directional data. *J. Multivar. Anal.*, 73(1):18–40.

Magnus, J. R. and Neudecker, H. (1999). *Matrix Differential Calculus with Applications in Statistics and Econometrics*. Wiley Series in Probability and Statistics. John Wiley & Sons, Ltd., Chichester.

Magnus, W., Oberhettinger, F., and Soni, R. P. (1966). *Formulas and Theorems for the Special Functions of Mathematical Physics*, volume 52 of *Die Grundlehren der mathematischen Wissenschaften*. Springer, Berlin.

Mardia, K. V. and Jupp, P. E. (1999). *Directional Statistics*. Wiley Series in Probability and Statistics. Wiley, Chichester.

Pewsey, A. (2026). On Jeffreys's cardioid distribution. *Comput. Stat. Data Anal.*, 213:108248.

Pewsey, A. and García-Portugués, E. (2021). Rejoinder on: Recent advances in directional statistics. *Test*, 30(1):76–82.

Pewsey, A., Neuhäuser, M., and Ruxton, G. D. (2013). *Circular Statistics in R*. Oxford University Press, Oxford.

van der Vaart, A. W. (1998). *Asymptotic Statistics*, volume 3 of *Cambridge Series in Statistical and Probabilistic Mathematics*. Cambridge University Press, Cambridge.

Wang, M. and Shimizu, K. (2012). On applying Möbius transformation to cardioid random variables. *Stat. Methodol.*, 9(6):604–614.

Wehrly, T. E. and Johnson, R. A. (1980). Bivariate models for dependence of angular observations and a related Markov process. *Biometrika*, 67(1):255–256.

Wolfram Research, Inc. (2021). Mathematica. Computer software, Version 13.0.